

THE CREEP AND CREEP RUPTURE OF SMC-R50
UNDER
DIFFERENT THERMOMECHANICAL CONDITIONS

By

Shing-Chung Yen

ABSTRACT

The creep and creep recovery behavior of a random fiber composite (SMC-R50) at elevated temperature and constant humidity were investigated experimentally and theoretically. The short time creep response for four constant stress levels at each of four selected temperature levels was experimentally determined. It was found that repeatable results can be obtained by applying a mechanical conditioning prior to each creep and creep recovery test. Creep data were modelled using the Findley equation which contains three parameters, ϵ_0 (the instantaneous creep response), m (the amplitude of transient creep), and n (the time exponent). It was found that the time exponent is a function of time but approaches to an asymptotic value when the duration of creep is long. Thus, at a constant temperature level, one long-time creep test and four short-time creep tests were conducted. The long-time creep results were used to determine the proper time exponent n . The short time creep data for constant load were used to determine the Findley parameters ϵ_0 and m . It was found that the Findley equation represented the creep results very accurately.

Based on the short-time creep results, the Findley equation was used to predict the long time creep response and the creep response due to multiple step loadings. Five long time creep experiments were conducted. Four of them were 10,000 minutes long and were conducted at the same stress level (6,510 psi) but different temperature levels. The fifth creep experiment was conducted at 5,425 psi and 185°F over a three week period. Three multiple step creep experiments were conducted. These tests were of different load steps and durations. In all cases, it was found that the Findley equation predicted both long time creep response and multiple step creep response very accurately.

Since repeatable results were obtained from conditioned specimens, the test results were compared to experimental data obtained from unconditioned specimens. It was found that experimental results of the conditioned specimens fell within the scatter band of the data for the unconditioned specimens.

A free energy based failure criterion (proposed by Reiner and Weisenberg) was coupled with the Findley equation to predict the creep rupture time of SMC-R50. It was found that the critical free energy at the time of failure is temperature dependent. For a constant temperature, the critical free energy required for rupture is essentially a constant. It is also concluded that, for limited data, the Reiner-Weisenberg Failure criterion provides overall good prediction of the time to failure for SMC-R50.

ACKNOWLEDGEMENTS

The author would like to express his deep appreciation to the chairman of his committee, Dr. D. H. Morris, for his guidance, support, and encouragement during the course of this study. The author would also like to thank Dr. C. Hiel for his invaluable ideas and suggestions to this study. Gratitude is also extended to Dr. H. F. Brinson for allowing the author to use the equipment in his laboratory.

Also, the author would like to extend his appreciation to his fellow graduate students for their encouragement, and in particular to _____ for many helpful discussions. Special thanks are extended to _____ who helped edit the original manuscript.

The author would like to express his gratitude to his father, brother, and parents-in-law for their love and encouragement. Finally, the author would like to express special acknowledgement to his wife for her love and understanding during this work.

TABLE OF CONTENTS

	Page
ABSTRACT	ii
ACKNOWLEDGEMENTS	iv
TABLE OF CONTENTS	v
LIST OF FIGURES	vii
LIST OF TABLES	xii
 <u>CHAPTER</u>	
1 INTRODUCTION	1
2 BACKGROUND INFORMATION	4
2.1 Viscoelasticity	4
2.2 Creep Rupture	6
3 ANALYTICAL MODEL	10
3.1 The Findley Equation	10
3.2 Data Reduction Procedure	12
3.3 Modified Superposition Principle	15
3.4 Reiner-Weissenberg Failure Criterion	18
3.5 Remarks	22
4 EXPERIMENTAL CONSIDERATIONS AND PROCEDURES	27
4.1 The Material and Specimen	27
4.2 Selection of Specimens	29
4.3 Effect of Moisture	29
4.4 Static Ultimate Tensile Strength	31
4.5 Mechanical Conditioning	32
4.6 Edge Replication	35
4.7 Strain Gages	39
4.8 Creep Experiments	39
5 RESULTS AND DISCUSSION	42
5.1 Moisture Effect	42
5.2 Effect of Damage on Creep Response	57
5.3 Parameters as Functions of Duration of Creep Experiment	84

<u>Chapter</u>		Page
	5.4 Short Time Creep Response	92
	5.5 Predictions	101
	5.6 Creep Rupture Results	123
	5.7 Summary	128
6	CONCLUSIONS	130
	REFERENCES	131
	VITA	138

LIST OF FIGURES

Figure	Page
3.1 Path of the minimization of square error using the Levenberg-Marquardt algorithm	14
3.2 Illustration of modified superposition principle	17
3.3 The generalized Kelvin model [7]	20
3.4 Creep and creep recovery response of a typical nonlinear viscoelastic material exhibits flow behavior.	24
3.5 Modification of load history as applied for modified superposition principle.	26
4.1 Configuration of the SMC-R50 specimen	28
4.2 Creep response due to 3 minutes creep and 30 minutes creep recovery	36
4.3 Mechanical conditioning procedure suggested by Jerina, Schapery, Tung and Sanders [32]. . .	37
5.1 Absorption and desorption of SMC-R50 moisture for SMC-R50 specimens at various conditions . .	44
5.2 Stress-strain curve of the post-cured SMC-R50 specimens	47
5.3 Stress-strain curve of the SMC-R50 specimens which were stored at 200°F for two months . . .	48
5.4 Stress-strain curves of the SMC-R50 specimens which were stored at room temperature and 40% relative humidity for two months.	49
5.5 Stress-strain curves of the SMC-R50 specimens which were soaked in water at room temperature for two months.	50
5.6 Typical types of failure of SMC-R50 specimens .	51
5.7 The static ultimate strength of SMC-R50 due to different moisture conditioning	52

Figure	Page
5.8 The static ultimate strain of SMC-R50 due to different moisture conditioning	54
5.9 The ultimate strength of SMC-R50 at elevated temperatures	56
5.10 Creep response of SMC-R50 specimen during mechanical conditioning	58
5.11 Accumulated permanent deformation of SMC-R50 during the mechanical conditioning	60
5.12 Creep response of SMC-R50 for the same test conditions but different mechanical conditions	61
5.13 Creep response of SMC-R50 conditioned at different temperatures	62
5.14 Creep response of SMC-R50 conditioned at different temperatures	63
5.15 Creep response of SMC-R50 conditioned at different temperatures	64
5.16 Edge replica of SMC-R50 at zero load	66
5.17 Edge replica of SMC-R50 at 7782 psi (obtained immediately after load application)	67
5.18 Edge replica of SMC-R50 at 18,500 psi (obtained immediately after load application)	68
5.19 Edge replica of SMC-R50 at creep time = 465 min. and creep stress = 18,500 psi	69
5.20 Edge replica of SMC-R50 at creep time = 700 min. and creep stress = 18,500 psi	70
5.21 Edge replica of SMC-R50 at creep time = 1,300 min. and creep stress = 18,500 psi	71
5.22 Edge replica of SMC-R50 at creep time = 1,640 min. and creep stress = 18,500 psi	72

Figure	Page
5.23 Edge replica of SMC-R50 at creep time = 2,000 min. and creep stress = 18,500 psi. . . .	73
5.24 Edge replica of SMC-R50 at creep time = 4,195 min. and creep stress = 18,500 psi. . . .	74
5.25 Creep response of SMC-R50 obtained from different previous loading history, ($\sigma = 6,510$ psi, room temperature)	76
5.26 The relation between the Poisson's ratio in creep and the mechanical conditioning stress. .	79
5.27 The relation between the time exponent n and the mechanical conditioning stress.	81
5.28 Findley parameter ϵ_0 as a function of applied stress and the conditioning stress.	82
5.29 Findley parameter m as a function of applied stress and the conditioning stress.	83
5.30 Effect of time on n , and the resulting creep response for $n = 0.26$	85
5.31 Variation of parameters, ϵ_0 and m , as a function of time.	87
5.32 Prediction of long time creep response using the short time and long time Findley parameters	88
5.33 Parameters, ϵ_0 and m , as a function of time for a given asymptotic n value.	89
5.34 Creep time required to obtain an asymptotic n value as a function of temperature.	91
5.35 Findley parameters as the functions of stress (conditioned at 7,782 psi).	93
5.36 Time exponent n as a function of temperature (conditioned at 50% of ultimate strength at a given temperature).	95
5.37 Hyperbolic sine fit of the Findley parameter, ϵ_0 , at elevated temperatures (conditioned at 50% of the ultimate strength at a given temperature).	96

Figure	Page
5.38 Hyperbolic sine fit of the Findley parameter, m , at elevated temperatures, (conditioned at 50% of the ultimate strength at a given temperature).	97
5.39 Variation of the Findley parameter, ϵ_0 , with temperature and applied stress	98
5.40 Variation of the Findley parameter, m , with temperature and applied stress	99
5.41 Prediction of the short time creep response using the Findley equation.	100
5.42 Prediction of the recovery response after the short time creep experiments.	102
5.43 Prediction of the short time creep response at elevated temperatures ($\sigma = 2,387$ psi) . . .	103
5.44 Prediction of the short time creep response at elevated temperatures ($\sigma = 4,340$ psi) . . .	104
5.45 Prediction of short time creep response at elevated temperatures ($\sigma = 6,510$ psi) . . .	105
5.46 Prediction of the short time creep response at elevated temperature ($\sigma = 7,782$ psi). . . .	106
5.47 Prediction of long time creep response at elevated temperature and at 6,510 psi	108
5.48 Prediction of the long time creep response at 185°F and 5,425 psi.	109
5.49 Prediction of the creep response at room temperature due to a two step loading	110
5.50 Prediction of the creep response at room temperature due to a three step loading	111
5.51 Load history for a five step loading.	113
5.52 Creep response of a five step loading at $T = 131^\circ\text{F}$	114

Figure	Page
5.53 Creep response of conditioned and unconditioned specimens at 73°F ($\sigma = 40\%$ of σ_u at 73°F)	116
5.54 Creep response of conditioned and unconditioned specimens at 73°F ($\sigma = 60\%$ of σ_u at 73°F)	117
5.55 Creep response of conditioned and unconditioned specimen at 73°F ($\sigma = 80\%$ of σ_u at 73°F)	118
5.56 Creep response of conditioned and unconditioned specimens at 200°F ($\sigma = 20\%$ of σ_u at 73°F)	119
5.57 Creep response of conditioned and unconditioned specimens at 200°F ($\sigma = 40\%$ of σ_u at 80°)	120
5.58 Creep response of conditioned and unconditioned specimens at 200°F ($\sigma = 60\%$ of σ_u at 73°F)	121
5.59 Creep response of conditioned and unconditioned specimens at 200°F ($\sigma = 74\%$ of σ_u at 73°F)	122
5.60 The relation between the critical free energy and temperature	126
5.61 Predictions of stress-rupture time using the Reiner-Weisenberg Criterion.	127

LIST OF TABLES

Table		Page
5.1	Mechanical properties of SMC-R50 after different moisture conditioning	55
5.2	Creep test program for the damage study	80
5.3	List of creep rupture data obtained from Denton [5] and Morris [18] and calculated values of critical free energy.	124

CHAPTER 1

INTRODUCTION

The automotive industry is faced with the challenge of reducing vehicle weight to achieve better fuel economy. While there are several approaches that can be taken to reduce vehicle weight, one of major interest today is the application of lighter weight materials. The material called 'fiber reinforced composite materials' is one of the candidates [1].

Since the early 1970's, fiber reinforced composites have received great attention by many investigators. For example, random fiber composites are valued not only because of their light weight, but also because of their durability, dimensional stability, and their favorable chemical, mechanical, and electrical properties [2]. In addition, the composite molding process for random fiber composites offers design flexibility and allows part consolidation, ultimately reducing the installed cost of complex components [3].

Advanced composites (continuous fiber composites using boron or graphite fibers, for example), have a well established reputation for structural applications in the aerospace industry. However, relatively slow, costly processes are employed to produce these composite structures. In high-volume industries, both high cost and long production

times are extremely detrimental. Therefore, the use of advanced composites in the automobile industry has been limited. On the other hand, random fiber composite materials are favorable because they can be manufactured in high volume, using low cost processes. In particular, sheet molding compound is one of the favorable materials to be used [4].

Sheet molding compound (SMC) may be defined as a molding compound in sheet form which is composed of a thermoset resin, fibrous reinforcement, and additives required for processing or specific product performance [5]. SMC usually consists of polyester resin and glass fiber reinforcement. However, other resin types, such as vinyl ester and epoxy, are finding increased use in SMC [5]. Other reinforcing fibers, namely carbon and aramid, are being considered for specific product performance [5].

The wide application of SMC is partially inhibited due to a lack of understanding of some aspects of its mechanical behavior. It is known that polymer matrices exhibit viscoelastic or time dependent effects which are significantly affected by stress, rate of loading, temperature, humidity, etc. Because of these effects, there is concern that time-dependent phenomena such as creep and creep rupture (the only response to be discussed herein) may be of importance in long term design. Creep and creep rupture tests

are both time consuming and expensive. Hence, it is necessary to use analytical techniques and short term laboratory tests to predict long term viscoelastic behavior. This is the central theme which has been utilized to characterize the viscoelastic response of a wide variety of materials [6,7,8].

The first goal of the current research is to investigate the effects of both stress and temperature on the creep behavior of composite materials, and further to use the Findley equation [9,10,11] to represent the creep data of a particular composite, SMC-R50. The Findley equation was selected based on the work of Cartner and Brinson [12]. They used Schapery's equations [13] to predict the response of SMC-R25; the Findley equation is a form of Schapery's equation. The second goal is to predict the creep response of this material under multi-step loading. The third goal is to predict the creep rupture strength or the time to rupture. The material selected for this study, SMC-R50, is a sheet molding compound containing 50% by weight of chopped glass fibers randomly oriented in the plane of the sheet. Further details of this material may be found in a monograph by Denton [5].

CHAPTER 2

BACKGROUND INFORMATION

2.1 Viscoelasticity

The theory of viscoelasticity as applied to composite materials has received much attention [13,14,15,16]. The theory of viscoelasticity has been used to predict the behavior of composite materials under service conditions, and ultimately to predict its service life (time to failure), [17,18,19].

Viscoelasticity is the study of materials whose properties are time dependent [6,7,20]. A viscoelastic material possesses a characteristic which can be described as a 'memory' effect [6,7,21]. That is, the response of a viscoelastic material is not only determined by the current state of stress, but is also influenced by all past states of stress; the material has a 'memory' for all past states of stress. Similarly, if the deformation is specified, the current stress depends on the entire past history of deformation.

Two fundamental methods, creep and relaxation tests, are frequently used to characterize viscoelastic materials [6,7,20]. A creep test is used to measure the strain-time response for a constant applied load. A relaxation test is used to determine the force-time response as a constant deformation is introduced. Creep and relaxation tests provide one

means of obtaining the static mechanical properties involved in the theory of viscoelasticity. Such tests are usually conducted under uniaxial deformation/force conditions. In a creep test the applied stress can be calculated from the applied load and initial cross-sectional area, the strain-time response can be measured at a designated gage section, and the compliance can be calculated from strain. In a relaxation test, a mechanical system is needed to keep a constant deformation in the specimen [7]. Creep tests were used throughout this study.

For linear viscoelastic materials under uniaxial creep loading, the constitutive equation under isothermal conditions is given by [6,7,20]

$$\epsilon(t) = D(t)\sigma_0 \quad (2.1)$$

where $\epsilon(t)$, $D(t)$ and σ_0 are creep strain, creep compliance, and applied constant stress, respectively. The creep compliance $D(t)$ can be further defined as,

$$D(t) = D_0 + D_1(t) \quad (2.2)$$

where D_0 = initial creep compliance and $D_1(t)$ = transient creep compliance.

To describe the viscoelastic response of a material, D_0 and D_1 in equation (2.2) need to be explicitly specified as functions of stress, temperature, humidity, etc. There are

a wide variety of approaches that could be used to model the constitutive properties of a viscoelastic material. The approaches are well documented, and some of the approaches as applied to composite materials may be found in references such as [13,14,17,22-33]. Of all the approaches, the creep power law is one of the most frequently used and is given as

$$\epsilon = \sigma_0 (D_0 + Ct^n) = \epsilon_0 + mt^n \quad (2.3)$$

This equation has been used by Findley to characterize the creep behavior of unfilled thermoplastics [34], laminated plastics [35], and metals at high temperatures [36,37,38]. More recently, Dillard et al. [16,19] and Gupta et al. [39] have applied equation (2.3) to describe the creep response of composite materials. More will be said about equation (2.3) (herein called the Findley equation) in the next chapter.

2.2 Creep Rupture

Creep reupture is characterized by failure which does not occur at the time of load application but rather after the passage of time. This time-dependent phenomenon has received considerable attention by a variety of researchers. The literature on the mechanics of polymer fracture has been exhaustively reviewed by Knauss [40], and by Regel and Tamuzh [41]. Previous studies of time dependent failure of

composites have included such material systems as graphite/epoxy [16,17,24], sheet molding compound [5,12,18], glass-fabric based plastic lamintes [42], and glass/epoxy composites [43].

Creep rupture in composite materials may be studied from several different viewpoints including a microfailure analysis [44], a phenomenological failure analysis [18,45], or a deformational failure analysis [12,46]. Microfailure investigations can include the study of the microscopic or small scale failure mechanisms that produce creep ruptures. Such phenomena as fiber-matrix interfacial failure, matrix crazing, delamination, or other damage formation, are potential areas of study. This approach was not used in this study.

Phenomenological approaches attempt to correlate the measured data with some form of failure law. Usually, these approaches represent the empirical observation of the general failure process. One of the phenomenological approaches that has been applied to composites is due to Zhurkov [47], who used a modified Arrhenius equation. The most common form of this equation is given as,

$$t_f = t_o \exp[(U_o - \gamma\sigma)/KT] \quad (2.4)$$

where t_f = rupture time

t_o = a constant

U_0 = activation energy = a constant

γ = a constant

σ = applied uniaxial stress

K = Boltzman's constant

T = absolute temperature

Chiao et al. [45] have found the Zhurkov relation to be valid for composites. However, the composite they studied consisted of only several strands of aramid fiber impregnated with epoxy primarily for protection, and therefore their results may not be applicable to more commonly encountered composite material systems.

Deformational approaches to creep rupture utilize knowledge of the state of stress, strain and time. The classic approach to this phenomenon is given by Landel and Fedors [48]. To perform this type of analysis, a property surface in stress-strain-time space is developed to establish the constitutive behavior for a material. The failure envelope is the boundary to this surface. Thus, the property surface uniquely establishes the stress-strain-time relationship for any load path, and the surface will also give the stress and strain at the time of failure.

A mathematical model for the characterization of a delayed yield phenomenon was proposed by Crochet [49]. He assumed that yield stress is a time dependent property, in particular, it is dependent upon the transient creep strain.

This approach was modified by Cartner et al. to predict the creep rupture of SMC-R25 [12].

CHAPTER 3

ANALYTICAL MODEL

As indicated in the previous chapter, there are many theories in viscoelasticity which might be potentially used in the characterization of SMC-R50. The Findley equation, even though it is an empirical equation, represents an approximation of a mechanical model of springs and dashpots [25]. The Findley equation is easy to use since data reduction and testing procedures are simple [25]. It has been shown in the literature [34,35,36] that the Findley equation represents creep data very accurately.

3.1 The Findley Equation

The Findley equation consists of three material parameters: the instantaneous (or initial) response (ϵ_0), the amplitude of transient creep (m), and the time exponent (n). For a unidirectional situation, this creep law for isothermal conditions can be expressed as [50],

$$\epsilon = \epsilon_0 + mt^n \quad (3.1)$$

Further, the assumptions are made that [51]

1. n is independent of stress, but a function of temperature, moisture etc.
2. ϵ_0 and m are functions of stress, temperature, moisture, etc.

Note that while ϵ_0 is often referred to as the initial strain, it is actually a curve fitting parameter in a data reduction procedure [10]. As such, ϵ_0 may not necessarily correspond to an actual instantaneous strain even if this value can be physically determined. Perhaps one of the reasons that the Findley equation has found wide usage is its great versatility to represent a variety of material responses [19,34,35,36,39].

As previously mentioned, the value of n has been assumed to be independent of the stress level. The published data of Findley et al. [50] indicates wide scattering in the value of n . This is probably due to the nature of the data reduction methods (which will be discussed in a later section), in which n is determined using only three data points. Another problem often observed in the literature is due to the fact that n is calculated using short time creep data where the transient creep strain is small. To deal with this problem, the average value of n is taken to be constant [19,50,51].

In his study of laminated plastics, Findley [52] discovered that the creep parameters ϵ_0 and m can be expressed as

$$\epsilon_0 = \epsilon_0' \sinh\left(\frac{\sigma}{\sigma_e}\right) \quad (3.2)$$

$$m = m' \sinh\left(\frac{\sigma}{\sigma_m}\right) \quad (3.3)$$

where ϵ_0' , m' , σ_e , and σ_m are material parameters and are functions of temperature, moisture, etc..

3.2 Data Reduction Procedure

Several techniques can be used to determine the material parameters in the Findley equation from experimental data. If the initial creep response ϵ_0 is known, the relation between $\epsilon - \epsilon_0$ and time (for constant stress) is simply a straight line on a log-log scale. The slope of this line gives the time exponent n and the $t=1$ intercept is the value m . A trial and error approach is needed to determine ϵ_0 because in practical situations it is very difficult to measure the initial response experimentally.

In some cases, Findley used another procedure to evaluate the values of ϵ_0 , m , and n . The approach was to record the strains ϵ_1 , ϵ_2 , and ϵ_3 at times t_1 , t_2 and t_3 where

$$t_3 = \sqrt{t_1 \cdot t_2} \quad (3.4)$$

The power law parameters may be easily determined from the following equations as found by Boller [42].

$$n = \frac{\log(\epsilon_3 - \epsilon_1) / (\epsilon_2 - \epsilon_1)}{\log(t_2 / t_1)} \quad (3.5)$$

$$\epsilon_0 = \frac{\epsilon_1 \epsilon_3 - \epsilon_2^2}{\epsilon_1 - 2\epsilon_2 + \epsilon_3} \quad (3.6)$$

$$m = \frac{\epsilon_1 - \epsilon_0}{t_1^n} \quad (3.7)$$

This approach is probably not as accurate as the preceding method of using the log-log plot because the fit is based on only 3 data points. Extensive discussion of this process can be found in the work by Dillard [19].

Recently, a computer-based solution for evaluating the parameters in Schapery's nonlinear viscoelastic model was developed at VPI & SU by Bertolotti et al. [53]. This computer code has proven very accurate and effective. Keeping the same algorithm, the author has made some changes in the program to determine the parameters in the Findley equation. The key mathematical (or computational) basis of this computer program is the finite-difference, Levenberg-Marquardt algorithm which finds the minimum sum of squares of error between data points and a defined function, i.e. the Findley equation. For a random set of parameters ϵ_0 , m , and n , the sum of squares error, Error, of a set of data points is

$$\text{Error} = \sum_{i=1}^N \{\epsilon_i - [\epsilon_0 + mt_i^n]\}^2 \quad (3.8)$$

It is clear that the plot of $\frac{E}{\sigma}$ error versus the three parameters given a surface as in Figure 3.1. On this

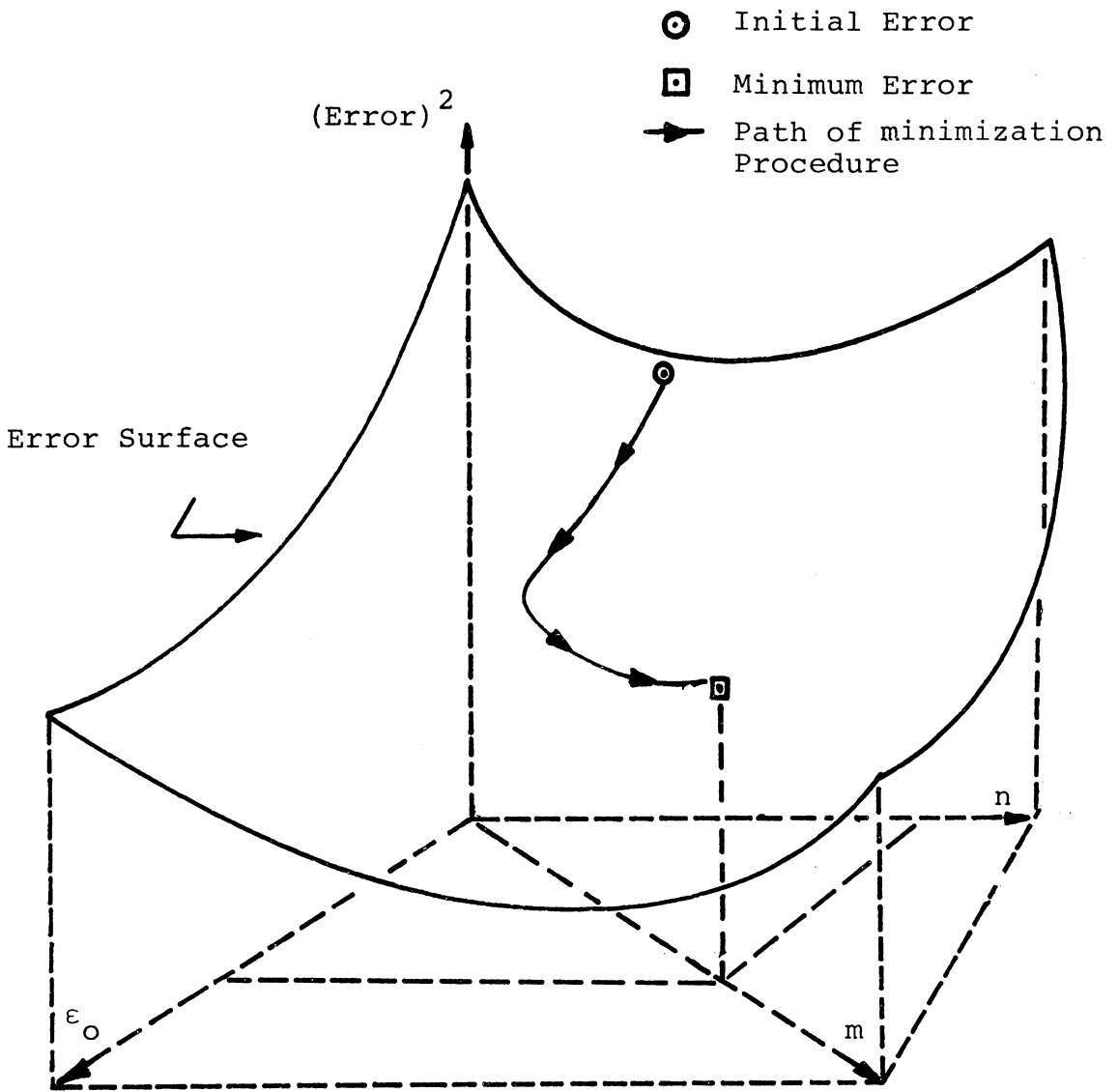


Figure 3.1 Path of the minimization of square error using the Levenberg-Marquardt algorithm.

surface, there is a point which defines the minimum squares error. The slope of the curve at such a point is zero. The Levenberg-Marquardt algorithm finds the direction of the steepest slope for a given initial set of values. In this direction, a new set of parameters is generated by the algorithm and repeats the same procedure. This procedure continues until a point is found where the slope increases in all directions. The parameters associated with this point essentially provide the best fit of experimental data. This method is more accurate than the other two methods mentioned previously and is currently used in this study.

3.3 Modified Superposition Principle

A structural member may frequently be subjected to abrupt changes of loading during service due to the failure of other members or a sudden load increase. The behavior due to a sudden load change in a viscoelastic media is complex. The mechanisms which dominate the viscoelastic response after an abrupt change of loading are the memory due to past loading histories and current loading history. To account for this kind of phenomenon, Findley and Lai [54] have developed a modified superposition principle. For uniaxial tension, this superposition method can be described as follows. When the state of stress is

abruptly changed from σ_1 to σ_2 at time t_1 , the creep behavior can be considered as if at this instant stress σ_1 is removed and at the same time stress σ_2 is applied to the specimen, both being considered as independent actions [54]. To illustrate this method consider a two-step loading as shown in Figure 3.2. The recovery strain ϵ_1 resulting from removal of σ_1 after loading time t_1 is given by

$$\epsilon' = \epsilon_o(\sigma_1) + m(\sigma_1)t^n - [\epsilon_o(\sigma_1) + m(\sigma_1)(t-t_1)^n]$$

or

$$\epsilon' = m(\sigma_1)[t^n - (t-t_1)^n] \quad (3.9)$$

The creep behavior due to σ_2 applied at t_1 , denoted by ϵ'' is

$$\epsilon'' = \epsilon_o(\sigma_2) + m(\sigma_2)(t-t_1)^n \quad (3.10)$$

The total strain will be the sum of equations (3.9) and (3.10) and equal to

$$\epsilon = \epsilon_o(\sigma_2) + m(\sigma_1)[t^n - (t-t_1)^n] + m(\sigma_2)(t-t_1)^n \quad \text{for } t > t_1 \quad (3.11)$$

In the same manner, the strain response due to stress changing k times is given as follows:

$$\epsilon = \epsilon_o(\sigma_k) + \sum_{p=1}^k [m(\sigma_p) - m(\sigma_{p-1})](t-t_{p-1})^n \quad \text{for } t > t_p \quad (3.12)$$

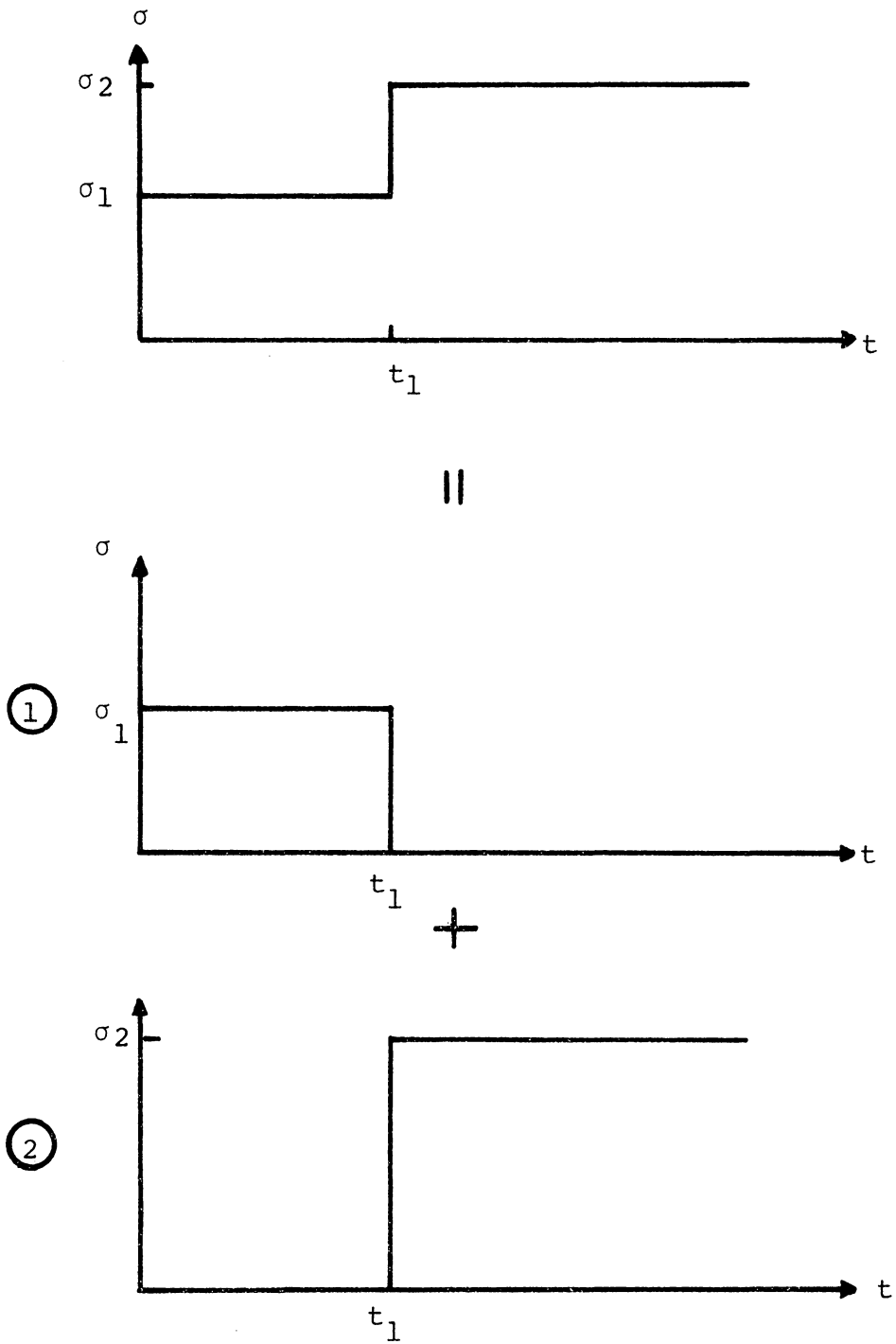


Figure 3.2 Illustration of modified superposition principle.

In this theory, the time-dependent part of the strain depends on both stress state and stress history, while the time-independent part depends only on the current state of stress.

Note that there are no additional parameters introduced in the Findley-Lai modified superposition principle. Thus, to predict the creep response due to multiple step loading, one needs only perform several single-step creep experiments to obtain the parameters needed for the mathematical model.

3.4 Reiner-Weissenberg Failure Criterion

A viscoelastic material under load behaves as a medium which both stores and dissipates energy. These energy components are related to the work performed by the applied stress as the deformation increases with time [25]. As time increases, the stored energy is accumulated and available for physical changes such as microcrack formations. According to Griffith et al. [24] and Hiel [25], Reiner and Weissenberg [55] proposed to use this fundamental property, stored energy, as a criterion to study the creep rupture behavior of viscoelastic materials. Hiel [25] assumed that a threshold value of the distortional free energy (i.e. the stored energy) is responsible for the final failure of a viscoelastic medium. For the viscoelastic behavior represented by a generalized Kelvin model

[6,7,20] (Figure 3.3), the free energy is equal to the sum of the energies stored in all springs and the dissipated energy is equal to the energy dissipated in all dashpots. The strain-time response of the generalized Kelvin model due to a constant stress, σ_0 , is as follows [6,7,20]:

$$\epsilon(t) = \sigma_0 D_0^S + \sum_{i=1}^N \sigma_0 D_i^S (1 - \exp^{-t/\tau_i}) \quad (3.13)$$

where the first term corresponds to the response of the free spring while the i -th component of the second term represents the response of the i -th Kelvin element. Note that in each Kelvin element, the spring and the dashpot are subjected to the same amount of deformation. Thus, each unit of the second term of the equation (3.13) also represents the amount of deformation imposed on the spring in a Kelvin element. The free energy stored in the springs is easily calculated and is given by Hiel [25],

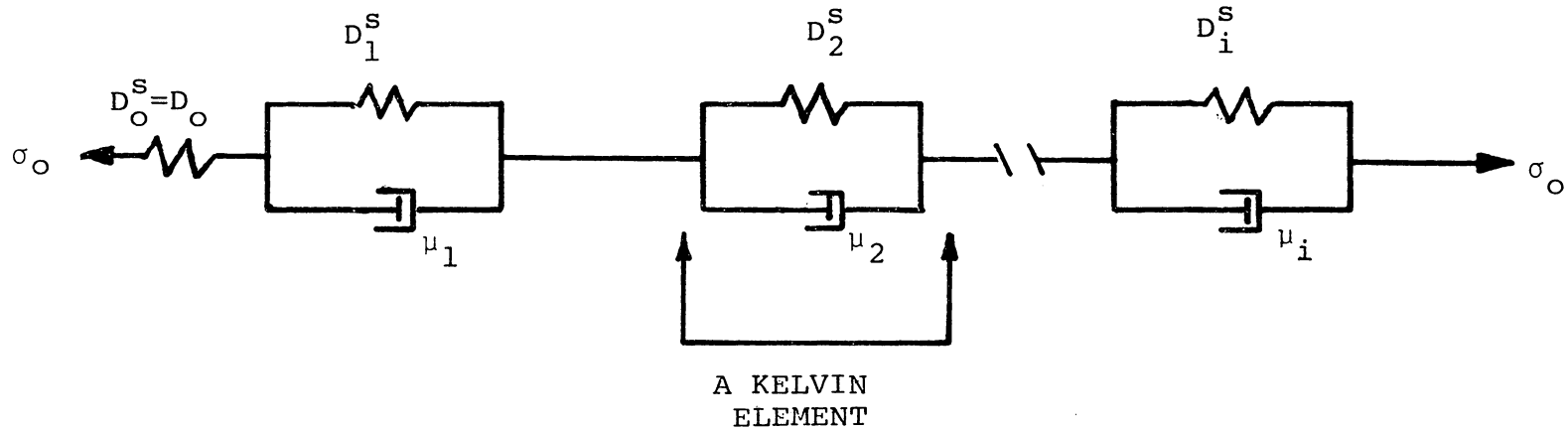
$$W_{\text{springs}} = \sigma_0^2 \left[\frac{D_0^S}{2} + \sum_{i=1}^N \frac{D_i^S}{2} [1 - \exp(-t/\tau_i)]^2 \right] \quad (3.14)$$

Similarly, the energy dissipated can be expressed as,

$$W_{\text{dashpots}} = \sigma_0^2 \sum_{i=1}^N \frac{D_i^S}{2} [1 - \exp(-2t/\tau_i)] \quad (3.15)$$

and the total energy is

$$W_{\text{total}} = \sigma_0^2 \left[\frac{D_0^S}{2} + \sum_{i=1}^N D_i^S [1 - \exp(-t/\tau_i)] \right] \quad (3.16)$$



D_i^S = COMPLIANCE FOR SPRINGS
 μ_i^S = THE COMPLIANCE FOR THE
 RATE OF DEFORMATION
 τ_i = RETARDATION TIME
 $\tau_i = D_i^S \mu_i$

Figure 3.3 The generalized Kelvin model [7].

Hiel also discovered that equations (3.14), (3.15), and (3.16) can be approximated by several constitutive laws of viscoelasticity [25]. In particular, they can be approximated by the Findley equation as follows,

$$\frac{W_{\text{total}}}{\sigma_0^2} - \frac{D_0^s}{2} = \sum_{i=1}^N D_i^s (1 - \exp(-t/\tau_i)) \approx Ct^n \quad (3.17)$$

and

$$\frac{W_{\text{dashpots}}}{\sigma_0^2} = \frac{1}{2} \sum_{i=1}^N D_i^s (1 - \exp(-2t/\tau_i)) \approx \frac{1}{2} C (2t)^n \quad (3.18)$$

An approximation for the stored energy can be obtained as,

$$\begin{aligned} W_{\text{springs}} &= W_{\text{total}} - W_{\text{dashpots}} \\ &\approx \sigma_0^2 \left[\frac{D_0}{2} + C \left(t^n - \frac{1}{2} (2t)^n \right) \right] \end{aligned} \quad (3.19)$$

Where $D_0 = \frac{\epsilon_0}{\sigma_0}$ = initial creep compliance

and $C = \frac{m}{\sigma_0}$ = transient creep compliance

According to Reiner et al. [55] and Hiel [25], the free energy reaches a critical value, the critical free energy W_c , at the instant of creep rupture. On the other hand, σ_0 becomes the failure stress, σ_f , and t becomes the failure time, t_f . Thus,

$$\sigma_f = \frac{\sqrt{W_c}}{\sqrt{\frac{D_0}{2} + C \left(t_f^n - \frac{1}{2} (2t_f)^n \right)}} \quad (3.20)$$

The critical free energy W_c has been found to be constant for a certain material at constant temperatures [25,56,57]. For a given value of W_c , one only needs to conduct a simple creep test to predict the time to failure for a given stress level.

As mentioned in the previous chapter, there are other failure criteria that may be used to predict creep rupture. Cartner et al. [12] used the Crochet criterion and the Schapery strain-time response to predict the creep rupture behavior of SMC-R25. This method requires both very short and very long time creep rupture data. Unfortunately, the creep rupture data available to the author, (from Denton [5] and Morris [18]) are short time failure data at very high stress or/and very high temperature levels. Therefore, the Crochet criterion is not considered in this study.

3.5 Remarks

The Findley equation requires only simple numerical and experimental procedures. In particular, for uniaxial creep, it requires only a single step creep test to determine the parameters ϵ_0 , m , and n for a given stress and temperature.

To apply the Findley modified superposition principle to describe the creep behavior due to multiple step loadings requires data from several single-step creep tests. Furthermore, the creep rupture time can be directly calculated using

the parameters of a single step creep test. Thus, to characterize creep response of a material over a range of thermomechanical conditions, only several single step creep tests are needed to determine the Findley parameters as a function of temperature and stress.

Because parameters ϵ_0 and m are hyperbolic sine functions of stress, the Findley equation is capable of predicting nonlinear creep response. For a nonlinear viscoelastic material that exhibits flow behavior [6], there exists an amount of non-recoverable strain when the creep load is released (Figure 3.4). Such a non-recoverable strain cannot be predicted by the modified superposition principle. As can be shown by letting t be large compared to t_1 in equation (3.9), the recovery strain becomes zero when time is sufficiently long. Furthermore, according to the Findley equation, the amount of strain released immediately following the removal of creep load, i.e. $\epsilon(t_1) - \epsilon'(t_1)$, is the same as the instantaneous creep strain. This is not always true for a nonlinear viscoelastic material. However, the non-recoverable strain and the difference between instantaneous creep and recovery are usually small and negligible at temperatures well below the glass transition temperature, T_g , [13].

Since the modified superposition equation is not of the integral form, its prediction for more complicated loadings

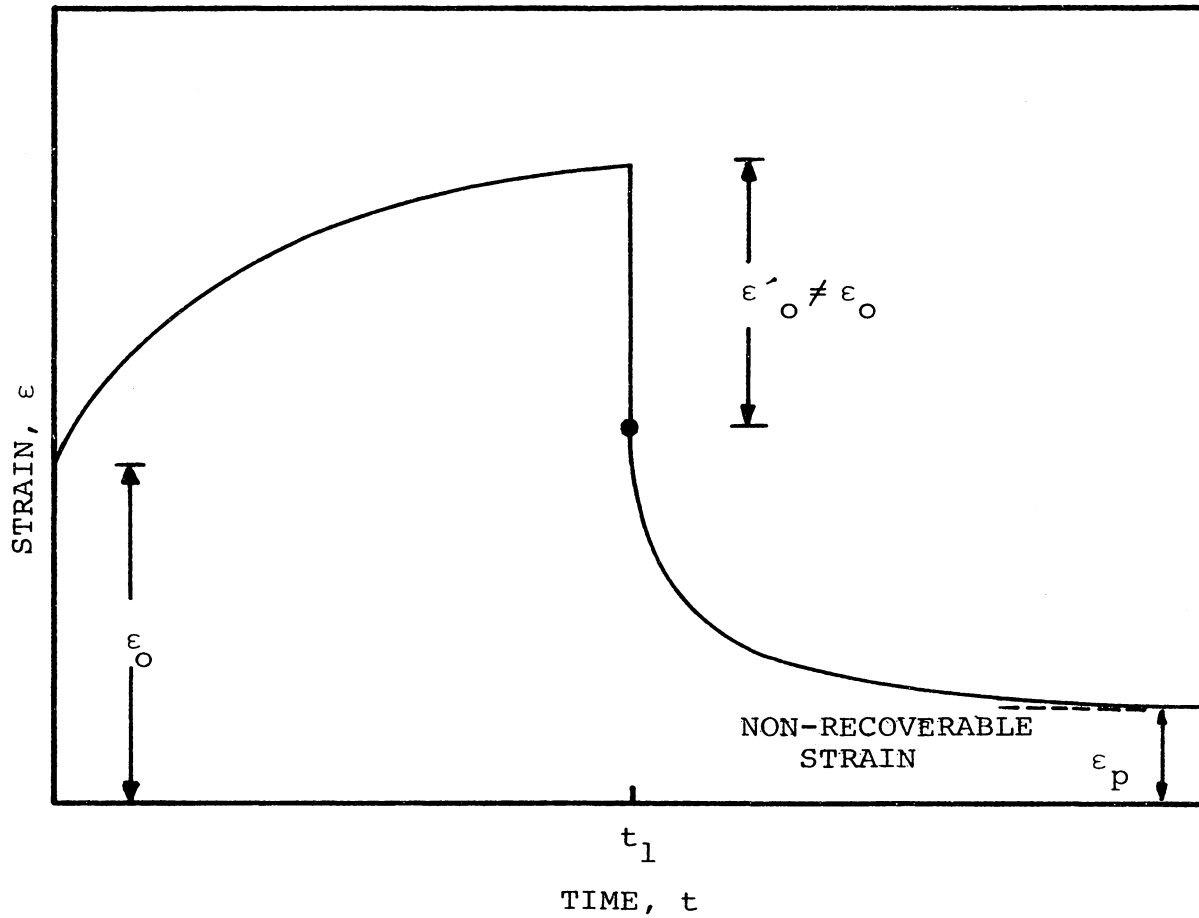


Figure 3.4 Creep and creep recovery response of a typical nonlinear viscoelastic material that exhibits flow behavior.

is doubtful (for example, such as monotonic varying loading and sinusoidal loading). However, these restrictions may be partially solved by treating the loading as having many fine steps of loading (Figure 3.5).

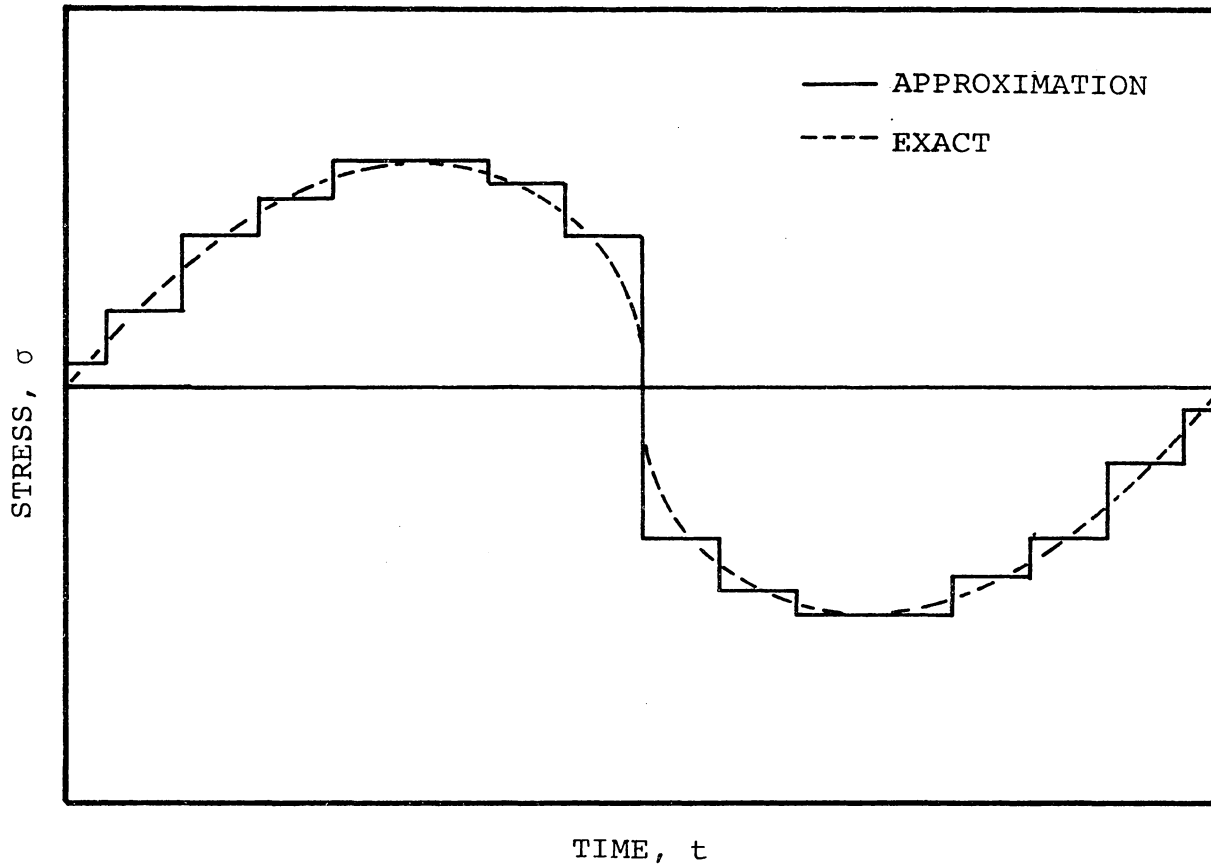


Figure 3.5 Modification of load history as applied for modified superposition principle.

CHAPTER 4

EXPERIMENTAL CONSIDERATIONS AND PROCEDURES

Several phases of experimental work were conducted so that the phenomenon of creep in SMC-R50 would be better understood. The considerations started with the effect of environmental conditions on the material, and the determination of a proper testing procedure which would provide repeatable results.

4.1 The Material and Specimen

The material used for the current experimental work was SMC-R50, a sheet molding compound containing 50% by weight chopped glass fibers randomly oriented in the plane of the sheet. The matrix material was polyester and the fiber length was approximately 1 in. Typically, SMC is compression molded at high temperature and pressure, 300°F and 1,000 psi [5]. It has been found [5] that SMC-R50 can be classified as a transversely isotropic material, where the plane of isotropy coincides with the plane of the sheet.

The dog bone shaped specimens (Figure 4.1) used for testing were rough-cut from SMC-R50 panels with a diamond abrasive disk; the final shape was formed using a high-speed router. Each specimen was labeled to indicate the location and the panel from which it was cut. The length of the specimen was 8 inches, while

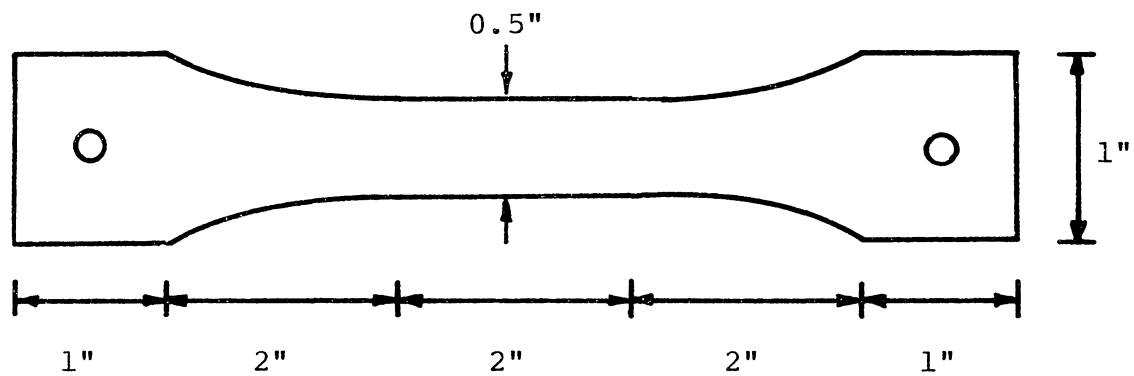


Figure 4.1 Configuration of the SMC-R50 specimen.

the gage section was 2 inches. The width of the specimen was 1 in. at the grip section and 0.5 in. at the gage section. One hole was drilled at each grip section to allow insertion of a pin which helped to prevent the specimen from slipping in the friction grips.

4.2 Selection of Specimens

During the molding process, glass fibers were randomly spread on the top of a layer of fluid like polyester matrix. Upon compression the polyester paste was squeezed. As a result, possible matrix rich and fiber rich regions might be formed during the manufacturing of SMC. Obviously, this material nonhomogeneity would cause a scattering of experimental data. To exclude this undesirable factor in the experimental result, specimens were subjected to a careful selection prior to testing. The method used to select specimens was simply placing the specimens on top of a light bulb. Due to the semi-transparent nature of SMC-R50 contrasted against the light background, a matrix rich (or fiber rich) region could be identified in the specimen. Specimens were selected that were as uniform as possible.

4.3 Effect of Moisture

Significant moisture content is known to have an

effect on the strength and stiffness of composite materials [58,59,60]. Particularly, according to Loos et al. [61] and Hosangadi et al. [62], SMC material systems tend to gain weight when they are exposed to high relative humidity or emersed in fluid. In addition, moisture has been considered as an agent to accelerate the viscoelastic behavior [59,60].

To study and to minimize the influence of moisture effect on the creep characterization, SMC-R50 specimens under four different conditions were investigated. Specimens were 1) post cured above the glass transition temperature T_g [20], 2) stored in an oven at 200°F for two months, 3) stored at room temperature at 40% relative humidity for two months, and 4) soaked in water at room temperature for two months.

To perform post cure, specimens were placed in an oven and heated to approximately 50°F above the glass transition temperature ($T_g=338^\circ\text{F}$ for SMC-R50 [5]). Before cooling, the specimens were stabilized at the high temperature for 48 hours. The temperature was decreased at a rate of 5°F/hour. The specimens were stored in a desiccator immediately after they had been cooled down.

The above mentioned treatments would indicate four cases of moisture content in SMC-R50 specimens. These cases were defined as extreme dry, dry, wet, and extreme wet and

were defined by the percentage of weight gain (or loss) with respect to the original weight of the specimen at room temperature. Before conducting the treatments, each specimen was weighed at room temperature. All the specimens except the post-cured one were weighed at room temperature periodically during the two-month period. Results are given in Chapter 5.

The weight measurements were conducted using an electronic balance. The maximum measuring capacity of the balance was 160 grams with accuracy up to 1/10,000 of a gram. To ensure accurate weight measurement, calibrations were performed before each use of the balance.

4.4 Static Ultimate Tensile Strength

The main purpose of weight measurement was to calculate the degree of moisture desorption (or absorption) in relation to the static ultimate strength of each SMC-R50 specimen. Also, one could then determine the extent to which the moisture content might affect the mechanical behavior of SMC-R50.

The static tensile strength tests were performed on an Instron testing machine. Tensile strain was measured using a strain gage extensometer, with a one-inch gage length and maximum strain of 25%. Load was measured using a load cell. A load-strain plot was recorded using an x-y recorder. Prior to each test the extensometer and load cell were

calibrated. Uniaxial tensile tests were conducted in a room at 73°F and 40% relative humidity. The tensile load was applied using a constant cross head rate of 0.05 in/min.

4.5 Mechanical Conditioning

Researchers have studied extensively the uniaxial tensile properties of SMC under a variety of conditions [1,5,12,32,63,64]. Considerable experimental scatter was found in their results. These results usually occurred not only from specimen to specimen but also occurred from the same specimen at the same test conditions (creep load, [1,32] for example). The fibers have preferred directions depending upon flow during the compressive molding process [3,4], also matrix rich and fiber rich regions exist in a panel. As a result, the mechanical response may be different from panel to panel and with the location and direction of a specimen taken from within a single panel. On the other hand, the same specimen may also exhibit data scatter for the same test conditions. For example, in their study of SMC-R25, Cartner and Brinson [12] found that repeatable stress-strain response for a constant cross head rate test occurs only after twenty cycles of loading and unloading. It has also been found that repeatable creep response of SMC-R50 can only be obtained after a few cycles of repeated creep and creep recovery [32]. Furthermore, SMC materials often exhibit discontinuous creep response, i.e. a sudden

increase in strain at a particular instant of time during the creep load [5,32]. This may be because of the existence of microcracks and non-recoverable deformations. In composite materials, microcracks are often introduced upon loading. These cracks often appear within the matrix material (or at the fiber/matrix interface) and continue growing as the loading is increased or repeated. While the exact crack growth behavior is not known, two distinct creep responses associated with it are thought to exist for a SMC material system [5,32]. They are unstable crack growth [5] and slow crack growth [32]. The slow crack growth behavior might be considered stable since it is a predictable continuous time event, while the unstable crack growth appears as a sudden jump in creep strain during the creep load and cannot be described by any of the theories available to-date [32]. Furthermore, there is no way of knowing when and how this sudden jump is going to occur. However, with the exception of these jumps in strain, creep strain of SMC is directly proportional to the logarithm of time [5]. This implies that if we can arrest the microcracks to a certain extent, the jump in creep strain may not occur during the creep loading.

The non-recoverable deformation previously mentioned may be plastic deformation, or residual microcrack openings, and due to the viscous flow of the matrix materials [32]. When this kind of deformation appears, the mechanical response

following the recovery of previous loading becomes more complicated. It is then necessary to keep track of the previous loading history and record the amount of irrecoverable strain to accurately measure the viscoelastic response.

In order to eliminate irreproducible results, it was necessary to mechanically condition specimens. There were different methods of mechanical conditioning used in the past. Cartner and Brinson [12] used a uniaxial loading (tension) and unloading procedure at a constant cross head rate to condition SMC-R25 specimens. They found that changes in the stress-strain diagram did occur with cycling up to about the 20th cycle, but thereafter the loading and unloading behavior was unchanged. A repeated creep and creep recovery procedure was used by Lou and Schapery [27] and Gupta and Lahire [39] to mechanically condition composite materials. Each cycle contained one hour of creep followed by 24 hours of creep recovery. Using this method, repeatable creep response was achieved in approximately 7 cycles (about one week). It was also noted that transient creep response was slightly decreased due to the nature of matrix cracking.

In a preliminary study for the work reported herein, the same procedure was taken except the creep time was three minutes and the recovery time was thirty minutes. Repeatable

results were obtained after twenty-two cycles (approximately 12 hours, see Figure 4.2). Since the conditioning period was extremely long, a procedure proposed by Jerina et al. [32] was adopted (Figure 4.3). The ratio of time between two subsequent load cycles was one to two, while in each cycle the time ratio between creep and creep recovery was one to ten. Jerina et al. have shown that for SMC-R50 specimens, it took approximately seven cycles (four hours) to obtain a repeatable creep response. It was also reported [32] that residual strains recovered after several days of sitting in the laboratory. Thus, mechanical conditioning was required prior to each test.

4.6 Edge Replication

Edge replication is a nondestructive technique which provides the details of the surface topography of specimens [65,66]. The replication technique is a basic metallurgical procedure used to study cracking in metals. For the present application, the edge replication technique was used to compare the microcrack pattern between different levels of applied creep load and between different times during a creep load.

To ensure better results, specimen edges were polished before testing (as suggested in [66]). The specimens were first polished on metallographic polishing paper beginning with 400 grit and following with 600 grit paper. The

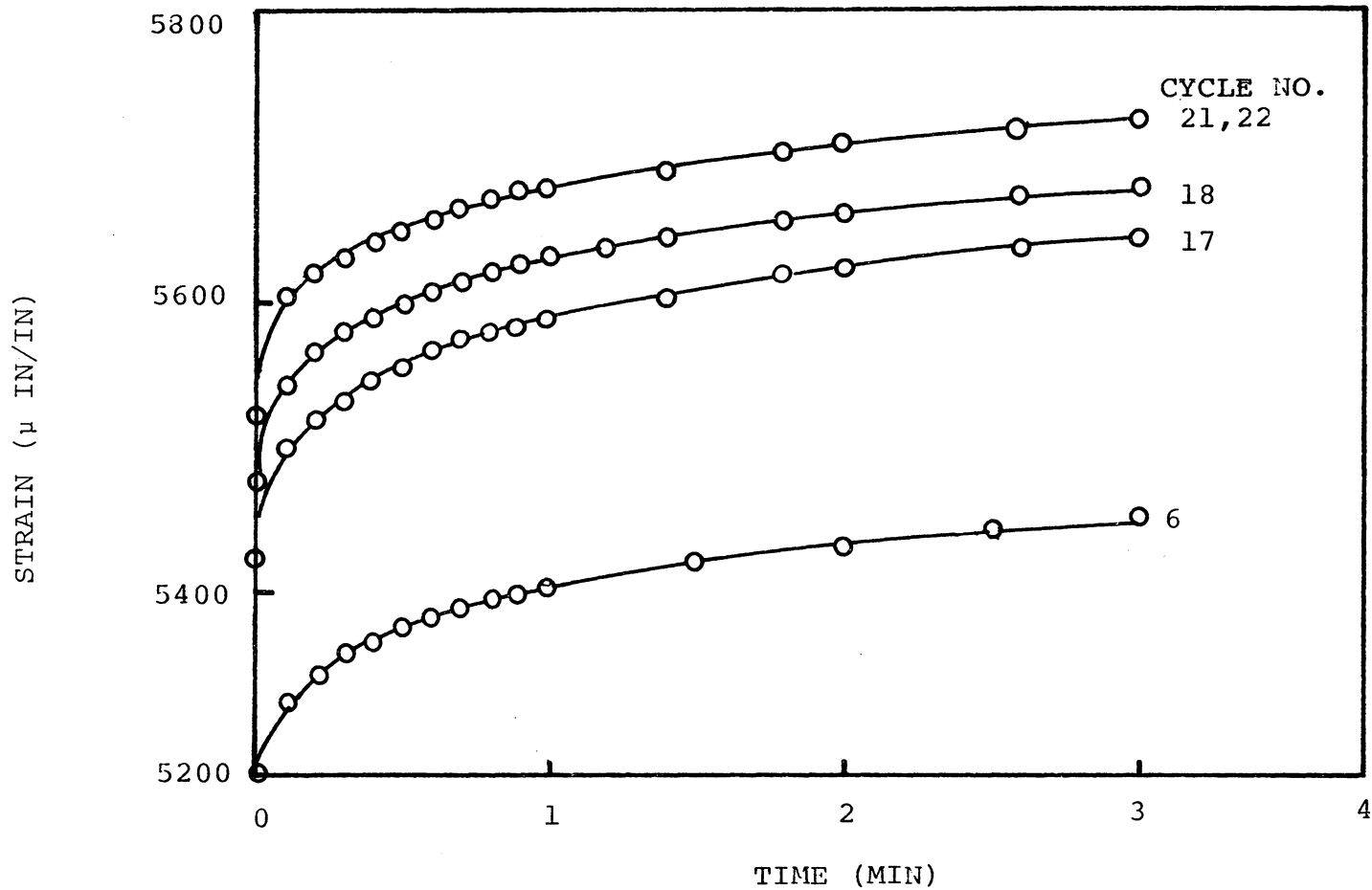


Figure 4.2 Creep response due to 3 minutes creep and 30 minutes creep recovery.

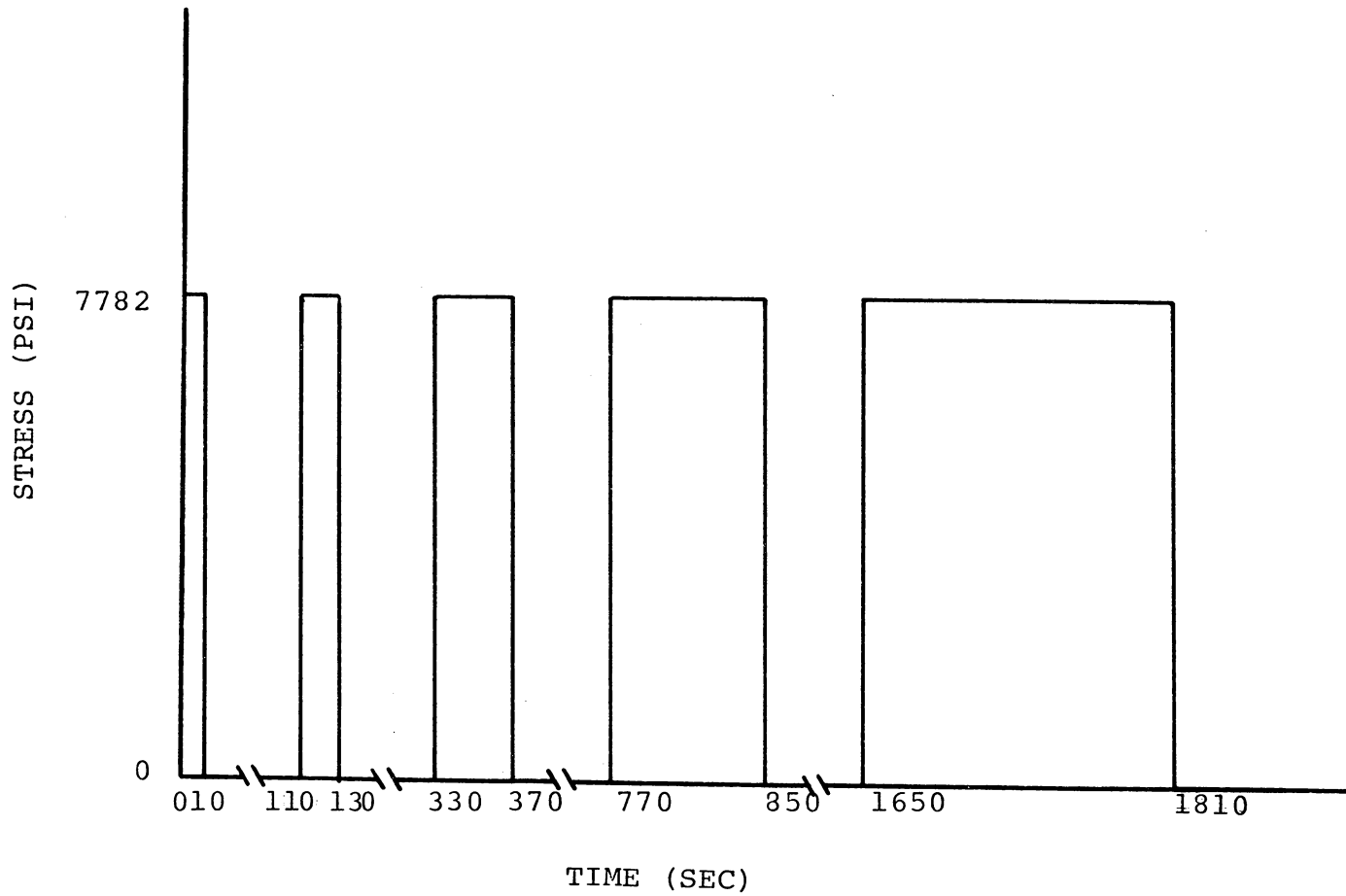


Figure 4.3 Mechanical conditioning procedure suggested by Jerina, Schapery, Tung and Sanders [32].

specimens were then polished with a 7 micron alumina slurry and finally with a 3 micron alumina slurry. Usually it took about 100 strokes for each of the coarse polishing steps and 50 strokes for each of the fine polishing steps to obtain the desired results. Polishing was applied with water to prevent unexpected heating of the specimens. With specimens prepared in this manner, one could distinguish individual fibers on the resulting replicas.

To obtain the edge replica, 0.005 in. thick cellulose acetate replicating tape was fixed in contact with the specimen edge at the gage section. A small amount of acetone was then injected between the replicating tape and the specimen. The acetone softened the tape while the capillary action of the SMC-R50 specimen drew the acetone and the softened tape to its surface. To ensure uniform application, a very slight pressure was applied to the tape immediately after the acetone injection. After a few minutes, the replicating tape hardened and was peeled from the specimen. These replicas provided a permanent record of the edge topography at the instant of time in which a particular loading was applied. Because these replica are transparent, copies of enlarged edge topography can be obtained using a microfiche reader.

4.7 Strain Gages

In all creep experiments the strain was measured using a strain gage manufactured by Micro-Measurements, Inc. Two types of strain gages were used; EA-06-125AC-350 and CEA-06-125UT-350. Except in the case of transverse strain measurements, the first gage type was used in all the creep tests. Micro-Measurement's M-bond 600 adhesive was used to mount the strain gage on the specimen. The specimen was placed in an oven at 175°F for 8 hours to cure the adhesive.

Gages were mounted on opposite sides of each specimen and wired in series in a Wheatstone bridge arrangement. This produced an effective 700 Ω configuration which minimized gage heating and eliminated specimen bending effects. A dummy specimen was used to compensate for temperature effects.

4.8 Creep Experiments

Two lever-arm creep frames were used for loading the specimens. Each machine was equipped with an ATS Series 2912 oven and a series 230 temperature controller. This control unit maintained oven temperatures within $\pm 5^\circ\text{F}$ of the desired temperature. Temperatures were determined with a Doric Model 412A Trendicator. Voltage to the strain gages was supplied by a Vishay 2120 strain gage conditioner. A Fluke 8200A digital volt meter was

connected to the conditioner to indicate creep strain. Creep strain was recorded at selected time intervals. The time was measured by a clock (manufactured by Engler). Hewlett-Packard 7100B strip chart Recorders were also used to monitor the strain data at initial times when strain changed rapidly.

Before being used for any experiment, the two creep frames were calibrated to determine the relation between the dead weight and the load applied to the specimen. A BLH load cell (type C3PlH) was used in the calibration. Repeatable results were found.

Four stress levels were used for the creep tests: 11%, 20%, 30% and 36% of the static ultimate strength of SMC-R50 at room temperature. Prior to each creep test, the specimen was mechanically conditioned. In room temperature testing, a desiccant was placed in the oven to minimize the moisture content.

The selection of the maximum temperature of the creep experiment was based on the design data used by General Motors [1]. The maximum temperature was limited to at least 50°F below the glass transition temperature. The four temperature levels used in this study were 73°F, 104°F, 158°F, and 212°F. Before performing elevated temperature creep tests, the temperature in the oven was maintained at the desired temperature for

at least 6 hours. To provide a uniform temperature distribution in the oven, a steel block was placed in the oven. The temperature gradient through the depth of the oven did not vary over $\pm 3^{\circ}\text{F}$. For all the tests, the strain was allowed to recover before the next test was started.

Multiple step loading was accomplished by simply removing or adding weight directly to the load pan of the load frame.

CHAPTER 5

RESULTS AND DISCUSSION

This chapter contains the experimental and numerical results of the current investigation. The static ultimate strength of SMC-R50 specimens with different moisture contents and at different temperatures are presented first to set a limitation on the testing environment. The nature of parameters ϵ_0 , m , and n in the Findley equation associated with the duration of a creep test are reported. Conditions under which repeatable results can be obtained are discussed. Elevated temperature creep characterization is presented. Predictions of long time creep and creep under multi-step loading are also outlined. Predictions of creep rupture are also presented.

5.1 Moisture Effect

As indicated in the previous chapter the effect of moisture on creep behavior of SMC-R50 will not be studied, however, in this investigation, creep experiments will be conducted at environments where relative humidity is not completely controlled. Therefore, it is necessary to know to what extent the mechanical properties of SMC-R50 are varied in terms of degree of moisture content. It is also necessary to estimate the amount of moisture content in a SMC-R50 specimen

during its exposure to a certain environmental condition (e.g. relative humidity). As a result, whether or not the mechanical properties of SMC-R50 are changed during exposure to a given environment can be determined.

To study the effect of moisture, twenty specimens from a SMC-R50 panel were divided into 4 groups (5 each). Each group was subjected to a different treatment to either decrease or increase the moisture content in the specimen. The four treatments (Section 4.3) were: 1) post-curing, 2) drying the specimens at 200°F, 3) storing specimens at room temperature (73°F) with 40% relative humidity, and 4) soaking specimens in water at room temperature. The weight of the specimens was measured prior to and after each treatment. Also, during each process except post-curing, the weight of specimens was periodically measured. The gain (or loss) of moisture of a specimen with time was calculated by the percentage of the weight change with respect to its initial weight.

$$\% \text{ Weight Gain} = \frac{\text{Current Weight} - \text{Initial Weight}}{\text{Initial Weight}} (100) \quad (5.1)$$

The plot of weight gain (or loss) of SMC-R50 due to each treatment with respect to the square root of time is shown in Figure 5.1. In this figure, each data

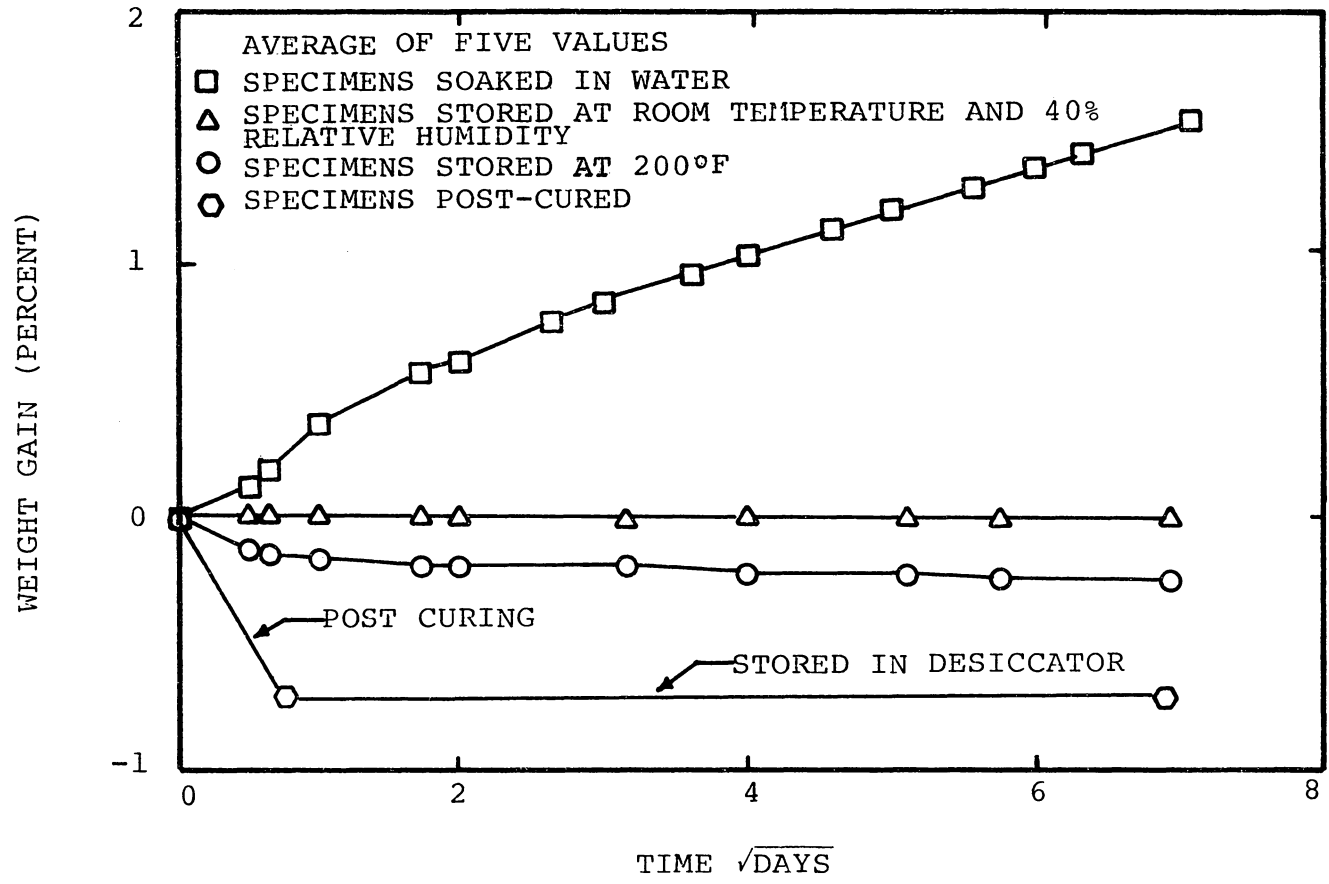


Figure 5.1 Absorption and desorption of moisture for SMC-R50 specimens at various conditions.

point represents an average of five values of moisture content of specimens which were side by side in the same panel. Specimens soaked in water (treatment 4) gained approximately 1.6% by weight of moisture during the test period. Until the termination of the test, specimens were still absorbing moisture at a constant rate. For specimens at room temperature and 40% relative humidity, a fluctuation in weight was observed. However, these specimens can be considered as having no weight gain (or loss) since the weight changes never exceed $\pm 0.003\%$. Approximately 0.25% of weight loss was observed for the specimens stored in the oven for two months at 200°F. The rate of losing moisture content largely decreased after a couple of days. Fluctuation of weight loss also was observed in this group of specimens. For the post-cured specimens, the total of weight loss was 0.75% which is three times that of the dried specimens (stored at 200°F). In addition, after the post-curing cycle the color of the specimens changed from creamy white to slightly brown. It should be noted that the post-cure procedure took only two days. Thereafter, specimens were stored in a desiccator for two months, with no apparent weight change occurring. In general the curves of weight gain (or loss) with respect to time are similar to those reported by Loos et al. [61]. Figure 5.1 represents the rate and the amount of absorbed (or desorbed) moisture with time under extreme dry, dry, wet and extreme wet conditions.

As a result, moisture content of SMC-R50 specimen at a given time and condition can be estimated.

After completion of moisture treatments, the twenty specimens were tested to rupture at a constant cross head rate of 0.05 in/min. Figures 5.2 to 5.5 present the stress-strain curves of SMC-R50 specimens after the four moisture treatments. In general, all the curves resemble the typical stress-strain curve of SMC-R50 [5] which can be represented as an initial straight line, a transition curve and then a straight line up to final failure. For most of the specimens the nonlinear stress strain behavior starts at approximately 5 ksi, except for the specimens which were soaked in water, where the nonlinearity starts at approximately 4 ksi. The last data point in each stress-strain curve represents rupture.

Two types of failure (Figure 5.6) were observed. The first type was a straight separation of two surfaces which is believed to be a pure tensile rupture. The second type of failure showed a combination of tensile and shear rupture. It was observed that lower ultimate strength (or strain) values occurred for the second type of failure. Specimens that ruptured outside the gage section also exhibited lower ultimate strengths. In each group of treated specimens, both types of failure were observed. Figure 5.7 shows a plot of static ultimate strength of SMC-R50 specimens versus

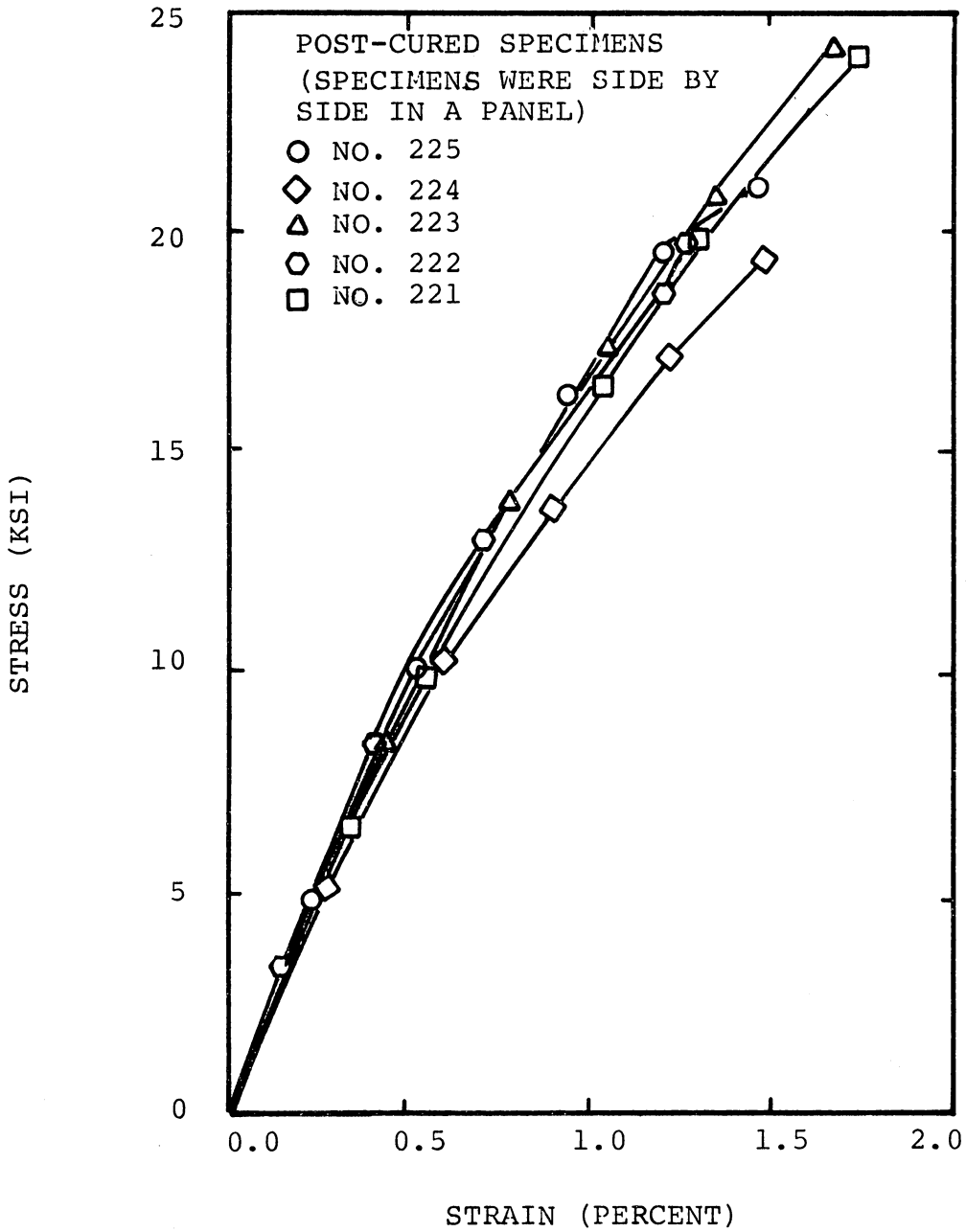


Figure 5.2 Stress-strain curve of the post-cured SMC-R50 specimens.

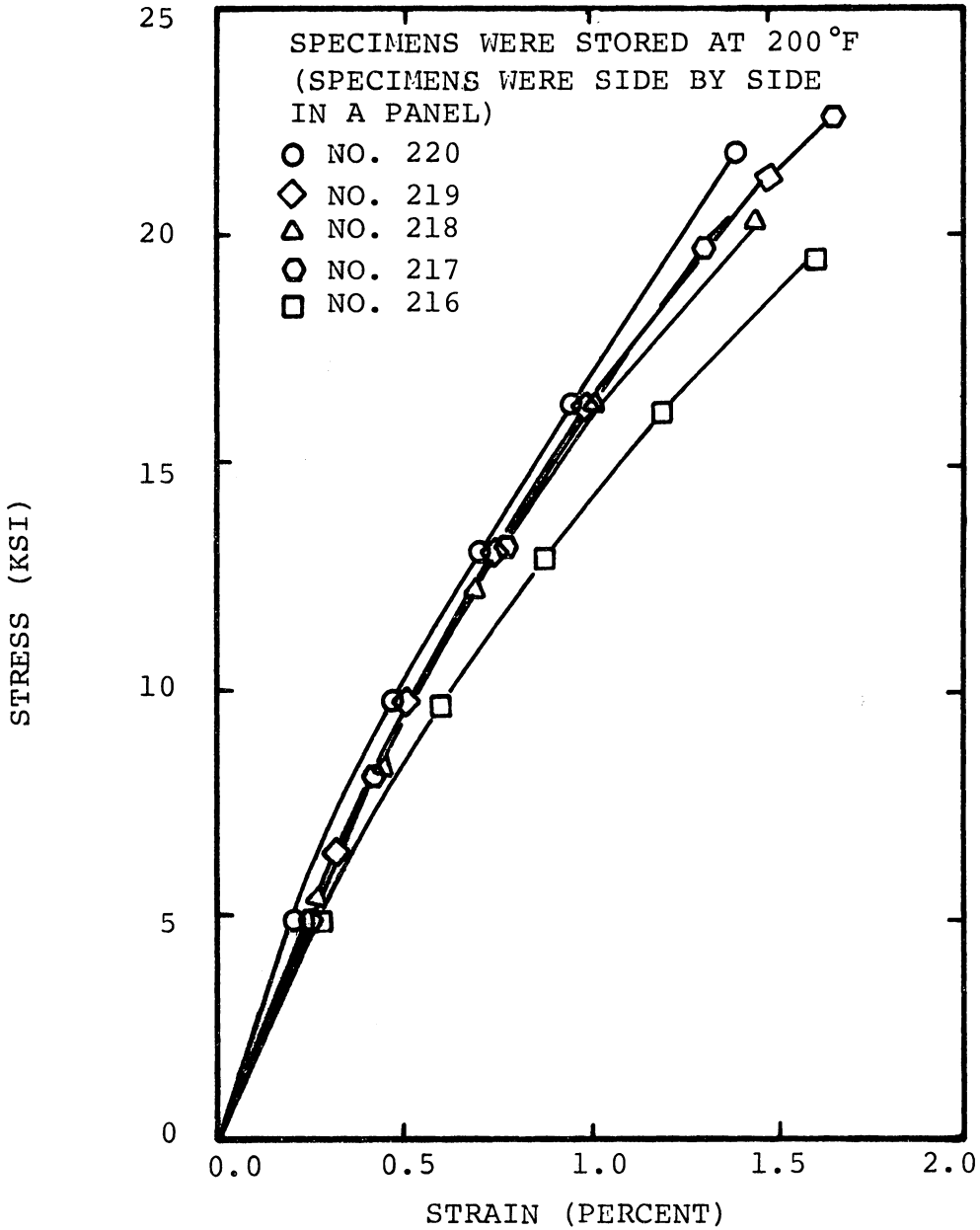


Figure 5.3 Stress-strain curve of the SMC-R50 specimens which were stored at 200°F for two months.

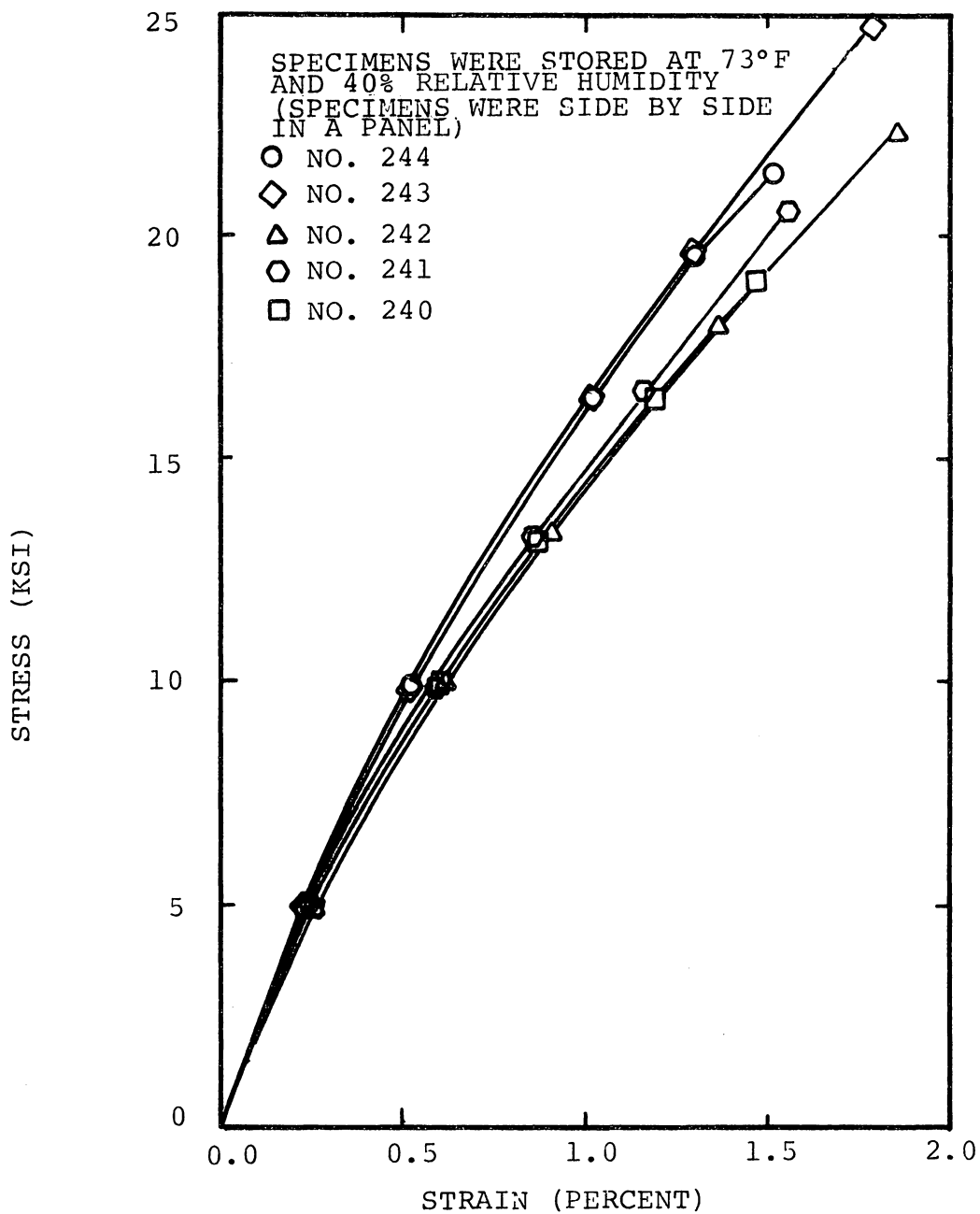


Figure 5.4 Stress-strain curves of the SMC-R50 specimens which were stored at room temperature and 40% relative humidity for two months.

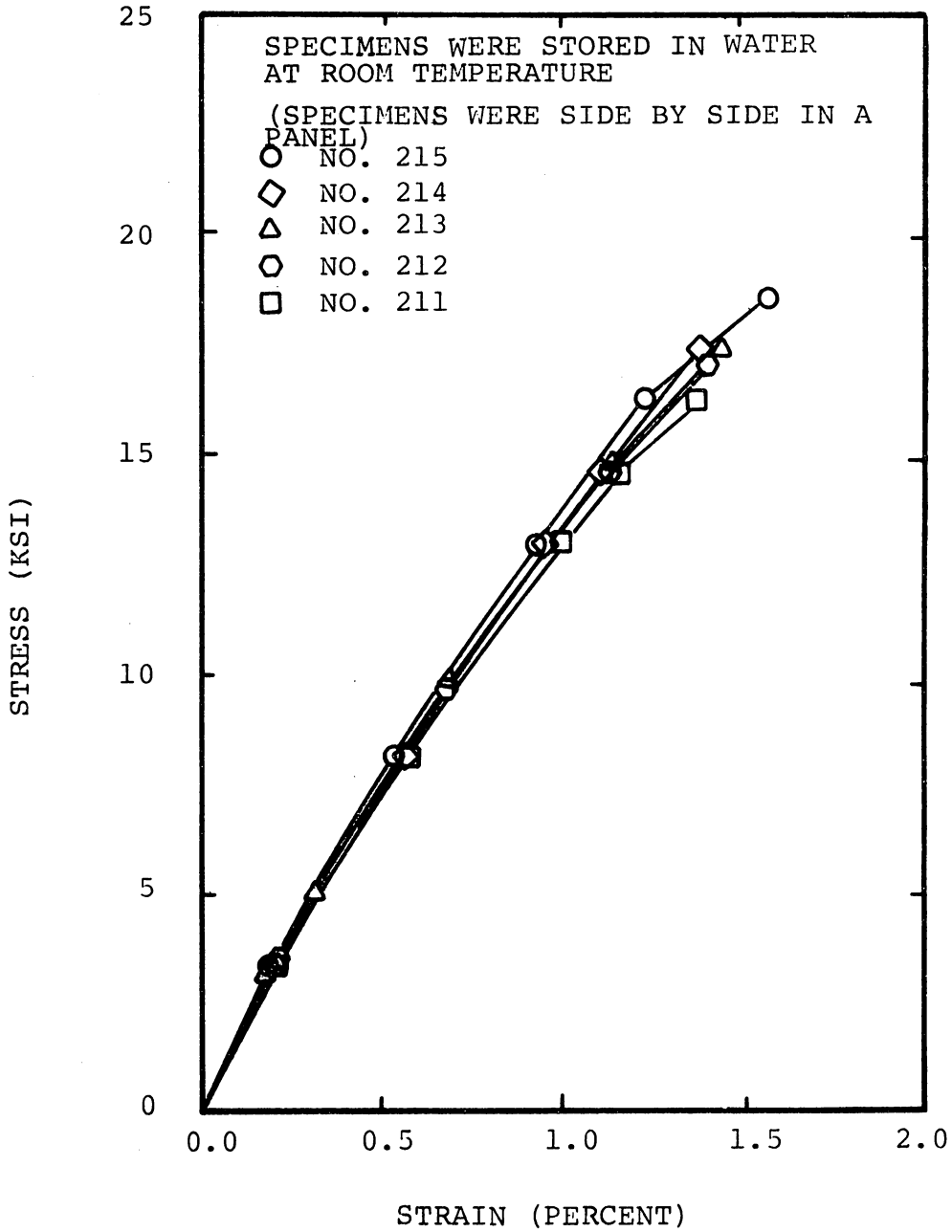


Figure 5.5 Stress-strain curves of the SMC-R50 specimens which were soaked in water at room temperature for two months.

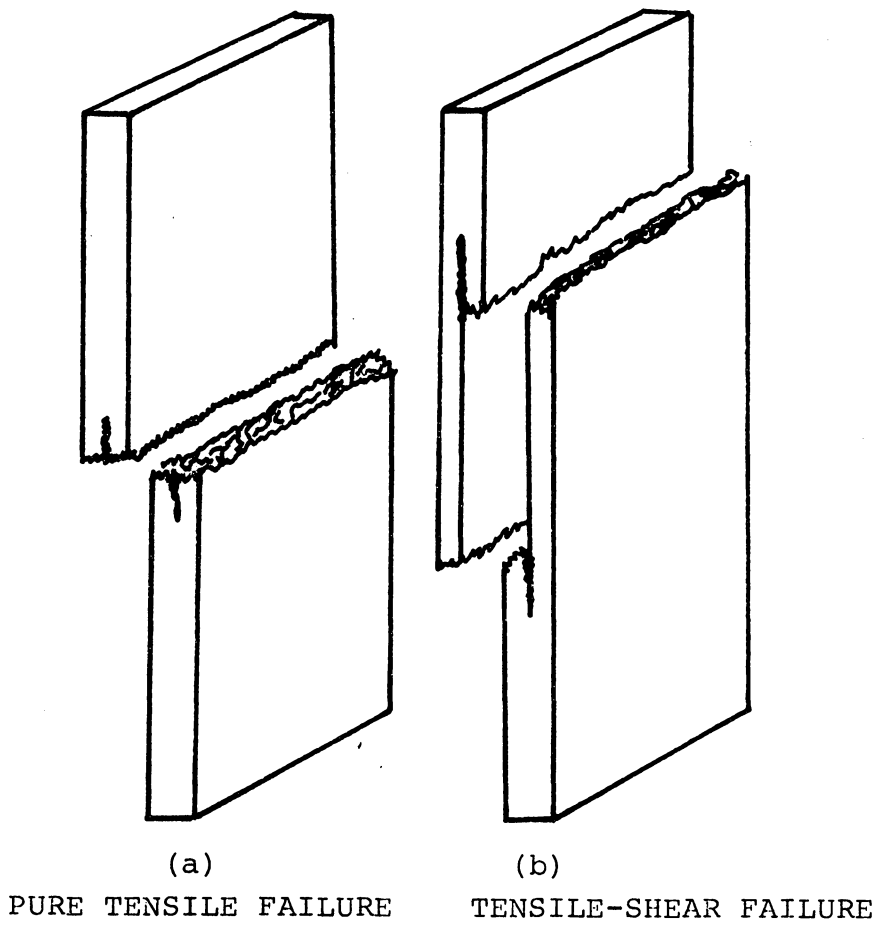


Figure 5.6 Typical types of failure of SMC-R50 specimens.

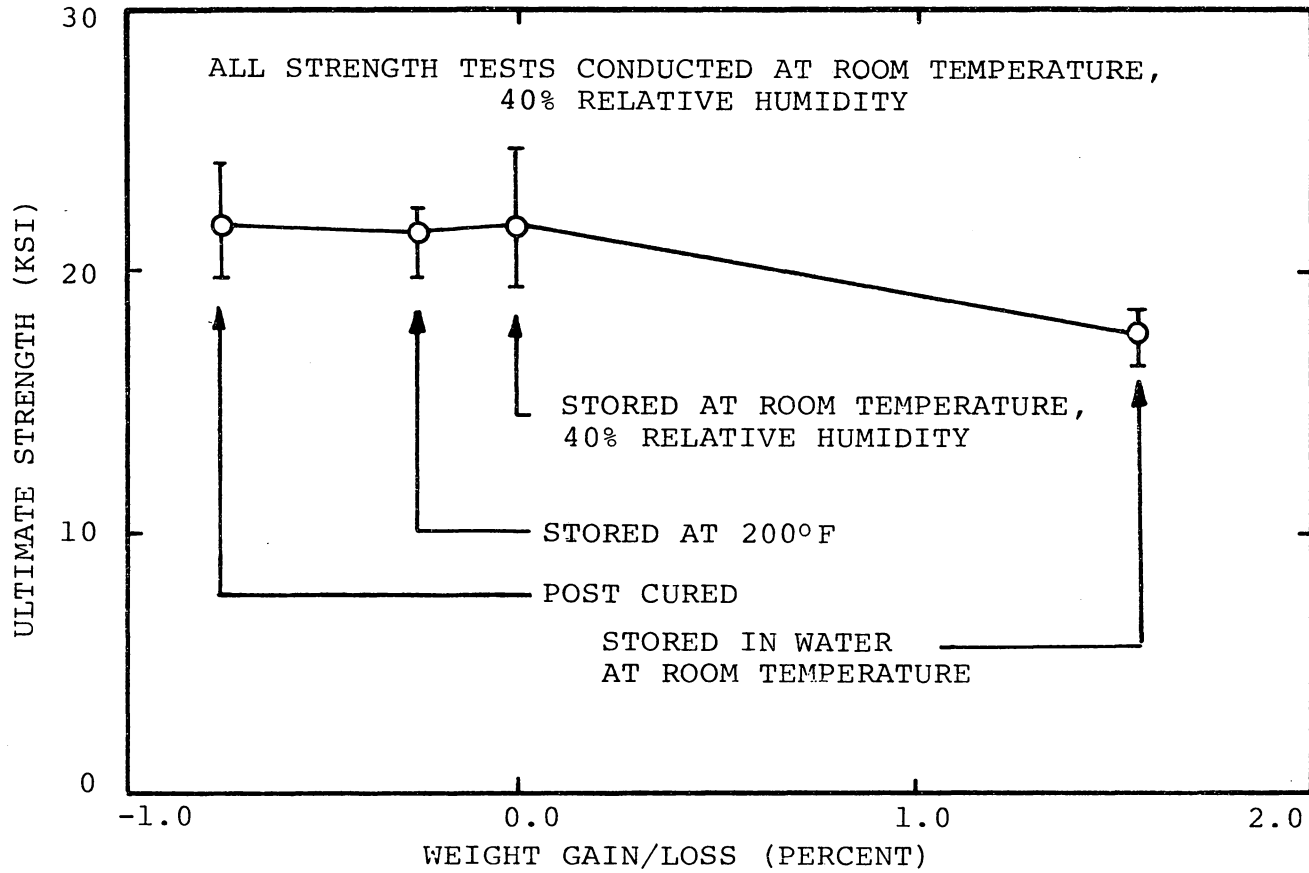


Figure 5.7 The static ultimate strength of SMC-R50 due to different moisture conditioning.

the moisture content due to four types of moisture conditioning. In the figure, there are three values, the maximum, the average (of 5 specimens), and the minimum strength for a given moisture content. Using Figure 5.7 as a guide, it was assumed that the effect of moisture was negligible for elevated temperature tests. However, for the room temperature creep experiment, specimens were isolated in an oven containing desiccant to minimize the effect of moisture.

A plot of static ultimate strain of SMC-R50 versus the moisture content due to the four types of conditioning is shown in Figure 5.8. The ultimate strain of SMC-R50 is nearly independent of the moisture content after the four types of conditioning.

Table 5.1 shows a list of specimens tested along with their ultimate strengths and strains, and the initial elastic modulus.

The static ultimate strength data of SMC-R50 at elevated temperatures were obtained from Denton [5]. Figure 5.9 shows two curves for ultimate strength versus temperature. The upper curve was obtained by Denton. The upper curve was adjusted by a factor which is equal to the ratio of the room temperature strengths obtained by the author and Denton. The lower curve in Figure 5.9 represents the adjusted strength data. The adjusted strength data were used to determine the stress level used in mechanical conditioning at elevated temperatures.

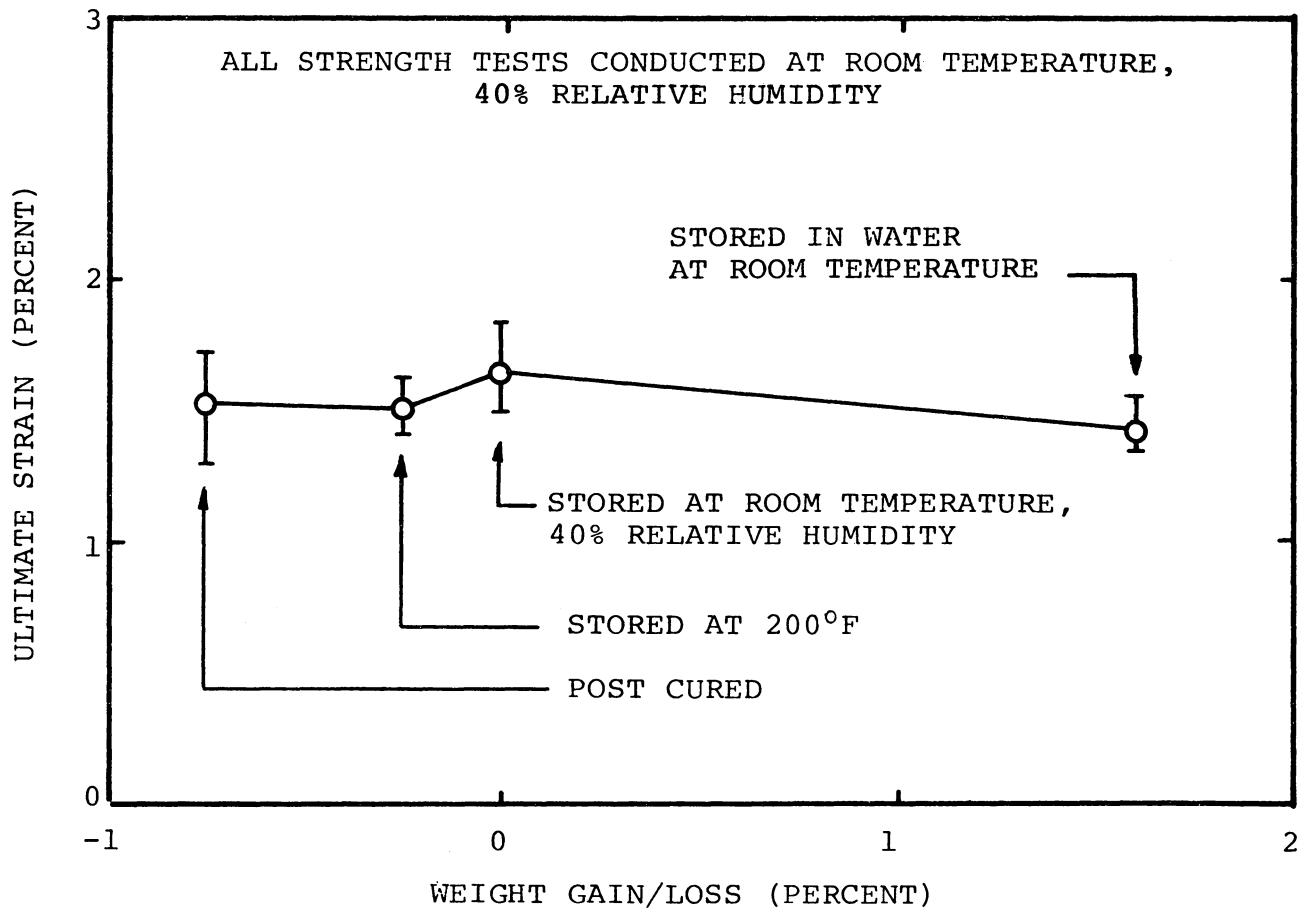


Figure 5.8 The static ultimate strain of SMC-R50 due to different moisture conditioning.

Table 5.1 Mechanical properties of SMC-R50 after different moisture conditioning.

Type of Moisture Conditioning	Specimen No.	Initial Modulus E , 10^6 psi	Ultimate Strength σ_u , 10^3 psi	Ultimate Strain ϵ_u , %
Post-cured	221	2.07	24.0	1.74
	222	2.18	21.1	1.46
	223	2.05	24.2	1.68
	224	2.03	19.5	1.48
	225	2.26	20.0	1.28
	Average	2.12	21.8	1.53
Stored at 200°F	216	1.90	19.5	1.60
	217	1.81	21.9	1.39
	218	2.05	20.3	1.45
	219	2.16	21.3	1.48
	220	2.19	22.6	1.65
	Average	2.02	22.1	1.51
Stored at room temperature, 40% relative humidity	240	2.05	19.1	1.48
	241	1.95	20.6	1.56
	242	1.96	22.3	1.86
	243	2.19	24.8	1.79
	244	2.28	21.5	1.54
Average	2.09	21.7	1.65	
Stored in water at room temperature	211	1.62	16.2	1.37
	212	1.71	18.6	1.57
	213	1.61	17.4	1.44
	214	1.62	17.4	1.38
	215	1.62	17.1	1.40
Average	1.64	17.3	1.43	

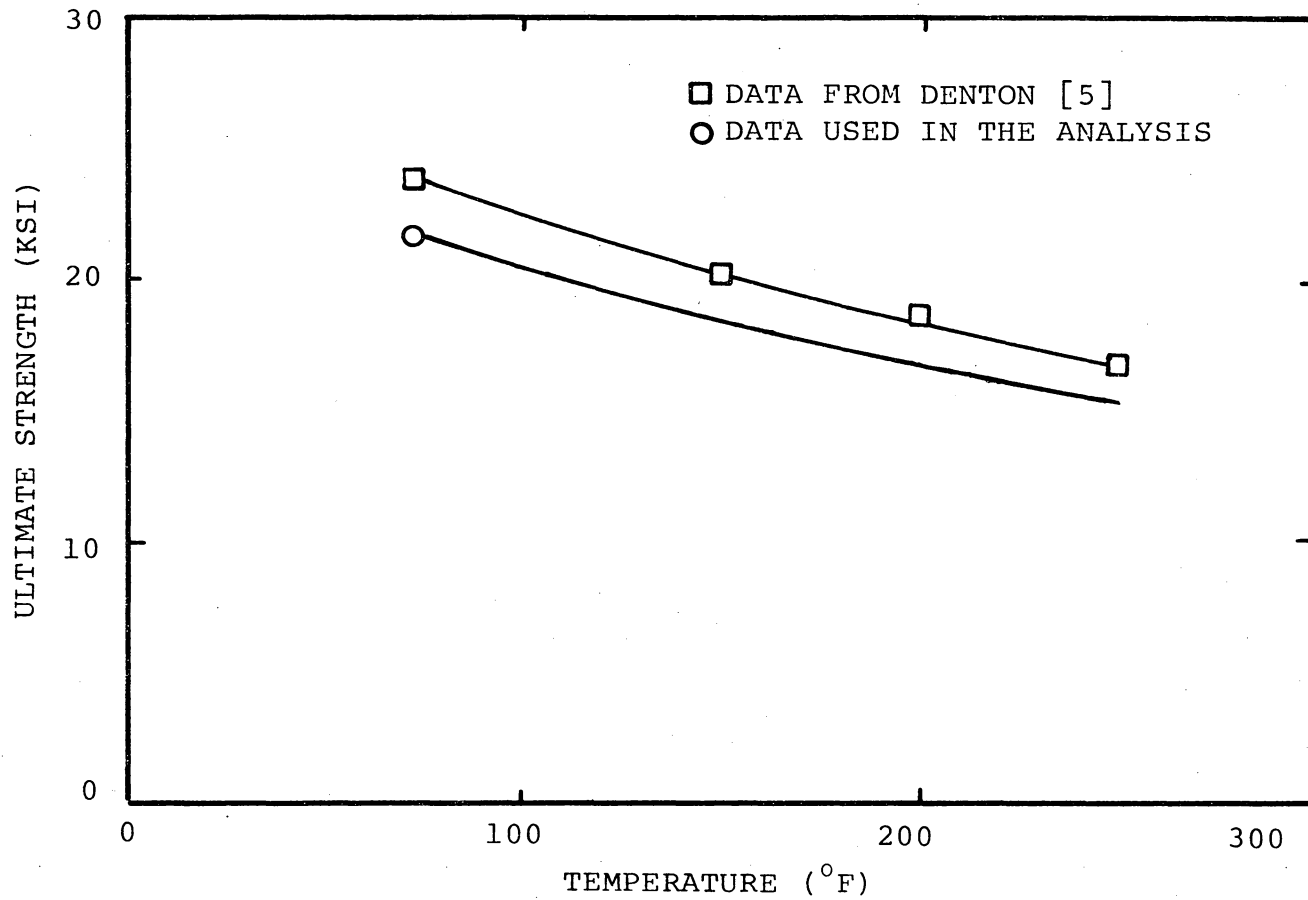


Figure 5.9 The ultimate strength of SMC-R50 at elevated temperatures.

5.2 Effect of Damage on Creep Response

Prior to each creep experiment, an SMC-R50 specimen was subjected to a mechanical conditioning procedure as described in Section 4.5. Usually, it took seven cycles to obtain such a repeatable result from an untested specimen. In the case where the specimen had been tested previously, fewer number of cycles were required to achieve the original conditioned state, and repeatable results were obtained as long as the next stress state was less than that of the mechanical conditioned stress state. For the purpose of comparison between the response of each cycle, the starting creep time for every cycle was plotted at time zero. A typical creep response during a mechanical conditioning process is shown in Figure 5.10. As can be seen, creep results of the seventh cycle are the same as those of the sixth cycle. The creep rates at earlier cycles were observed to be greater than that of the last two cycles (6th and 7th). It was also observed that the instantaneous response increased as the number of conditioning cycles increased but approached a constant value as the specimen was conditioned. It is believed that the increase of the instantaneous creep component of strain may be associated with the growth of instantaneous micro-crack opening upon loading.

During each cycle of the mechanical conditioning, permanent deformation was observed regardless of the

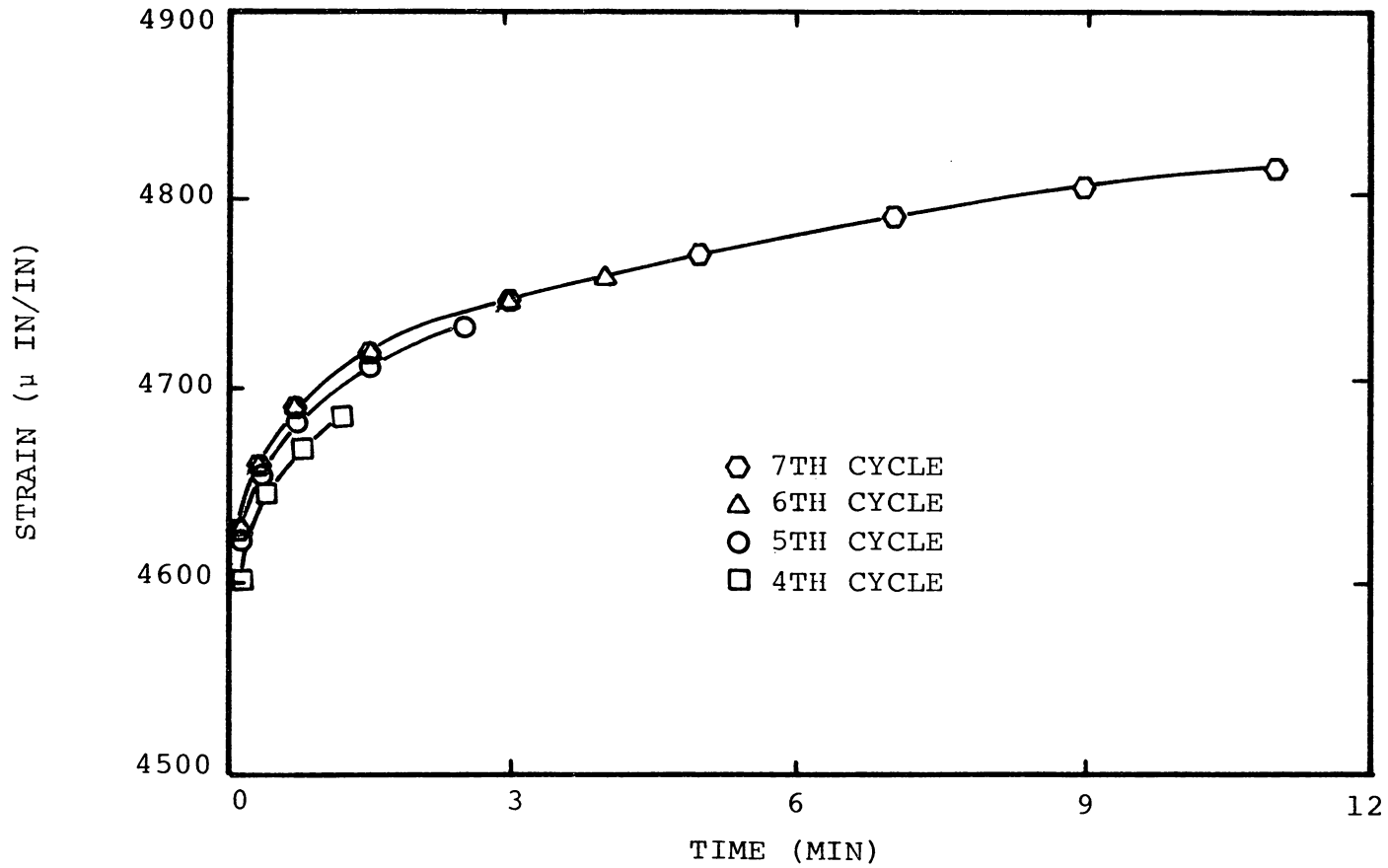


Figure 5.10 Creep response of SMC-R50 specimen during mechanical conditioning.

recovery time (at least up to 8 hours). The permanent deformation was recorded and subtracted electronically upon the end of recovery of each conditioning cycle. It was found that the amount of irrecoverable strain was the greatest for the first cycle. Additional amounts of irrecoverable strain were largely reduced to zero during the subsequent cycles. Figure 5.11 shows the accumulated irrecoverable strain versus the duration of the creep time of each cycle.

To further check the validity of the mechanical conditioning procedures, creep tests (at the same stress level) were conducted on a specimen that had been conditioned at different stress levels. Figure 5.12 shows three experimental creep curves for the same stress level except that prior to each test a different stress level was used to perform the mechanical conditioning. As can be seen, these curves apparently exhibit different creep responses. It was also found that temperature introduced a similar effect on the SMC-R50 specimens. Figures 5.13 to 5.15 show the creep curves due to various stress levels and the same mechanical conditioning stress, but the temperature levels under which the conditioning procedure was performed were different. Again, different creep responses were observed. These results were thought to be due to the different ratio of the same mechanical conditioning stress to the different ultimate strengths at elevated temperatures. In fact, when a fixed ratio of mechanical conditioning stress to ultimate

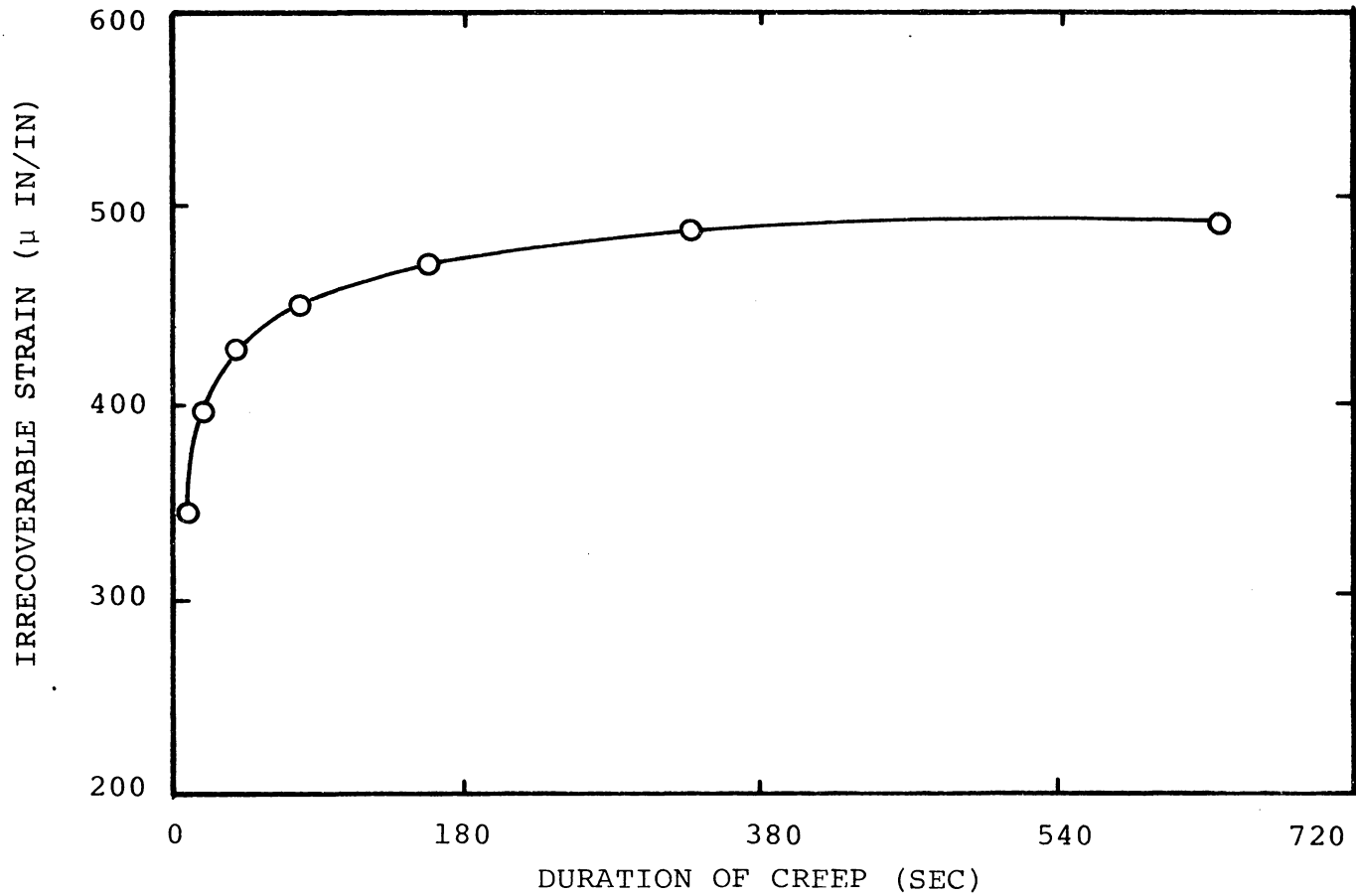


Figure 5.11 Accumulated permanent deformation of SMC-R50 during the mechanical conditioning.

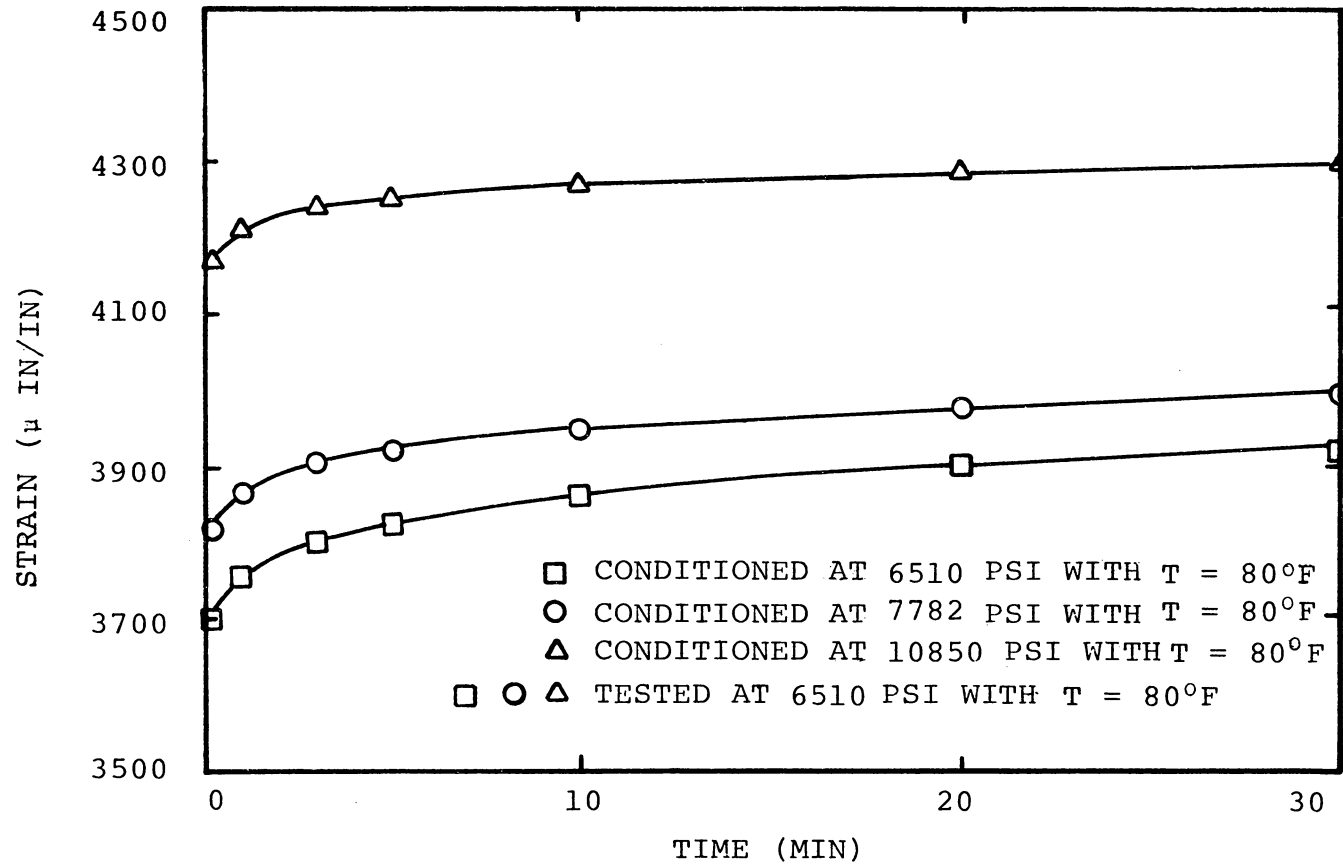


Figure 5.12 Creep response of SMC-R50 for the same test conditions but different mechanical conditioning.

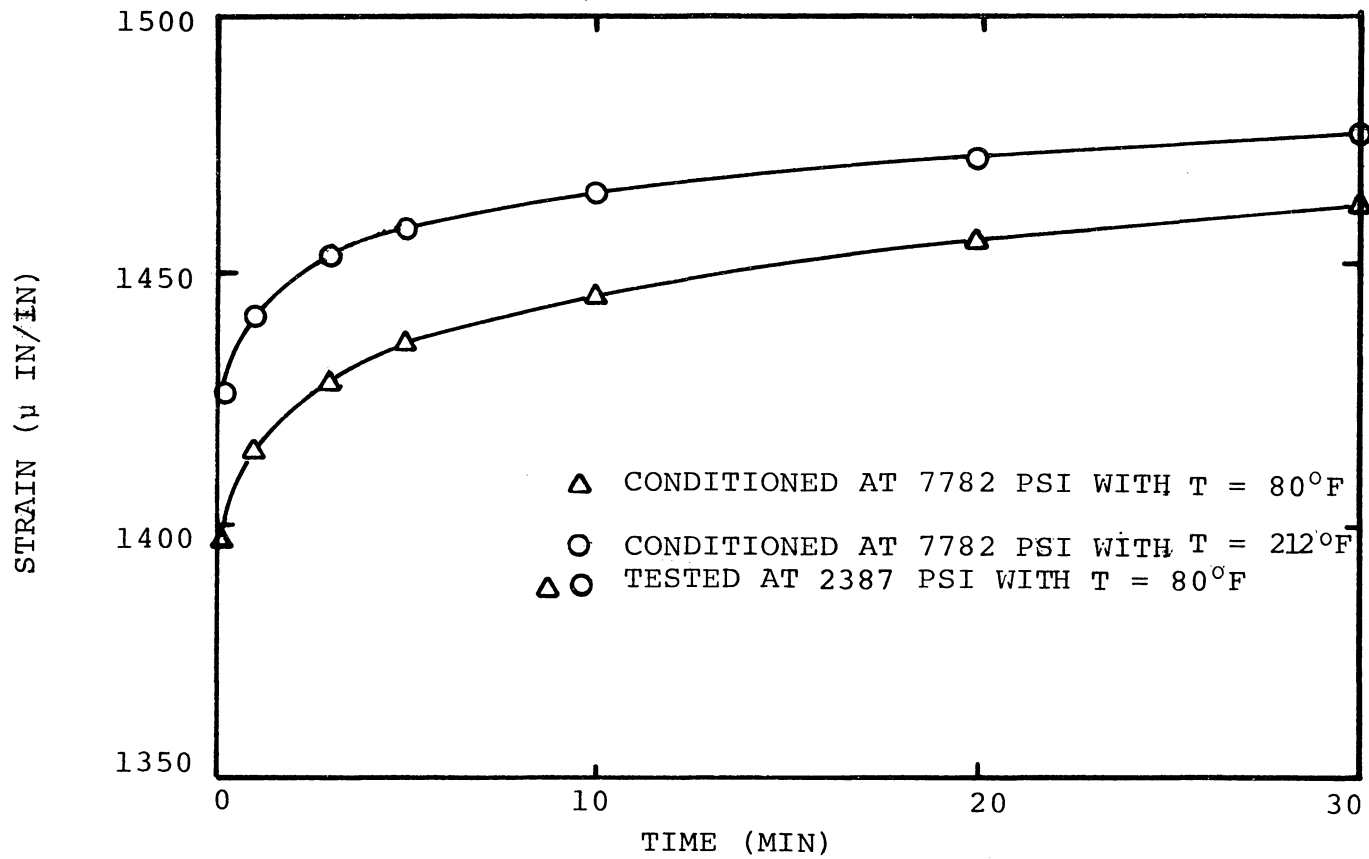


Figure 5.13 Creep response of SMC-R50 conditioned at different temperatures.

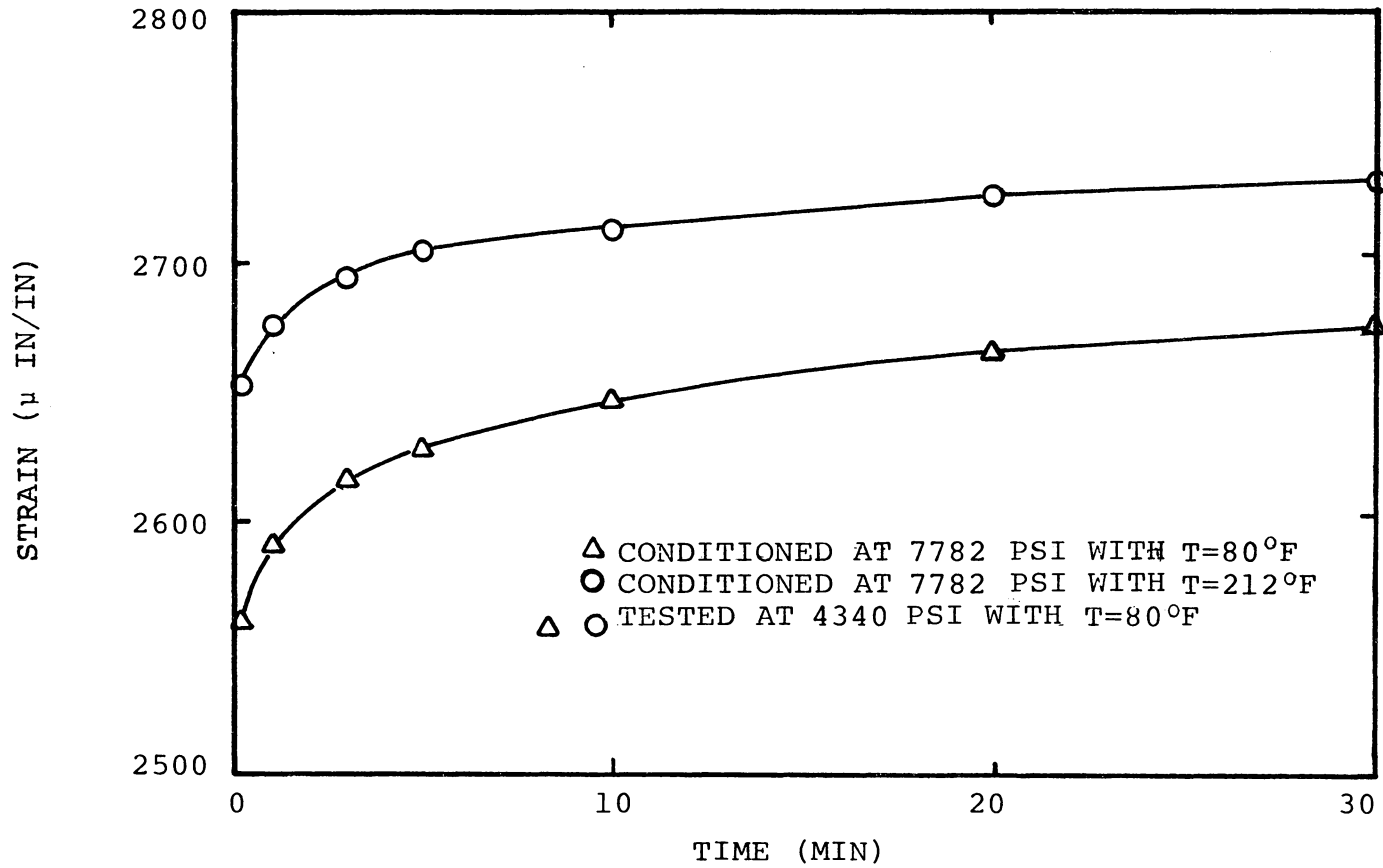


Figure 5.14 Creep response of SMC-R50 conditioned at different temperatures.

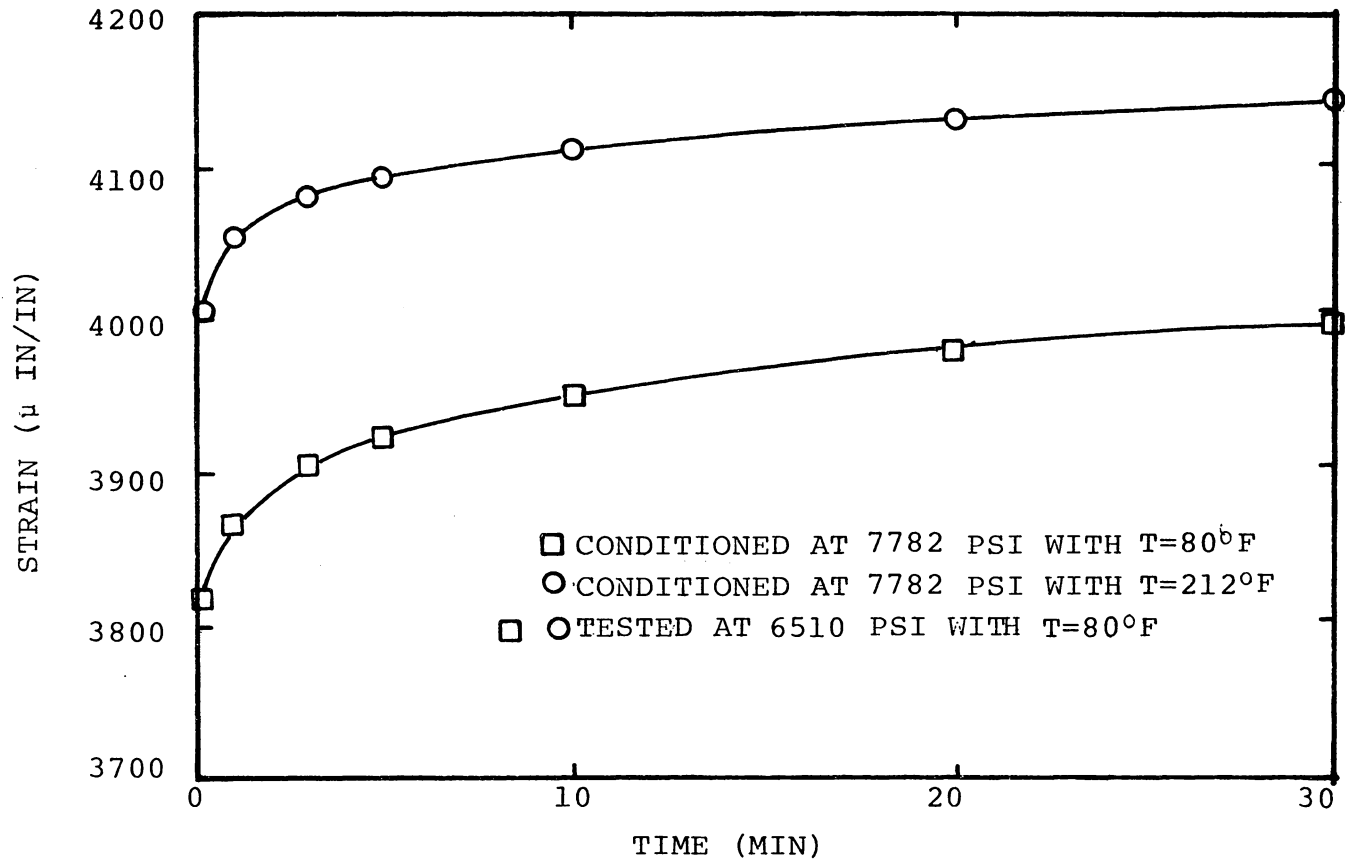


Figure 5.15 Creep response of SMC-R50 conditioned at different temperatures.

strength was used, repeatable results were obtained (these will be shown later in this section).

The development of micro-cracks in the matrix of the SMC-R50 specimen may be induced by stress and may be responsible for the changes of material response. To illustrate, edge replicas were obtained for the same specimen under different levels of creep stress (zero load, 7,782 psi, and 18,500 psi) at room temperature. The specimen was conditioned at the same stress level used for the creep test. Figures 5.16 to 5.18 represent the edge replicas obtained immediately after the application of the creep loadings. These replicas showed an increasing damage state as the creep stress increased. Most of the damage was micro-cracking which was transverse to the loading axis and occurred in the matrix region. The existence of such microcracks might affect the long time creep response, since microcracks may expand during the time of loading. A creep test (4,195 minutes in duration) was conducted at 85% of the room temperature ultimate strength of 21,700 psi. Edge replicas were obtained at different instances of time during creep. These edge replicas are shown in Figures 5.19 to 5.24. It was found that no new microcracks were initiated and no apparent change in the transverse microcracks occurred as time progressed.

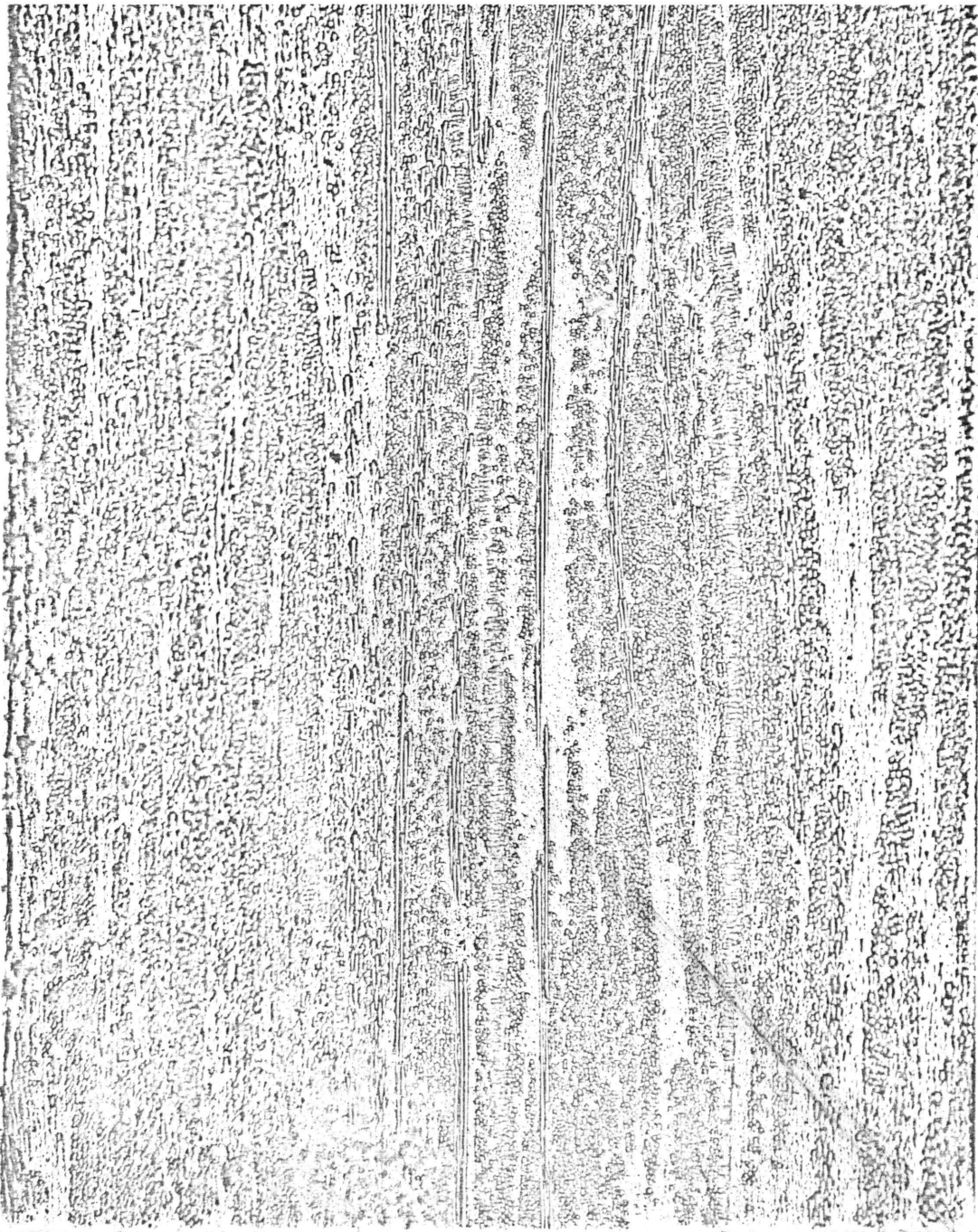


Figure 5.16 Edge replica of SMC-R50 at zero load.

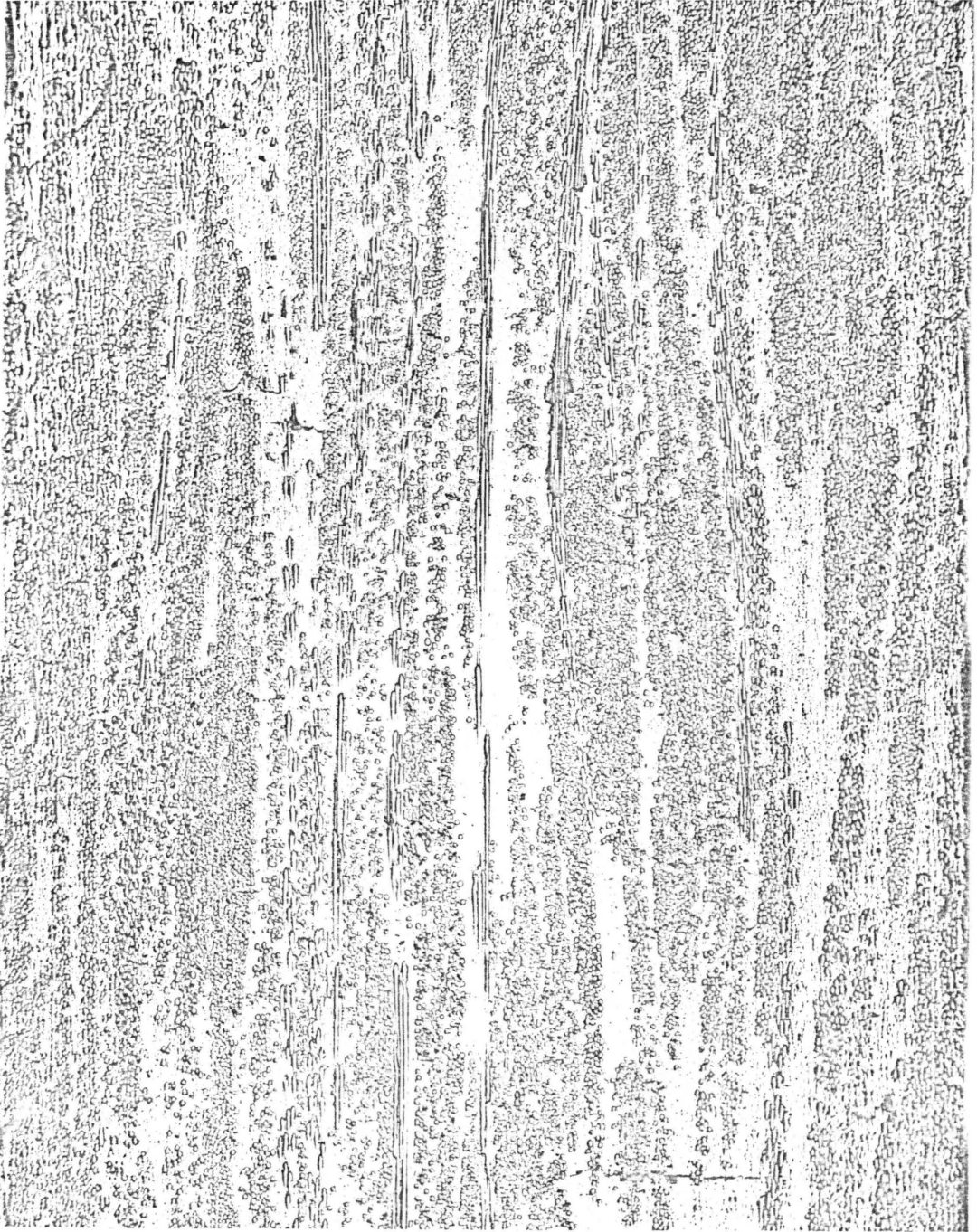


Figure 5.17 Edge replica of SMC-R50 at 7,782 psi (obtained immediately after load application).

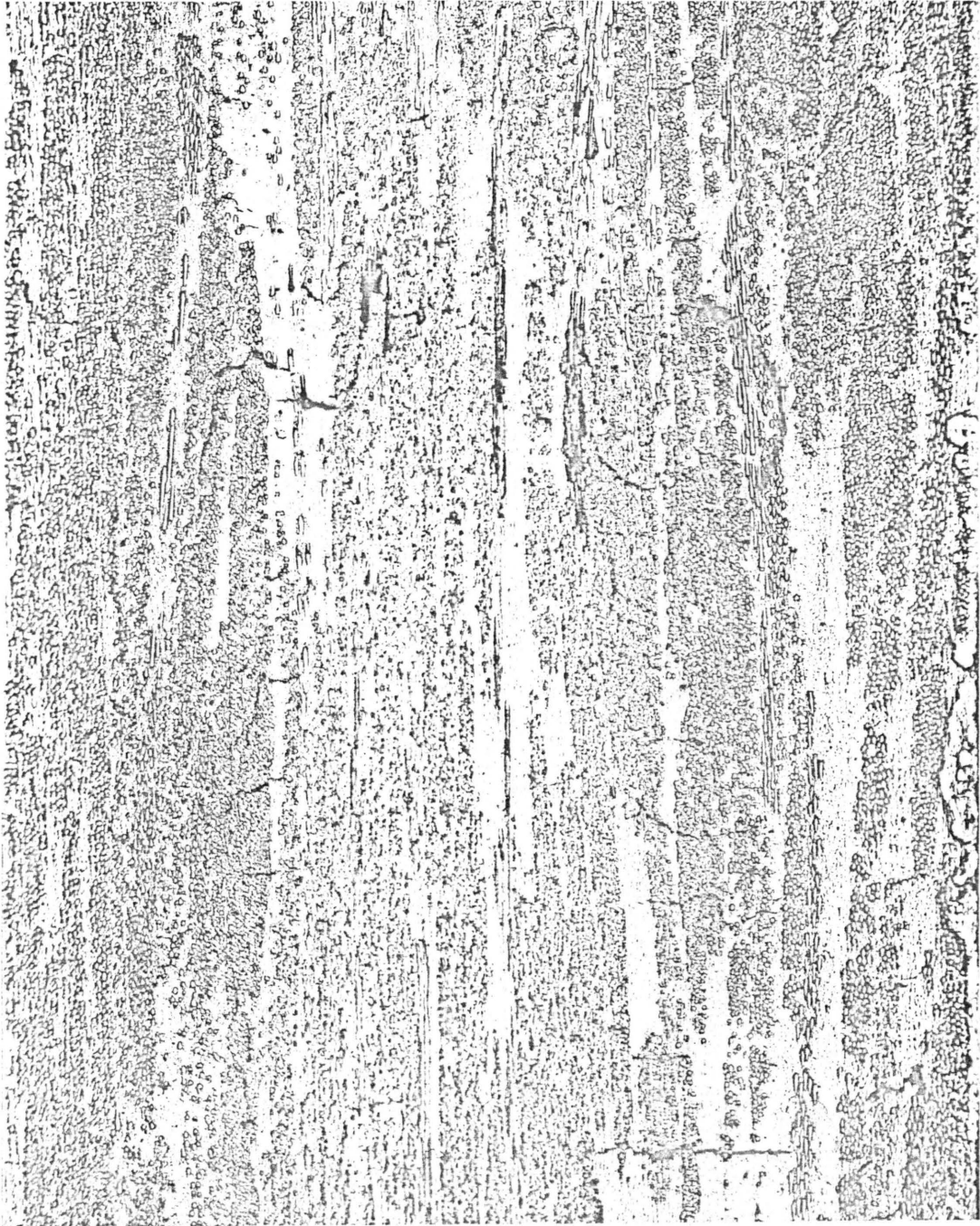


Figure 5.18 Edge replica of SMC-R50 at 18,500 psi (obtained immediately after load application).

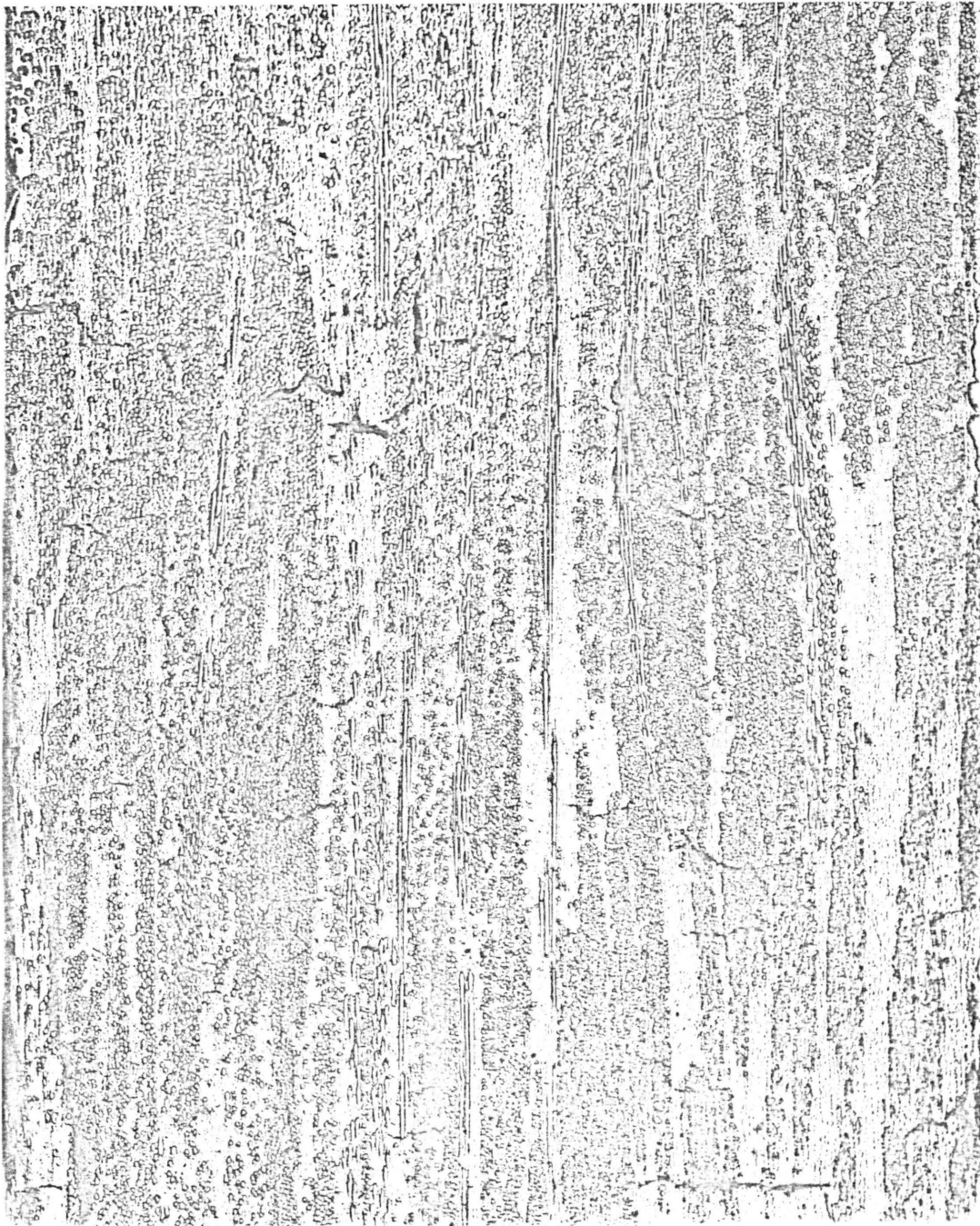


Figure 5.19 Edge replica of SMC-R50 at creep time = 465 min. and creep stress = 18,500 psi.

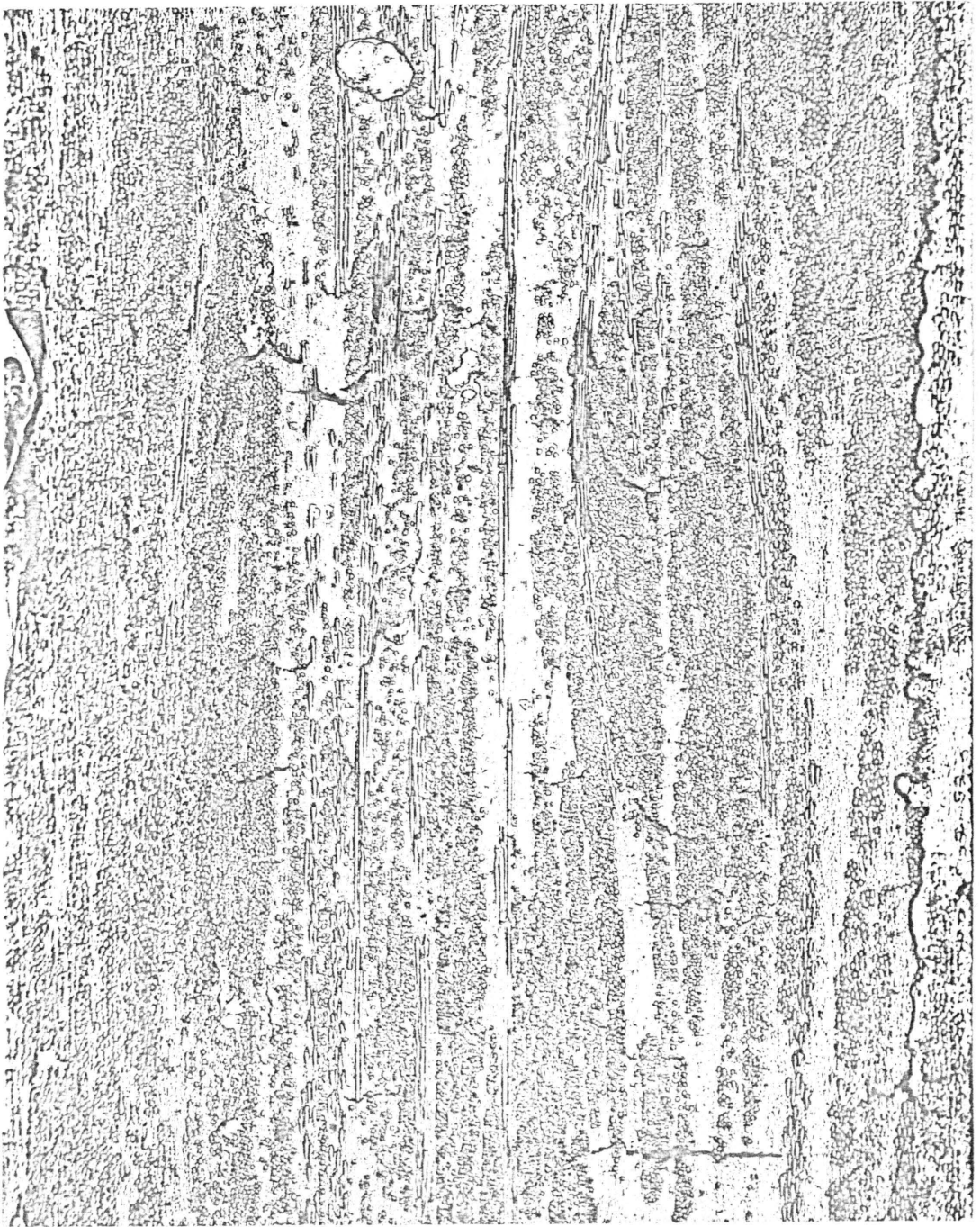


Figure 5.20 Edge replica of SMC-R50 at creep time = 700 min. and creep stress = 18,500 psi.

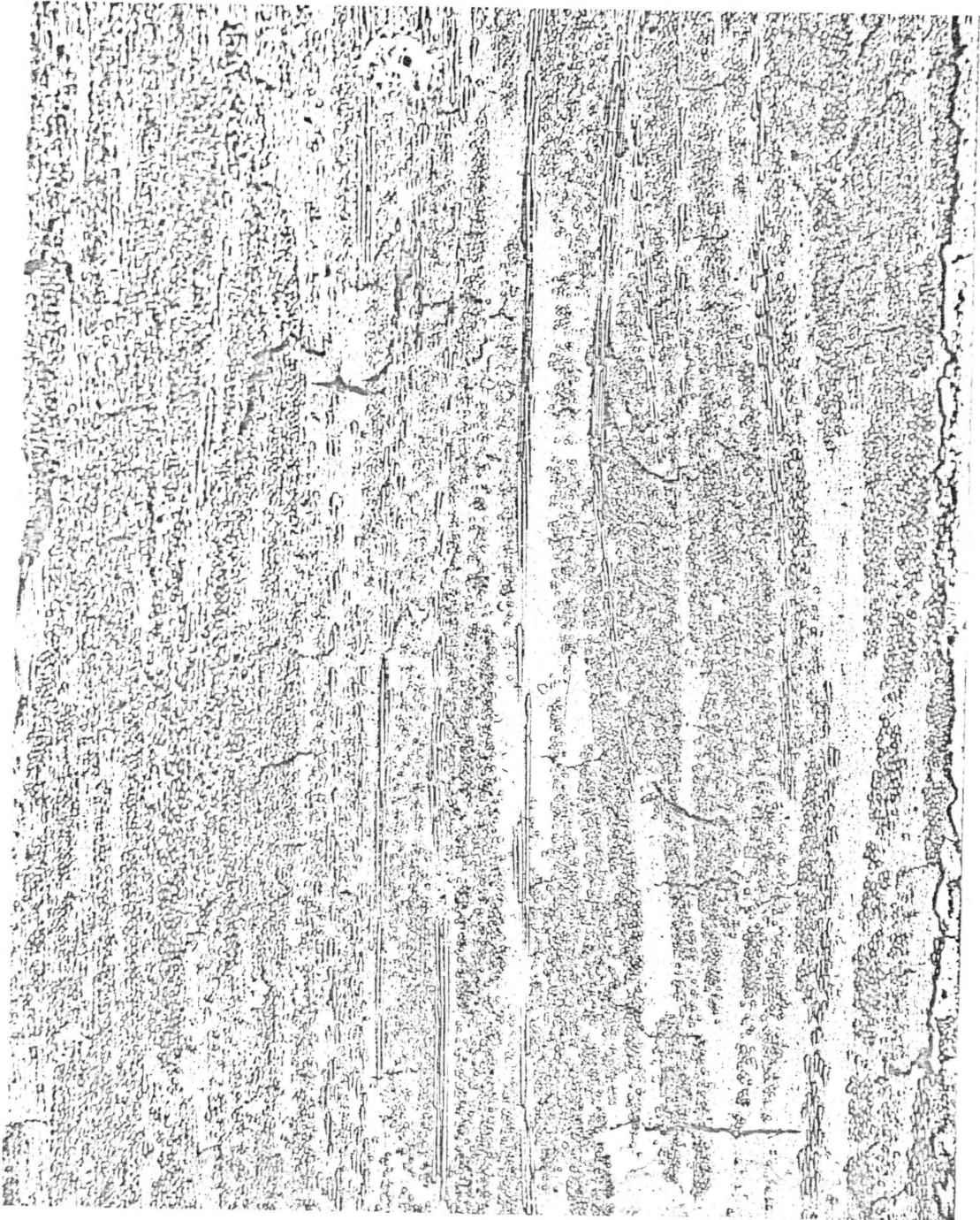


Figure 5.21 Edge replica of SMC-R50 at creep time = 1,300 min. and creep stress = 18,500 psi.

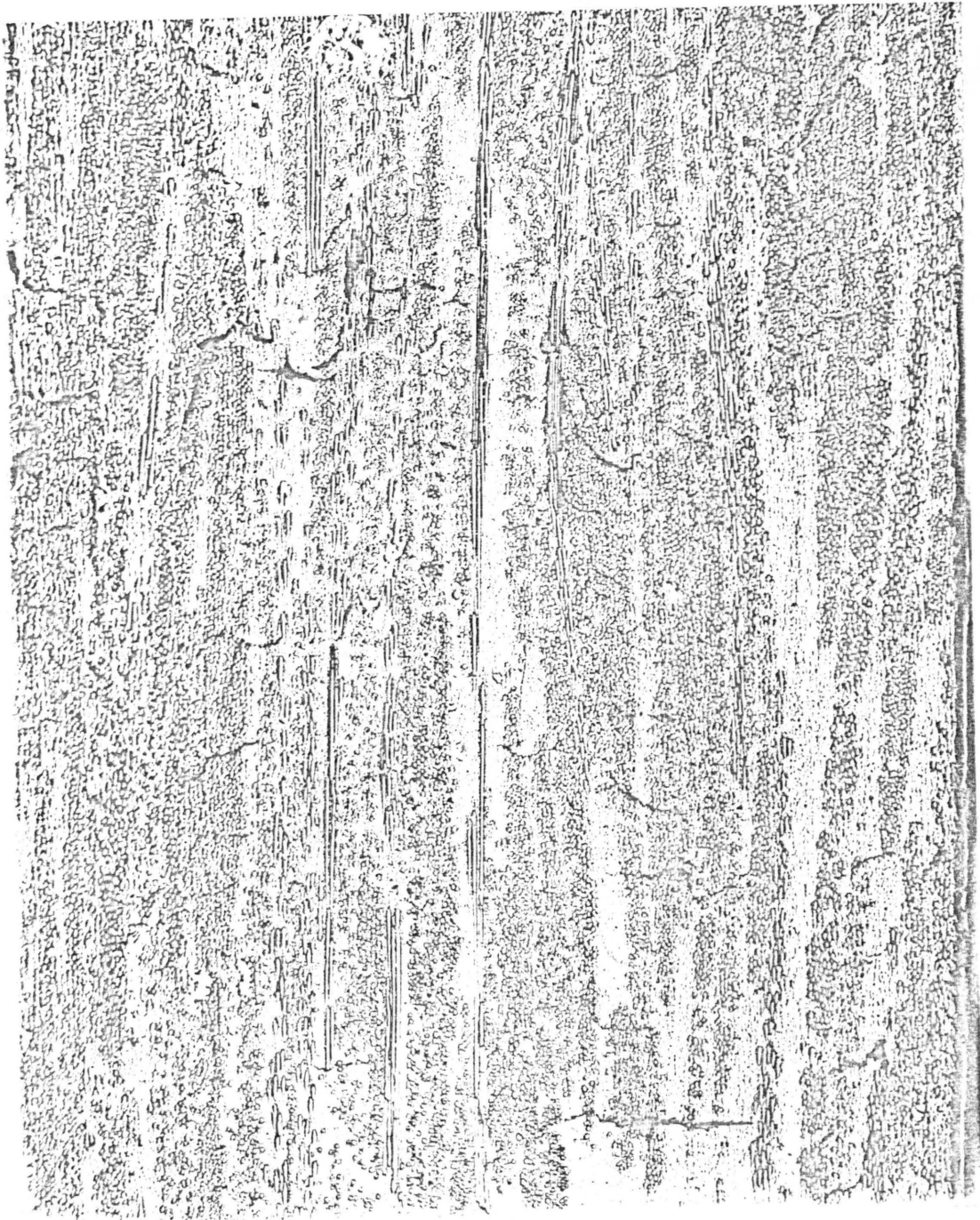


Figure 5.22 Edge replica of SMC-R50 at creep time
= 1,640 min. and creep stress = 18,500 psi.

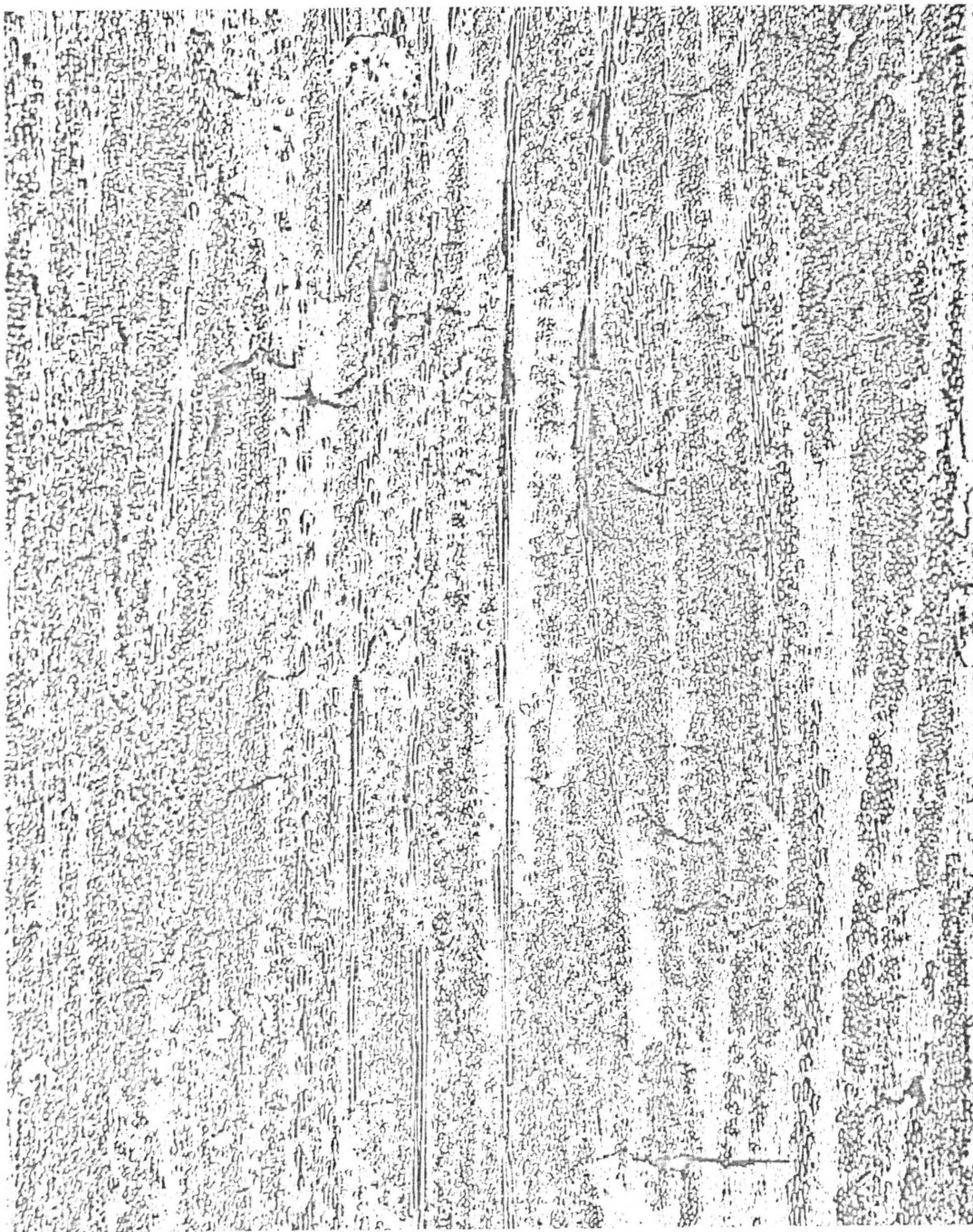


Figure 5.23 Edge replica of SMC-R50 at creep time
= 2,000 min. and creep stress = 18,500 psi.

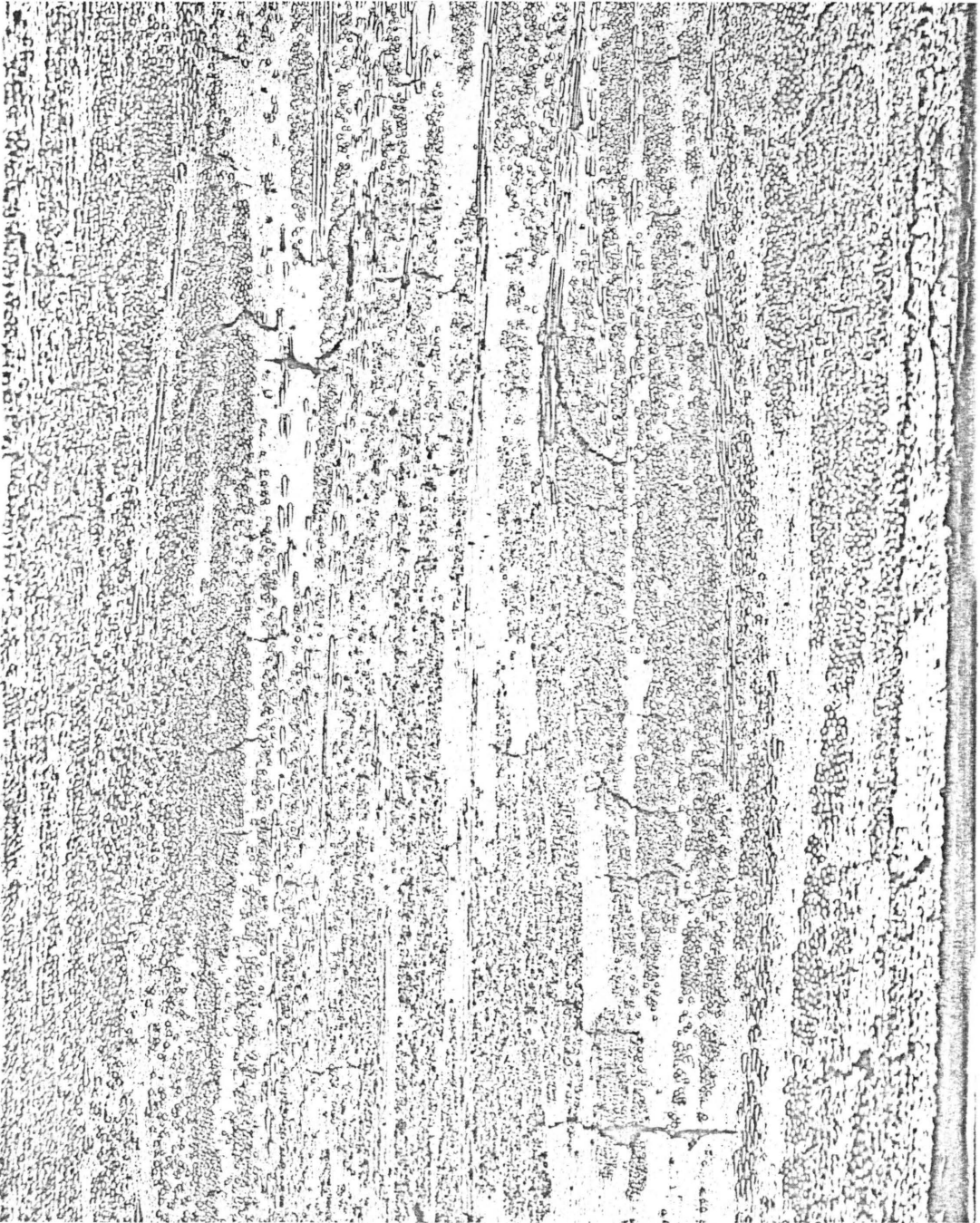


Figure 5.24 Edge replica of SMC-R50 at creep time = 4,195 min. and creep stress = 18,500 psi.

That the microcracks do not affect the long time response is further supported by the creep results shown in Figure 5.25. In this figure, three creep experiments are presented; the test conditions for each experiment are the same, 6510 psi at room temperature. These three creep curves are practically the same, the maximum difference being approximately $20 \mu\epsilon$. The first test was conducted at room temperature on a specimen that had been conditioned at 10,850 psi (50% of the ultimate strength at room temperature). Before conducting the room temperature test again, the specimen was allowed to recover and was tested at 104°F for about one month and then brought back to room temperature. A similar sequence was used except that a specimen was tested over approximately a two month interval (one month each at both 158°F and 212°F). In order to insure that the conditioned state of the specimen would not be altered after the initial mechanical conditioning, different stress levels were used to condition the specimen at the elevated temperature testings. These stress levels were selected so that they were 50% of the ultimate strength at that temperature. Thus, the creep response is affected by the degree of damage, and the damage is associated with the stress level. Repeatable results can be obtained as long as the damage state is not changed. The current damage state is defined as the previous highest ratio of applied

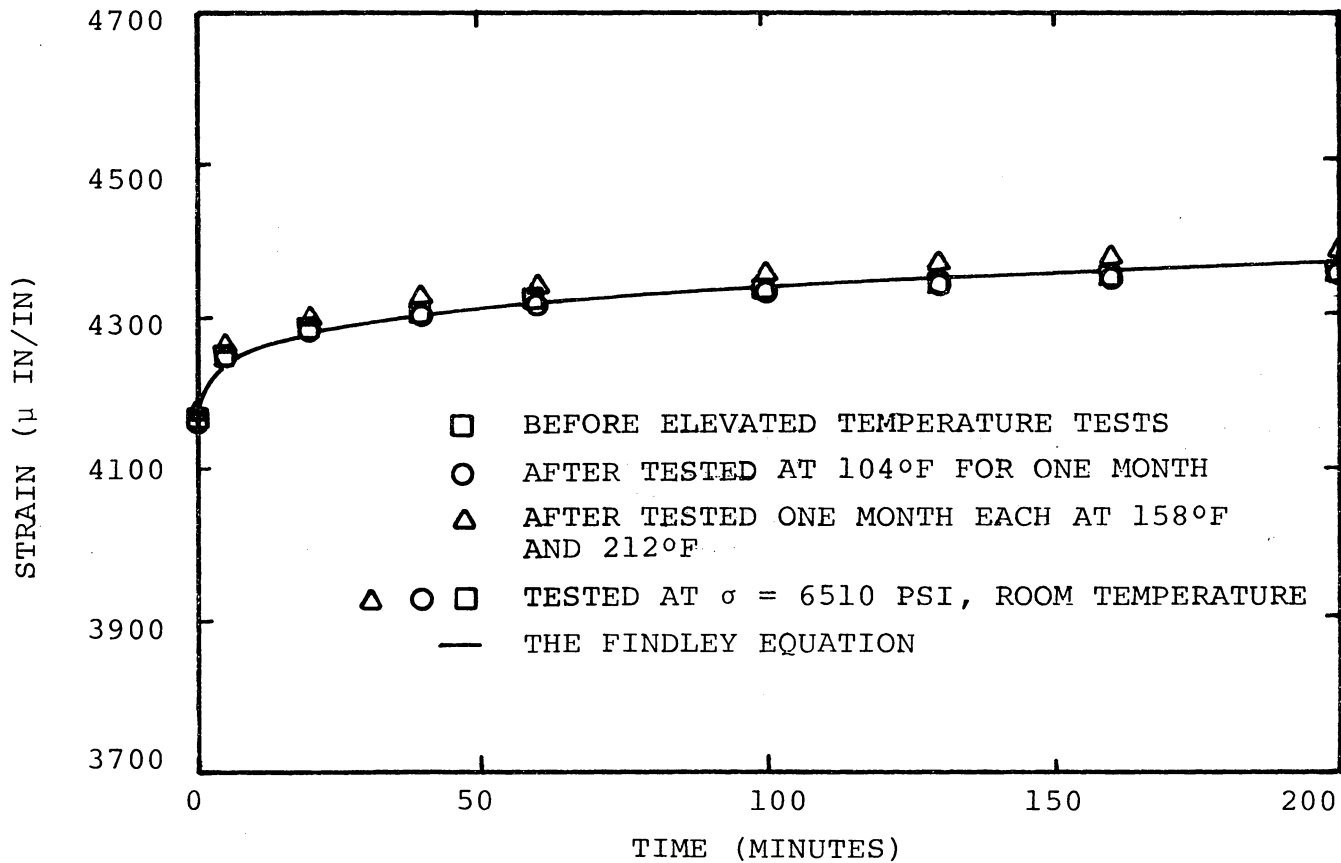


Figure 5.25 Creep response of SMC-R50 obtained from different previous loading history, ($\sigma = 6,510$ psi, room temperature).

stress (including that of mechanical conditioning) to the static ultimate strength at a given temperature.

Creep response due to different damage situations can also be examined by the initial and transient components of the Findley equation. For the same testing conditions, as the damage increases the initial creep response (ϵ_0) increases while the transient creep response decreases. Because more microcracks are present, the increase in the initial creep response due to higher damage is quite obvious. On the other hand, due to the presence of the microcracks the cross-section area of the specimen has decreased. It is natural to believe that for the same applied load the transient component should be larger for greater damage because the same amount of loading is now carried by a smaller cross-sectional area. This contradicts what has been observed and might be associated with change of fiber angle toward the loading axis. As the specimen elongates in the axial direction and contracts in the transverse direction due to the Poisson's effect, fibers tend to align in the loading direction. Due to the increase of transverse microcracks, the fibers carry a larger portion of the loading and the fiber angles become smaller. Thus, the transient creep component becomes smaller. Although the phenomenon mentioned above is a hypothesis, it seems to be capable of explaining the physical observation. Axial and transverse

creep strain were measured to calculate the Poisson's ratio in creep. It was found that during a creep test the Poisson's ratio stayed constant. The Poisson's ratio was also found to decrease as the damage level increased (Figure 5.26). This observation supports the hypothesis mentioned above, since it indicates a decrease of the load transferring mechanism from the axial to the transverse direction as the damage level increased.

A series of creep tests (Table 5.2) were conducted to study the effects of the damaged state, the results of which were used to calculate the parameters in the Findley equation. These tests were divided into five groups according to the different damage states (mechanical conditioning). In each group the maximum applied stress did not exceed the stress level used for the mechanical conditioning procedure. It was found that the asymptotic value of the time exponent n decreased almost linearly as the stress level used for the mechanical conditioning procedure increased (Figure 5.27). Approximately a 14 percent decrease of n -value was obtained for the creep response of a specimen conditioned at 10,850 psi as opposed to that at 2,387 psi. Using these n -values, the parameters ϵ_0 and m as functions of applied stress and the mechanical conditioning stress were calculated and are presented in Figures 5.28 and 5.29. For the creep response under the same mechanical conditioning the parameters ϵ_0 and

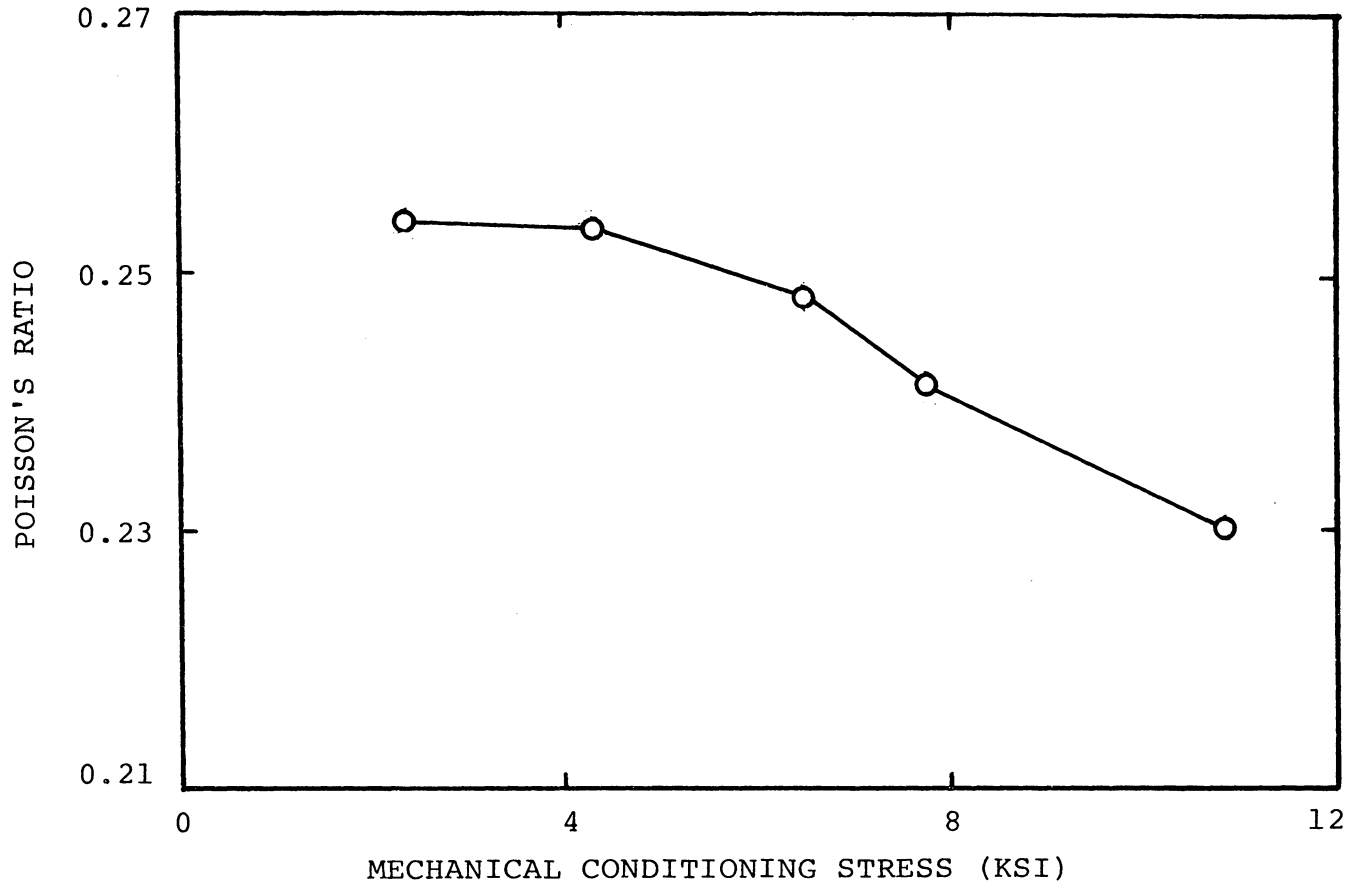


Figure 5.26 The relation between the Poisson's ratio in creep and the mechanical conditioning stress.

Table 5.2 Creep test program for
the damage study.

Applied stress, psi	Conditioning stress, psi				
	2387	4340	6510	7782	10850
2387	(1) *	(2)	(4)	(7)	(11)
4340		(3)	(5)	(8)	(12)
6510			(6)	(9)	(13)
7782				(10)	(14)

* (X) - indicates testing sequence

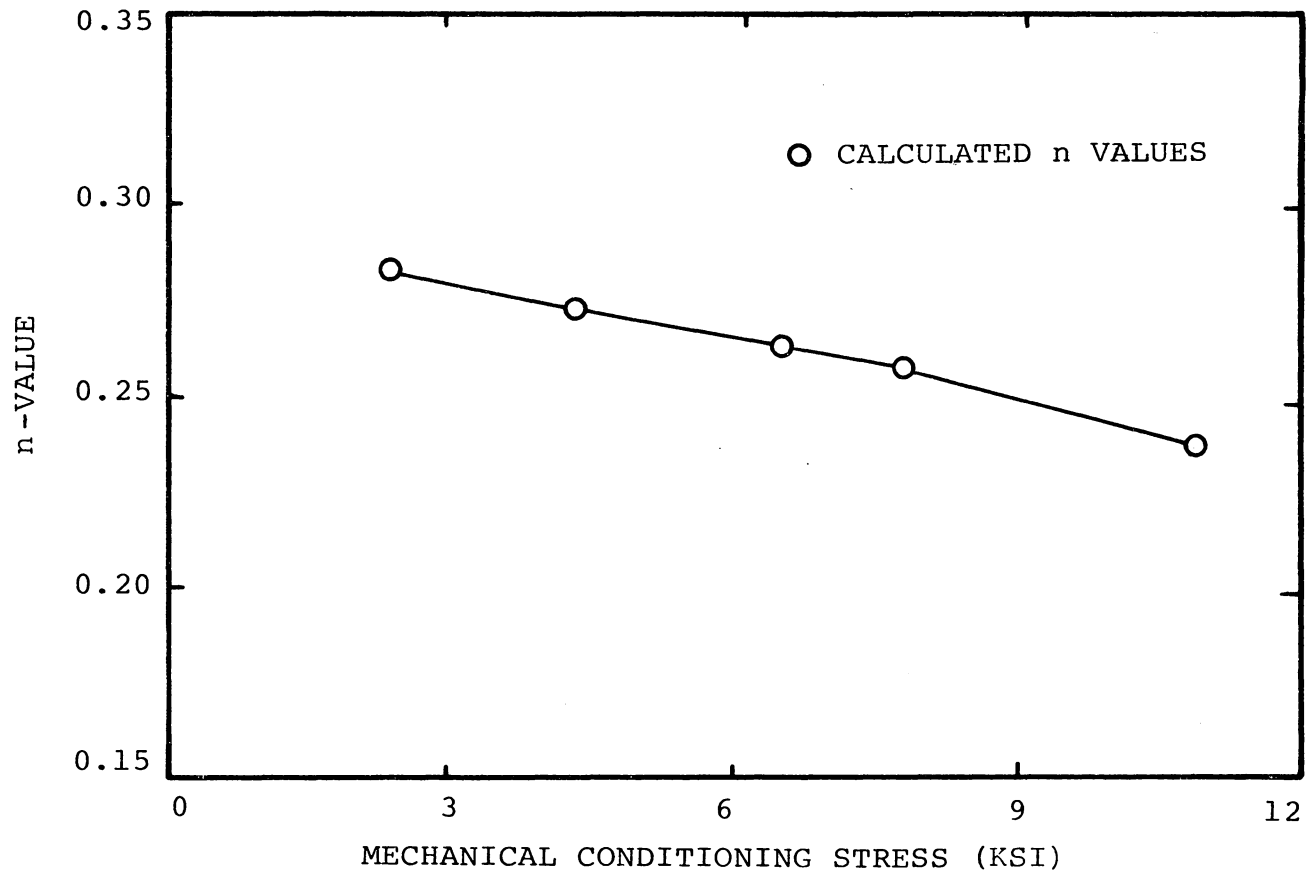


Figure 5.27 The relation between the time exponent n and the mechanical conditioning stress.

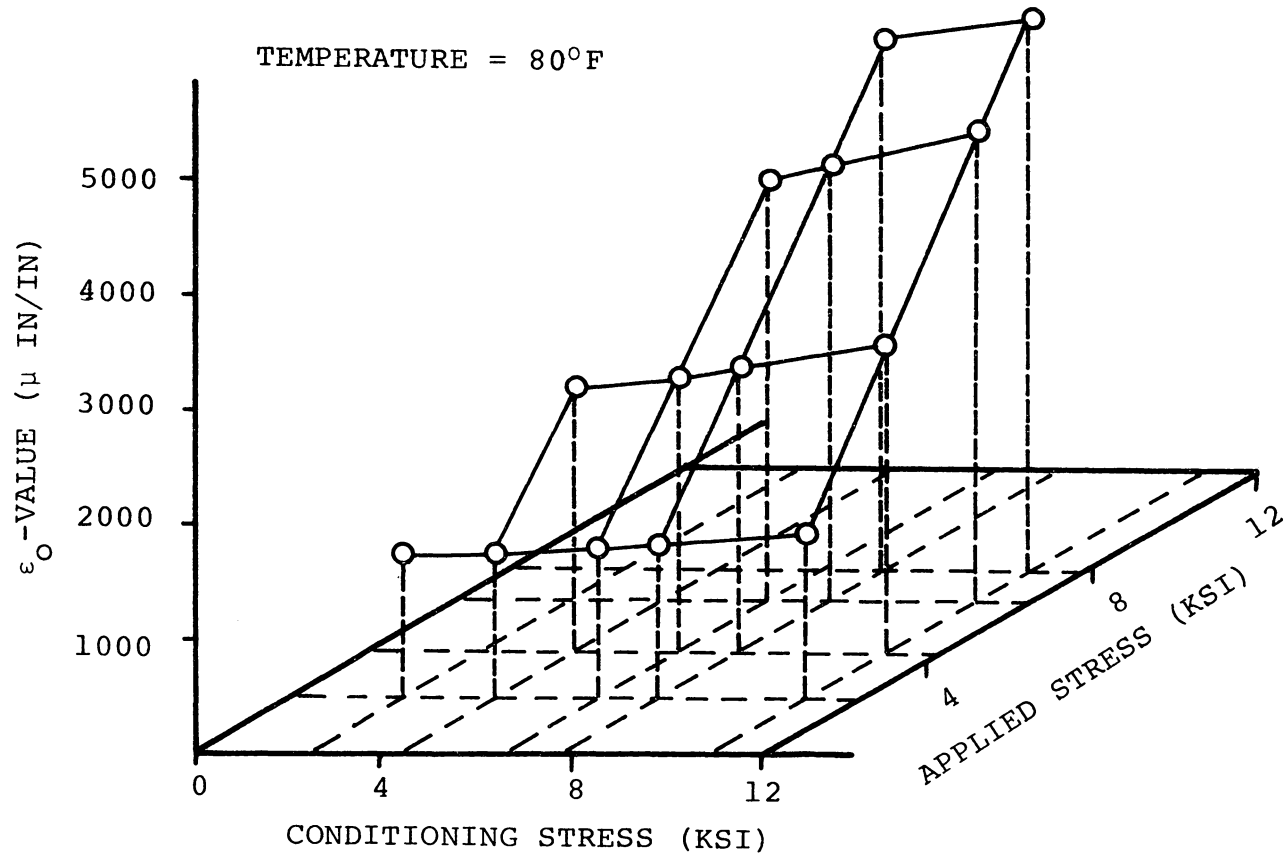


Figure 5.28 Findley parameter ϵ_0 as a function of applied stress and the conditioning stress.

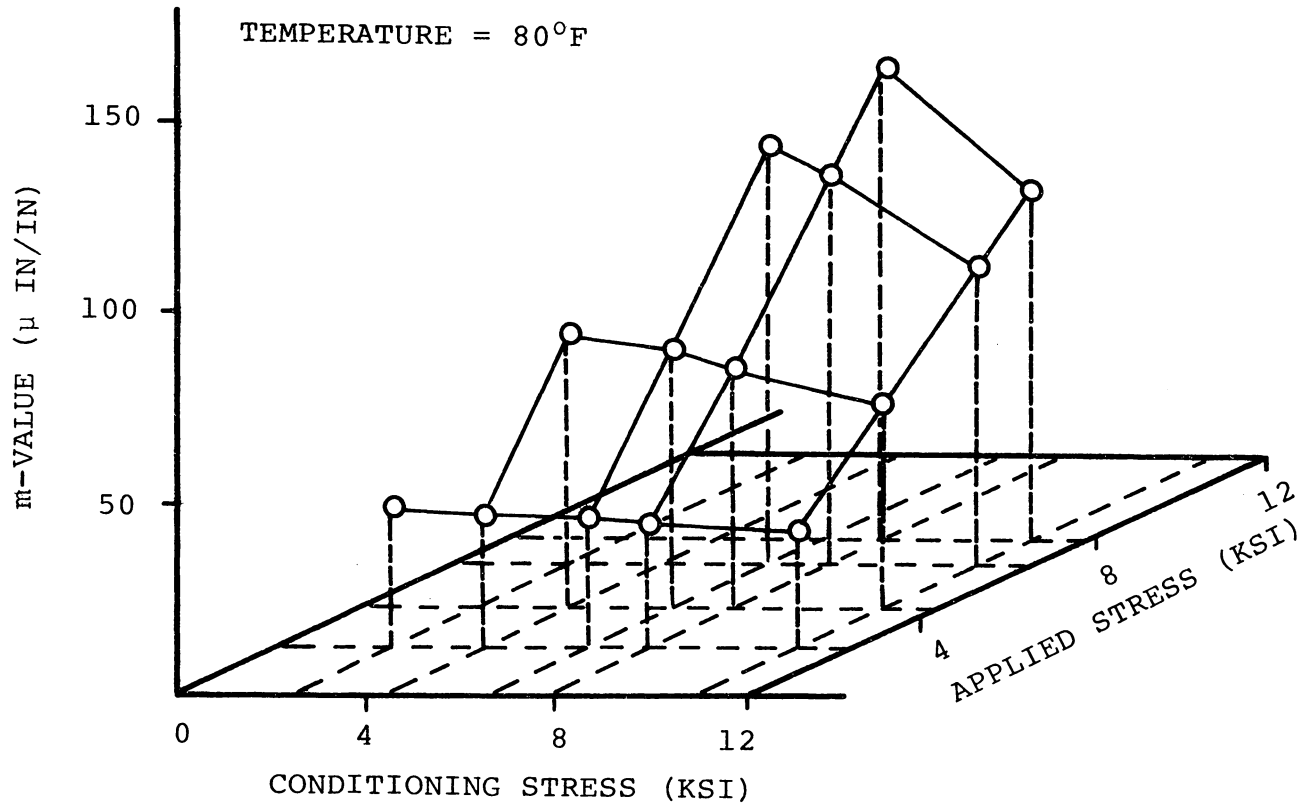


Figure 5.29 Findley parameter m as a function of applied stress and the conditioning stress.

m can be described as a hyperbolic sine function of the applied stress. For the same applied stress but different conditioning stress the initial response (ϵ_0) increases and the m-value decreases as the mechanical conditioning stress increases. It is also observed that the rate of increase (or decrease) of the parameters with respect to the mechanical conditioning increases as the applied stress increases.

The parameters ϵ_0 , m and n appear to be dependent upon the damage state in a specimen. This effect was eliminated by mechanical conditioning and the curve fitting procedure. No attempt was made to incorporate the state of damage into the Findley equation. However, the relationship between damage and the Findley parameters warrants further study.

5.3 Parameters as Functions of Duration of Creep Experiment

A one week creep test was conducted at room temperature, with 6,510 and 7,782 psi being the applied stress and the mechanical conditioning stress, respectively. The Findley parameters were computed at different times during the creep test. It was found that n varies with time (Figure 5.30). The value of n increased gradually as the creep time increased. The n-value approached an asymptotic value after 8,000 minutes. Note that a change of 150 percent was obtained between the initial and the asymptotic n value. The parameters ϵ_0 and m were also found to exhibit a time

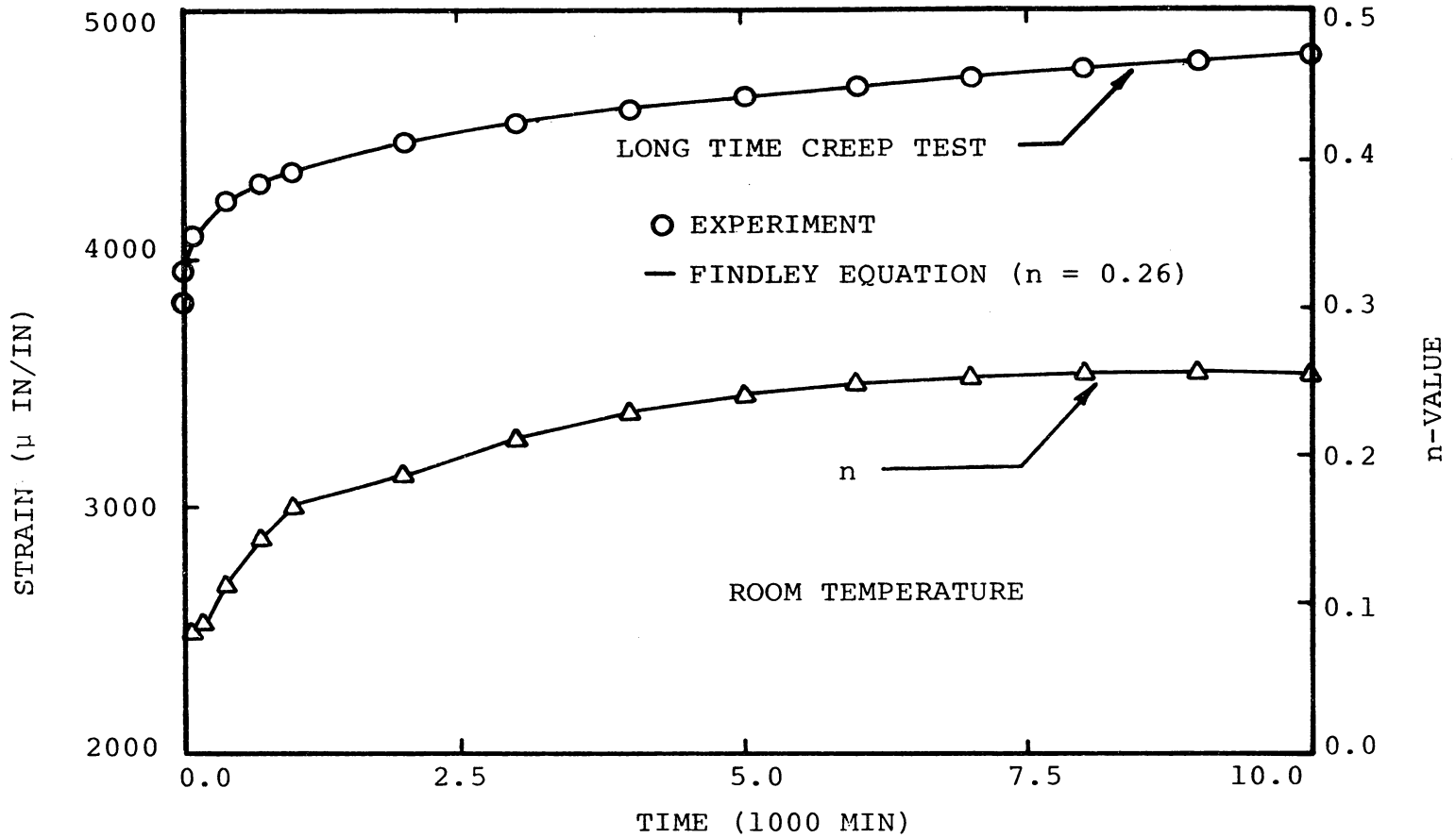


Figure 5.30 Effect of time on n , and the resulting creep response for $n = 0.26$.

dependent behavior (shown in Figure 5.31). Predictions using the Findley equation and asymptotic values of n , m and ϵ_0 are shown in Figure 5.30. Predictive capabilities of the Findley equation using the parameters obtained from both short time (30 minutes) and long time (10,000 minutes) creep data are shown in Figure 5.32. The Findley equation matches the experimental results when the asymptotic parameters are used (Figures 5.30 and 5.32).

The rate at which parameters ϵ_0 and m approach their asymptotic values can be accelerated if the asymptotic n -value is used to calculate them. As shown in Figure 5.33, with an asymptotic n value the parameters ϵ_0 and m approach their asymptotic values within 100 minutes rather than 8,000 minutes. For the predictions to stay within 3% of experiment, it has been found that short time creep tests of 200 minutes duration is adequate to evaluate ϵ_0 and m as a function of stress (using the asymptotic value of n). Since the n -value is independent of the stress level for an unchanged damage situation (i.e. the stress used for the mechanical conditioning is higher than the applied stress), only one long time creep test for each temperature level is needed to determine the asymptotic n value. Thus, for each temperature, the creep characterization contains one long term test and several short time tests. It was also observed that at elevated temperatures, the duration of long-time creep test, t^* , required to determine the

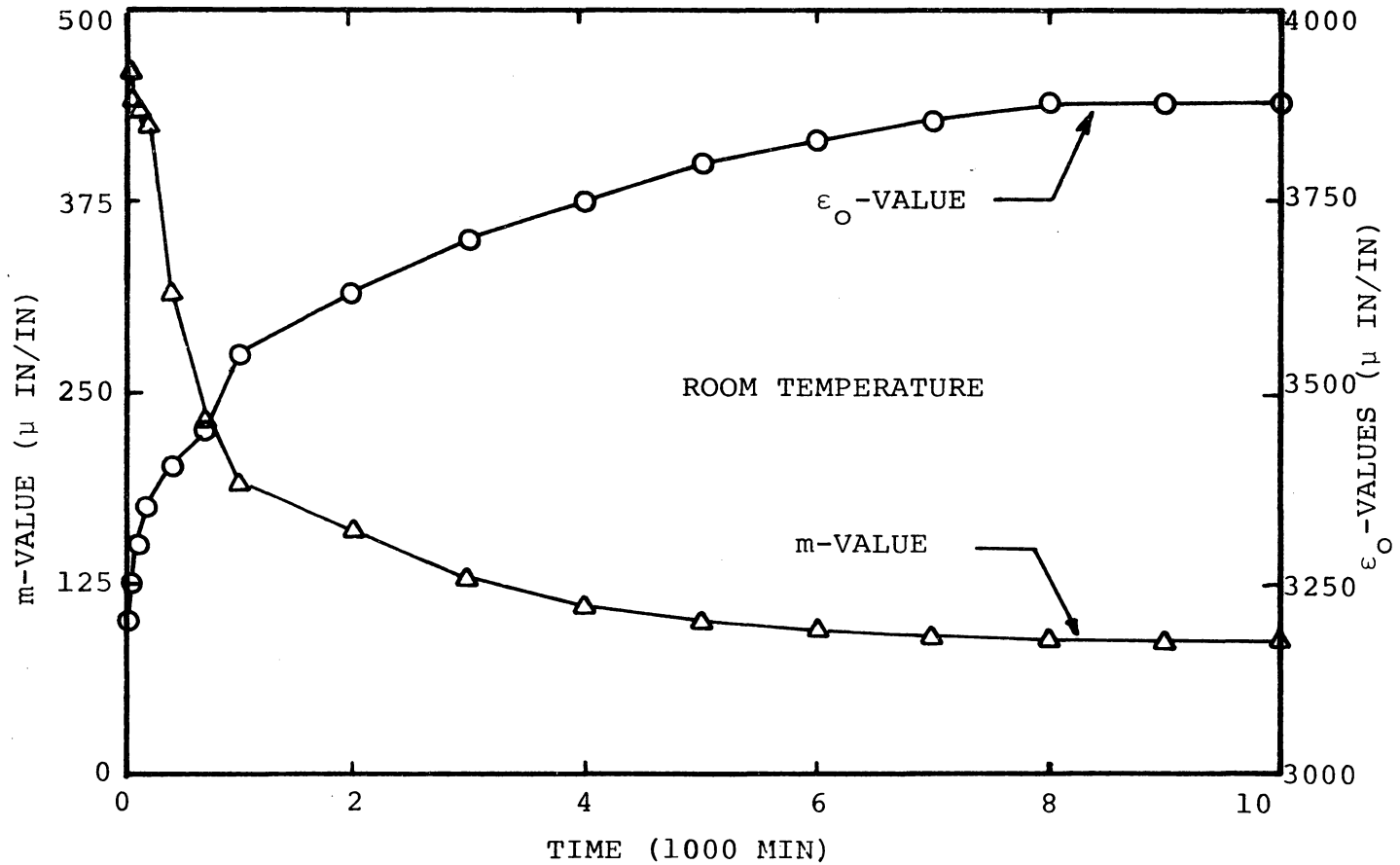


Figure 5.31 Variation of parameters, ϵ_0 and m , as a function of time.

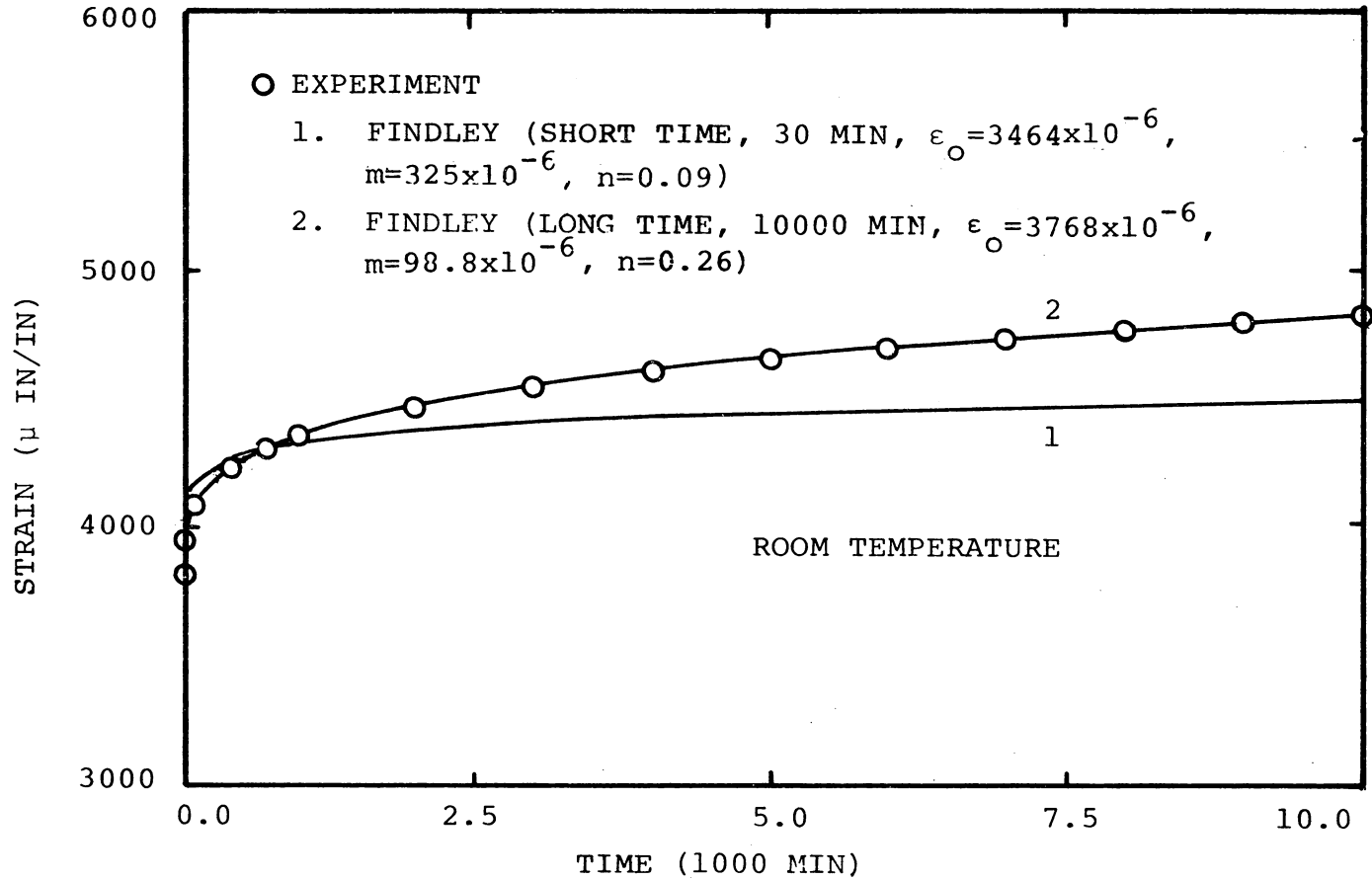


Figure 5.32 Prediction of long time creep response using the short time and long time Findley parameters.

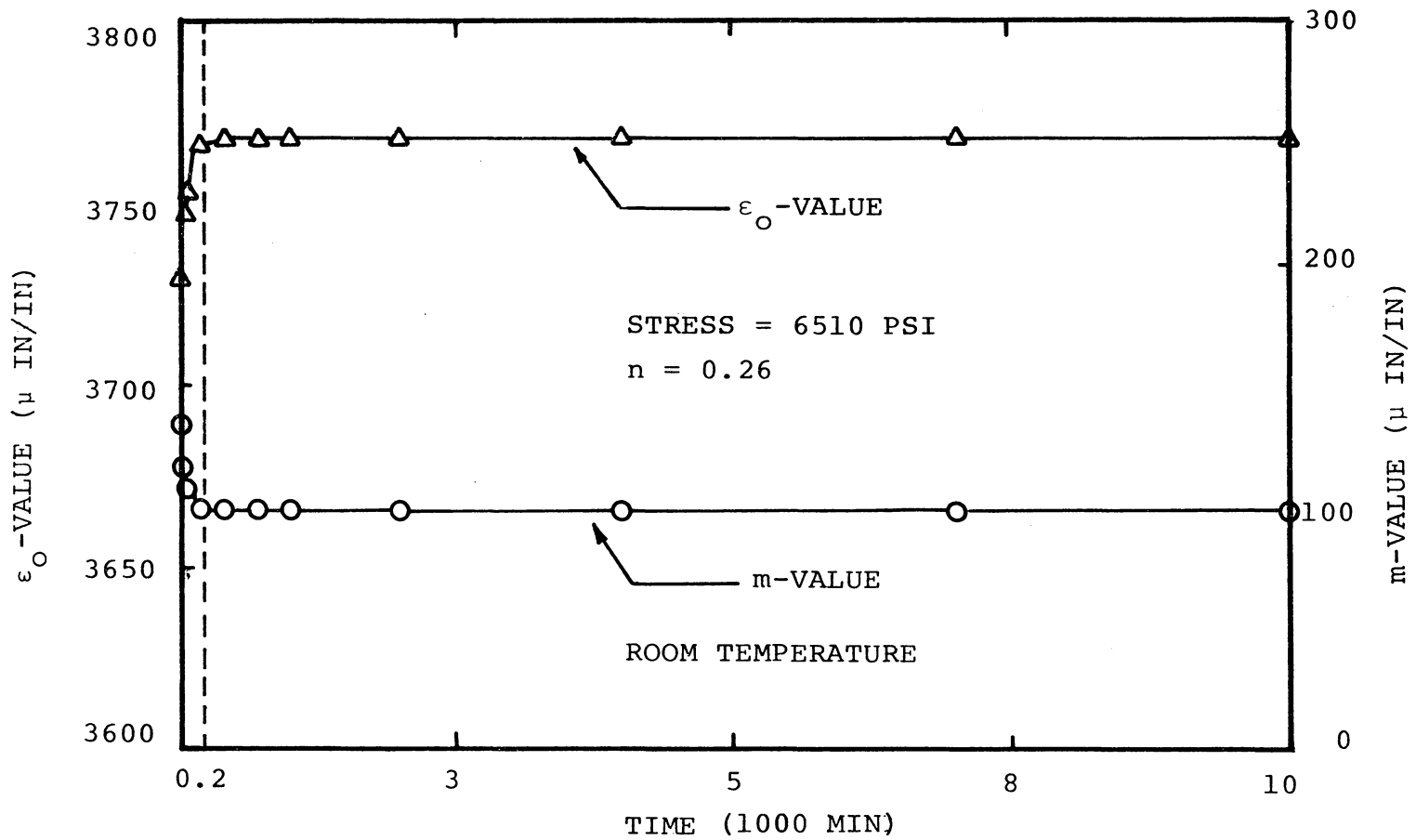


Figure 5.33 Parameters, ϵ_0 and m , as a function of time for a given asymptotic n value.

asymptotic n -value is shorter (Figure 5.34). However, a 200 minute test was still required to determine the asymptotic values of ϵ_0 and m .

It has been shown [25] that when using the creep recovery data of a short time creep test the same asymptotic n -value can be obtained as when using a long time creep test. While this procedure was not adopted in this study, it is considered to be a time saving method since there is no need to perform the long-time experiments. One other advantage of using the recovery data is that the calculation of parameters is not affected by the initial creep components [25].

A 200 minute creep test was performed at room temperature at 6,510 psi. The strain-time recovery data was recorded until the specimen was completely recovered. It was found that approximately the same n -value as that of long time creep was obtained. Note that due to the fast decay of the recovery strain, the recovery data in the first few minutes was taken from a strip chart recorder. Quite often, the data recording was influenced by undesirable noise from the oven controller, a keypunch machine in the next room, and small experimental error. These influences would often contribute a $\pm 10 \mu\epsilon$ fluctuation in the reading. This noise level may be 10 percent of the recovery data and result in incorrect values of m and n . Tuttle [67] has

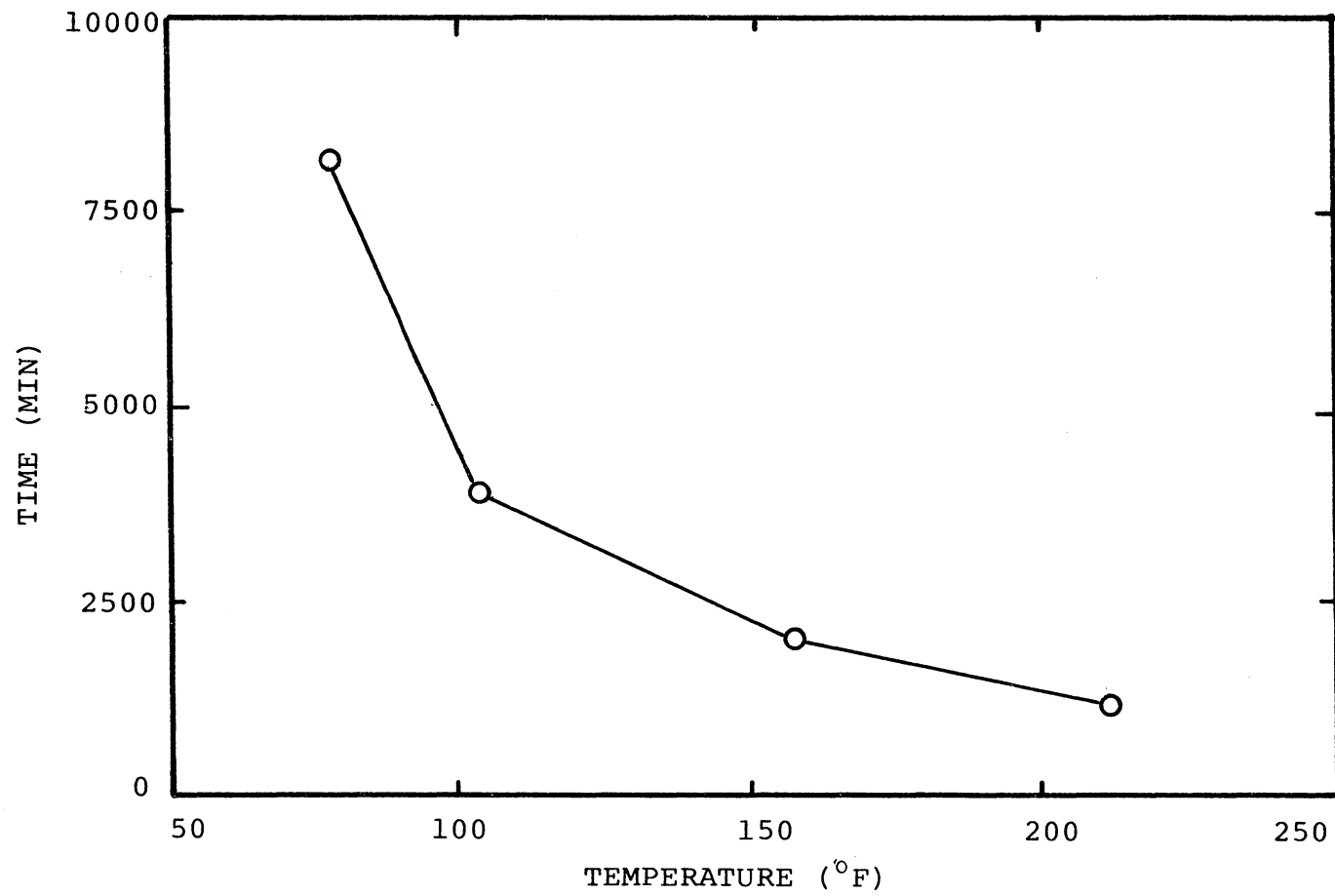


Figure 5.34 Creep time required to obtain an asymptotic n value as a function of temperature.

recently determined that slight change of recovery data may provide a drastic change in material parameters m and n . When creep data is used, the noise level is relatively small and does not affect the determination of the material parameters. This is the reason that the creep data were used in this study instead of the recovery data. However, the recovery data method of evaluating the Findley parameters warrants further study.

5.4 Short Time Creep Response

As discussed in the previous sections, repeatable creep results occur only when the specimen is under the same damage condition as that of the mechanical conditioned state. The main purpose of the short time creep experiments was to calculate the parameters ϵ_0 and m as functions of applied stress, mechanical conditioning, and temperature.

Figure 5.35 shows the Findley parameters at four stress levels at room temperature. The specimen was conditioned at 7,782 psi (36% of ultimate strength at room temperature). In this figure, n -values from two sources are presented. The solid dark triangles represent the n -value obtained from the long time creep tests; while the open triangles represent the n -values calculated from the 30 minute creep results. The asymptotic values of n are independent of stress. The parameters ϵ_0 and m calculated using the long

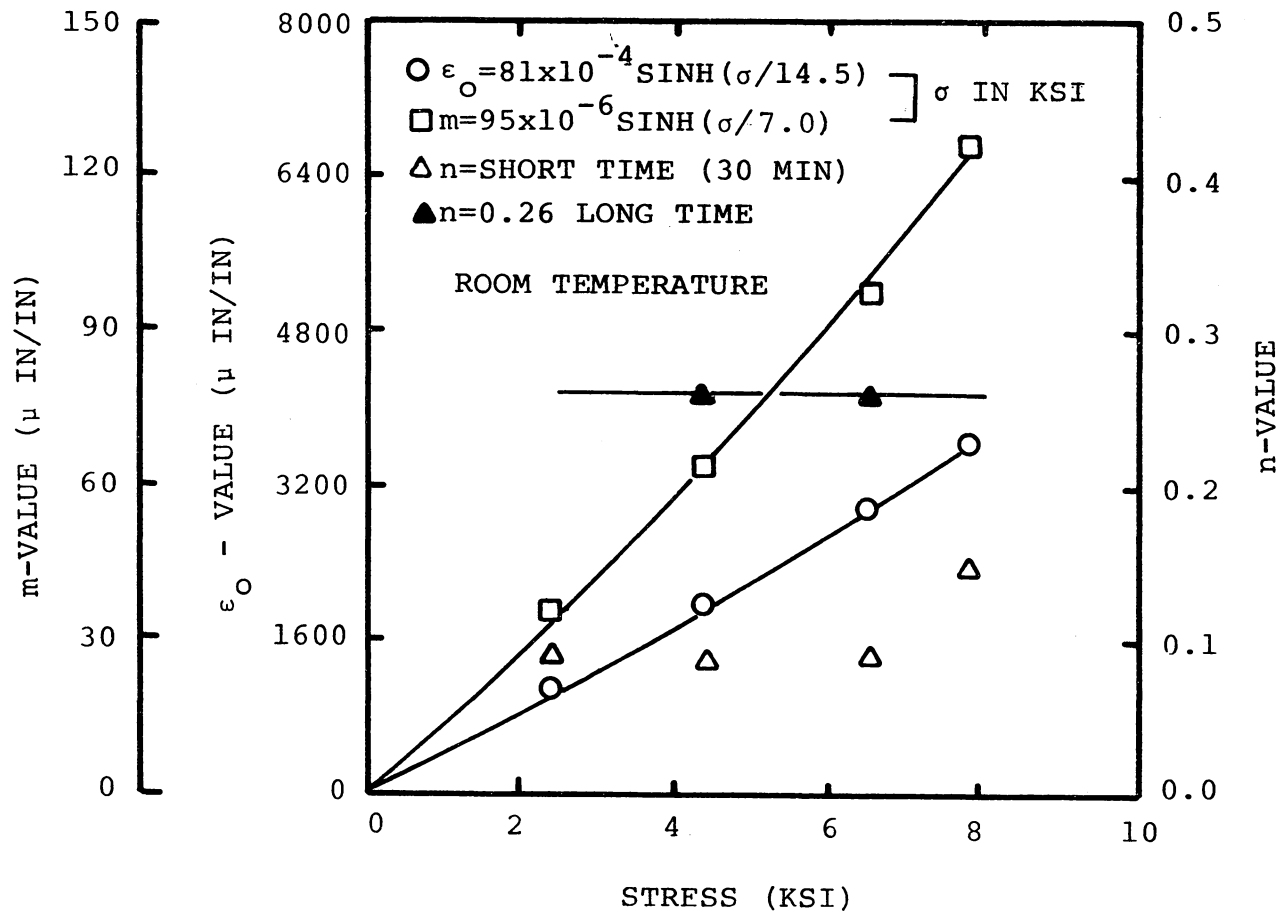


Figure 5.35 Findley parameters as functions of stress (conditioned at 7,782 psi).

time n -value are also shown in the same figure and can be described by hyperbolic sine functions of stress.

For the elevated temperature tests, specimens were conditioned at 50% of the ultimate strength at each test temperature. The duration of creep for evaluating ϵ_0 and m was 200 minutes as suggested by the room temperature studies. The long-time n -value varied linearly with temperature and is shown in Figure 5.36. The n -value was 0.24 at room temperature and increased to 0.30 at 212°F. Using the long time n -values and the 200 minute creep data, the parameters ϵ_0 and m were calculated. Figures 5.37 and 5.38 show the isothermal hyperbolic sine fit of ϵ_0 and m respectively. The nonlinear creep response is insignificant within the range of stress tested, as the hyperbolic sine curves can be approximated by straight lines. However, the nonlinearity increases as the temperature increases. For the same stress level, ϵ_0 and m increases linearly with the temperature (Figures 5.39 and 5.40).

Based on the appropriate ϵ_0 , m , and n parameters, a comparison can be made between experimental results and the Findley equation. Figure 5.41 shows the room temperature creep results at four stress levels. The stress level used for the mechanical conditioning was 7,782 psi. Excellent agreement between the theory and experiment was obtained. The recovery strains associated with these four

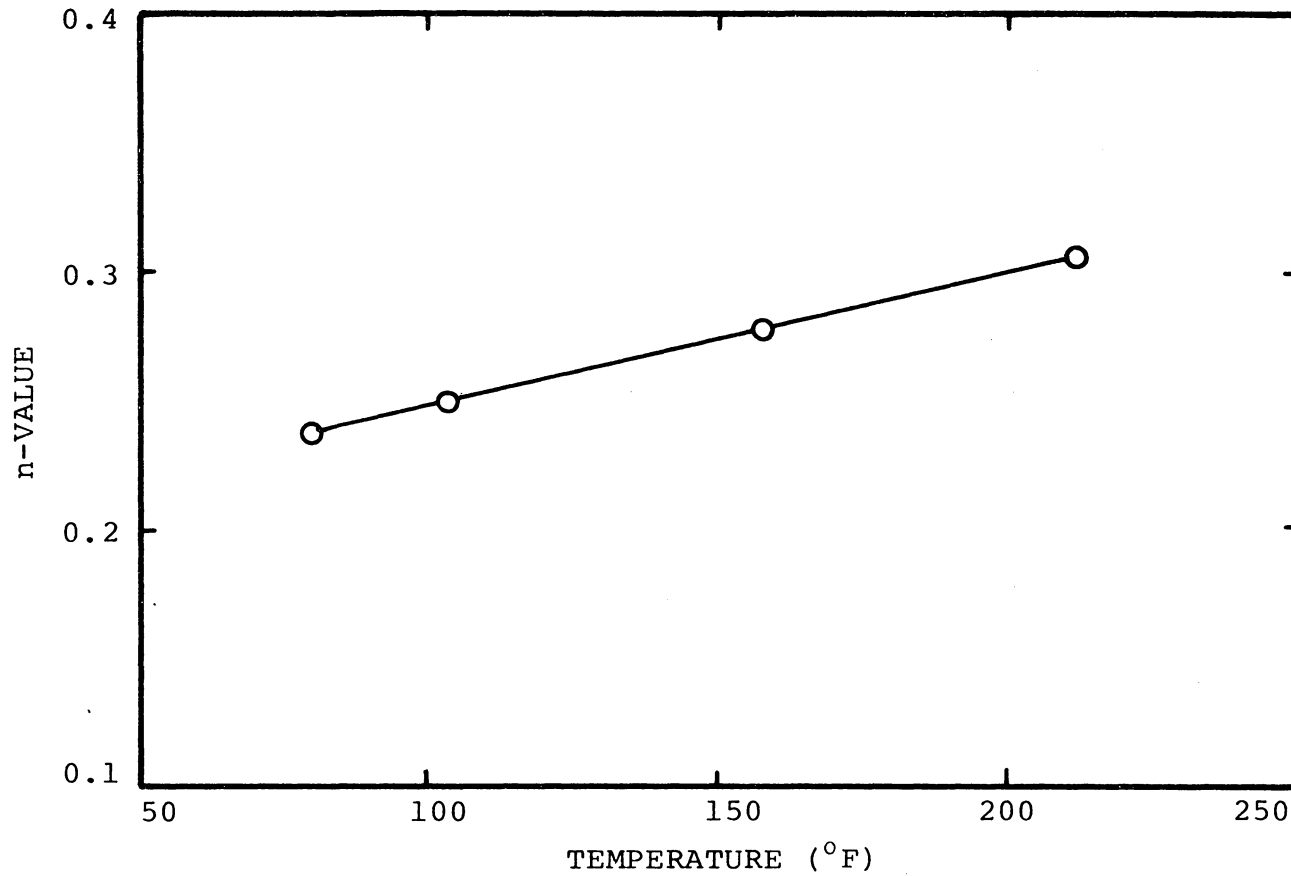


Figure 5.36 Time exponent n as a function of temperature (conditioned at 50% of ultimate strength at a given temperature).

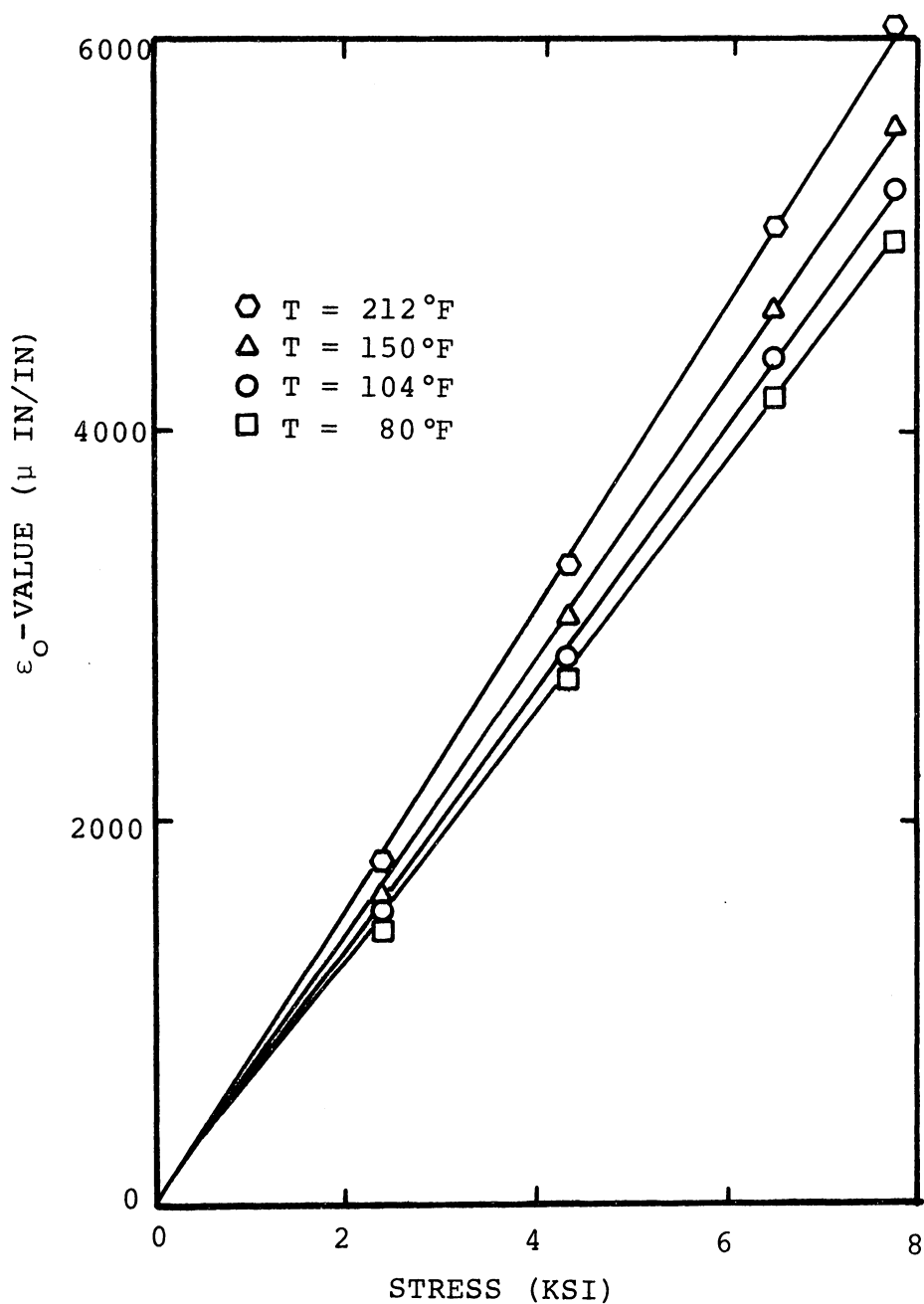


Figure 5.37 Hyperbolic sine fit of the Findley parameter, ϵ_0 , at elevated temperatures (conditioned at 50% of the ultimate strength at a given temperature).

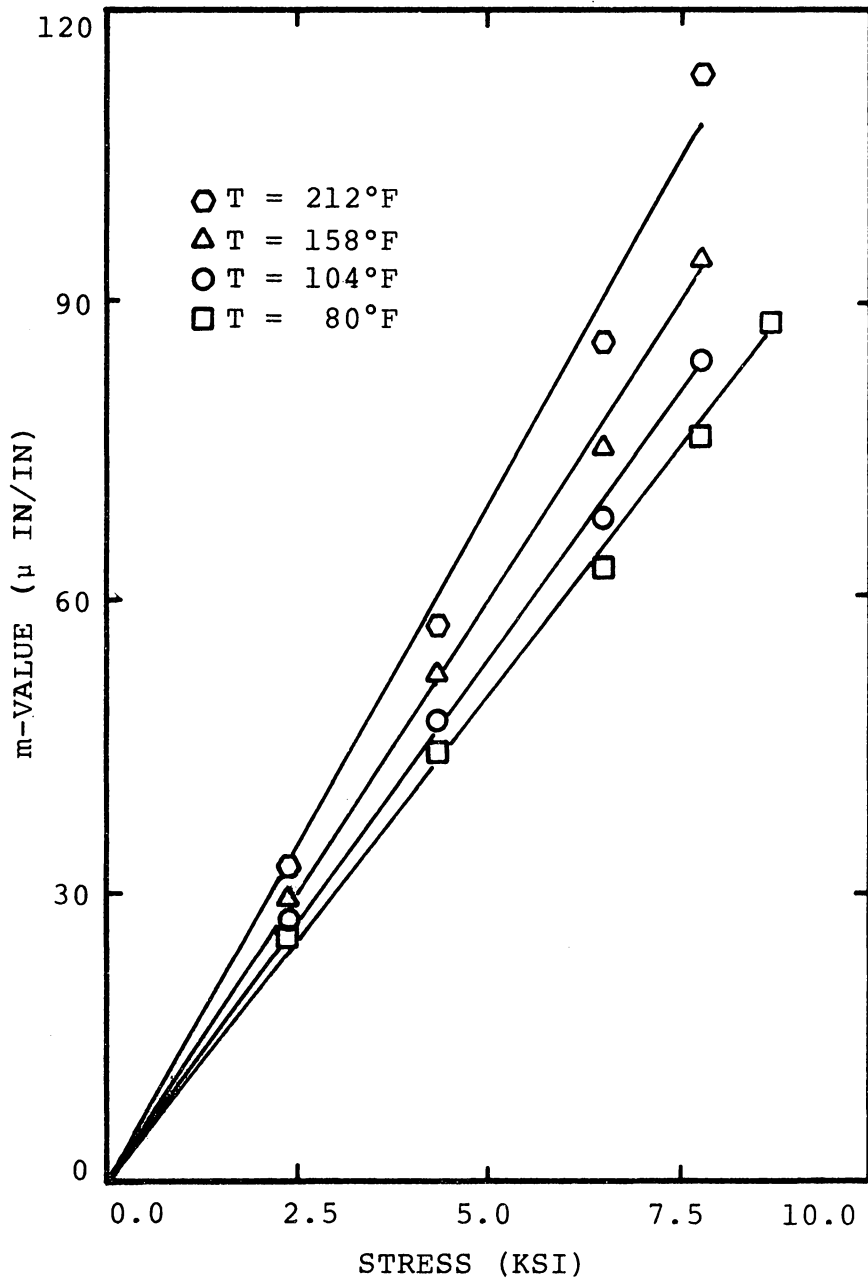


Figure 5.38 Hyperbolic sine fit of the Findley parameter, m , at elevated temperatures, (conditioned at 50% of the ultimate strength at a given temperature).

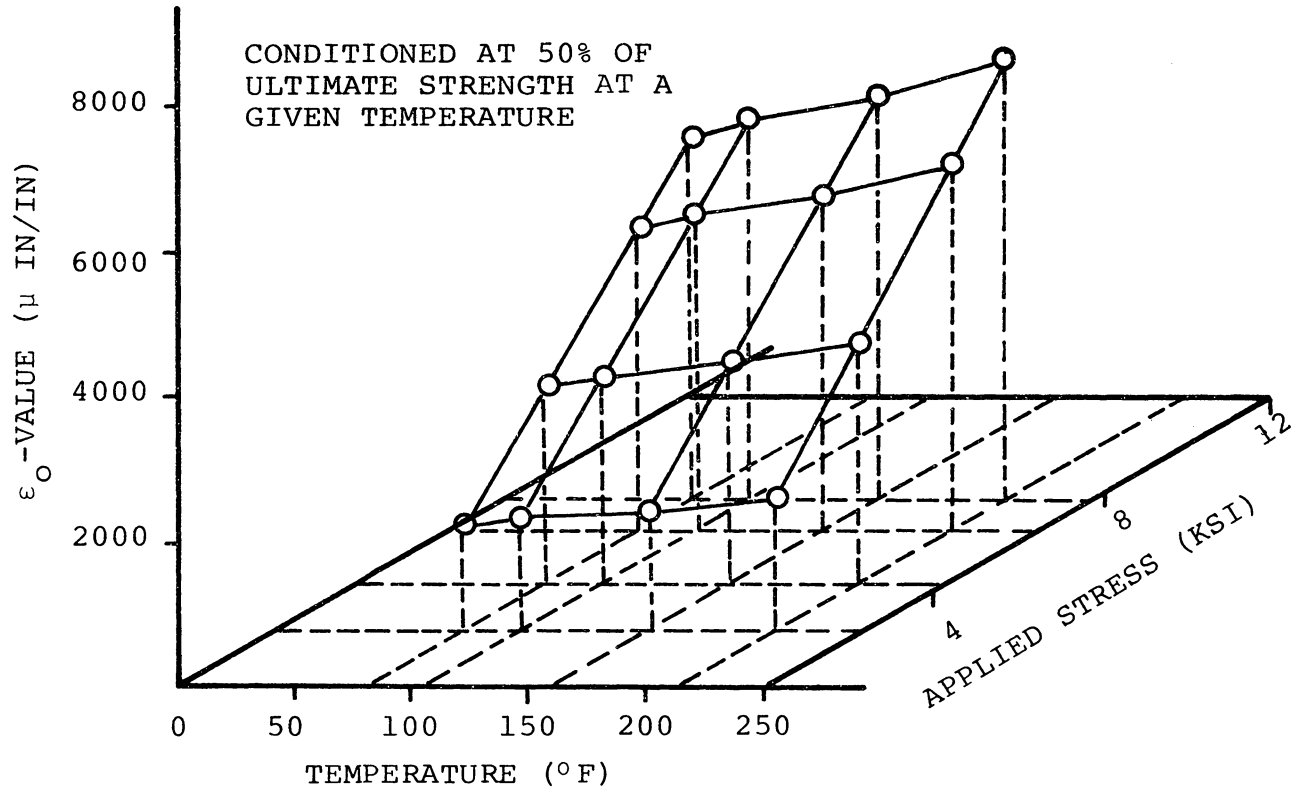


Figure 5.39 Variation of the Findley parameter, ϵ_0 , with temperature and applied stress.

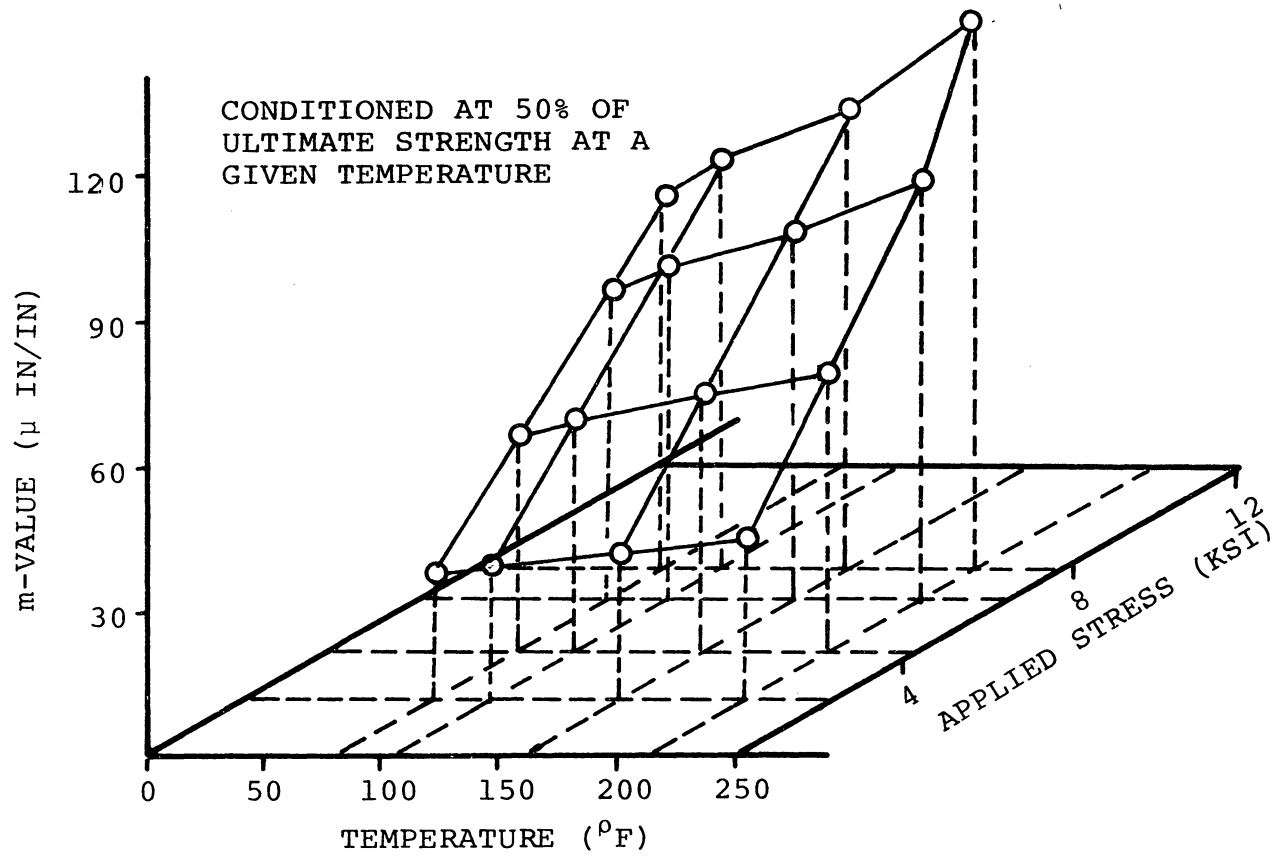


Figure 5.40 Variation of the Findley parameter, m , with temperature and applied stress.

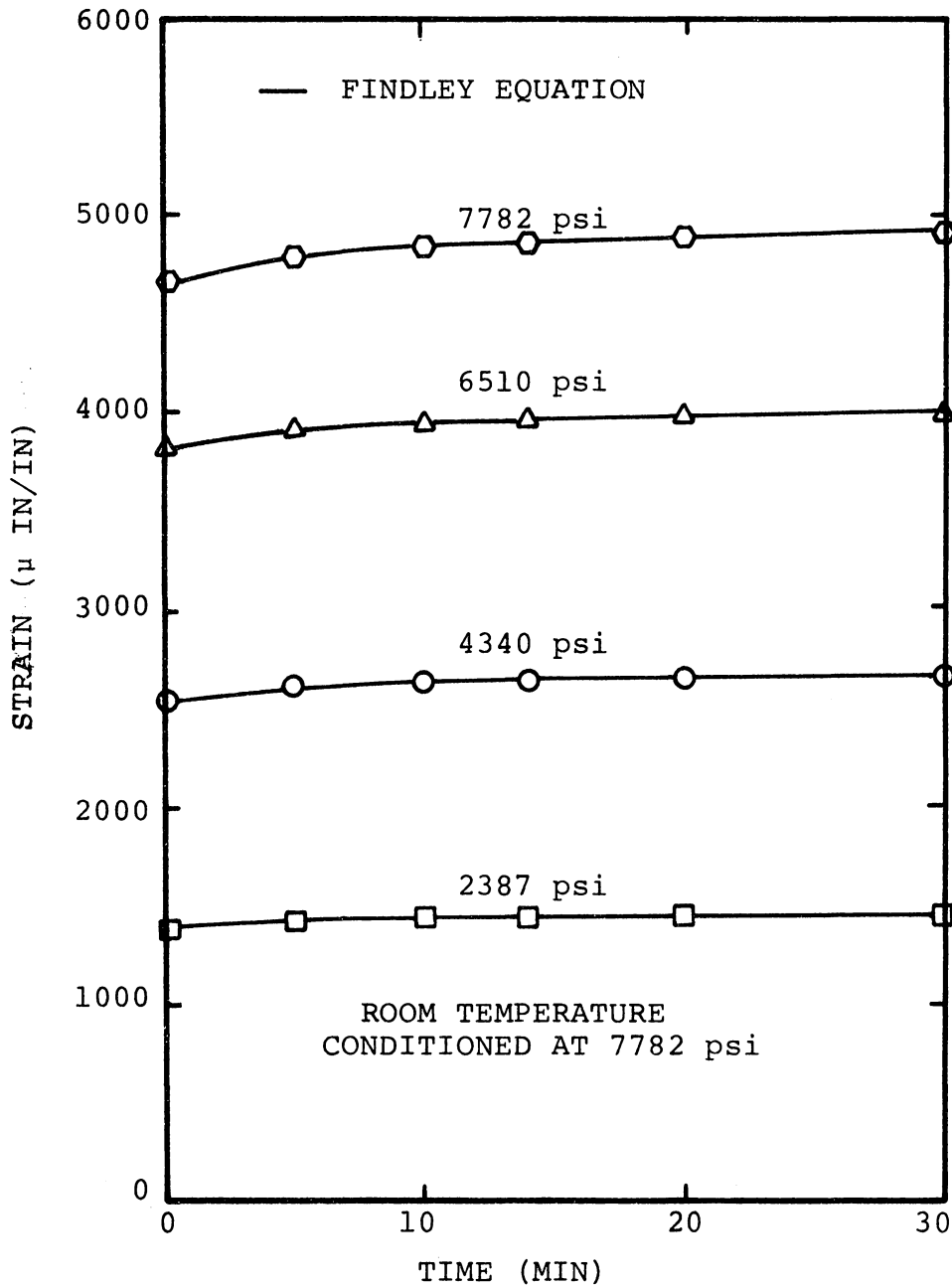


Figure 5.41 Prediction of the short time creep response using the Findley equation.

creep experiments are presented in Figure 5.42, where the solid lines are the predictions using the Findley equation. The maximum difference between the recovery strain and the prediction was $10 \mu\epsilon$. This difference usually occurred at times when the loadings were just released.

The short time (200 minute) elevated temperature creep results (mechanically conditioned at 50% of ultimate strength at a given temperature) are shown in Figures 5.43 to 5.46. As is shown, the creep behavior of SMC-R50 is temperature dependent. For a given stress, creep strain increases with temperature. Agreement was obtained between the experimental results and the predictions.

5.5 Predictions

One of the goals of this study was to use the Findley equation to predict the creep response at random stresses and temperatures. Predictions were classified in three categories: 1) long time creep response, 2) creep response due to multiple step loadings, and 3) the long time creep response of unconditioned specimens. Before conducting the creep experiments associated with categories 1) and 2), specimens were all mechanically conditioned at either 36% or 50% of ultimate strength at room temperature. Depending on the stress level of mechanical conditioning used in the creep experiments, the parameters of the Findley equation used in the predictions were determined from either

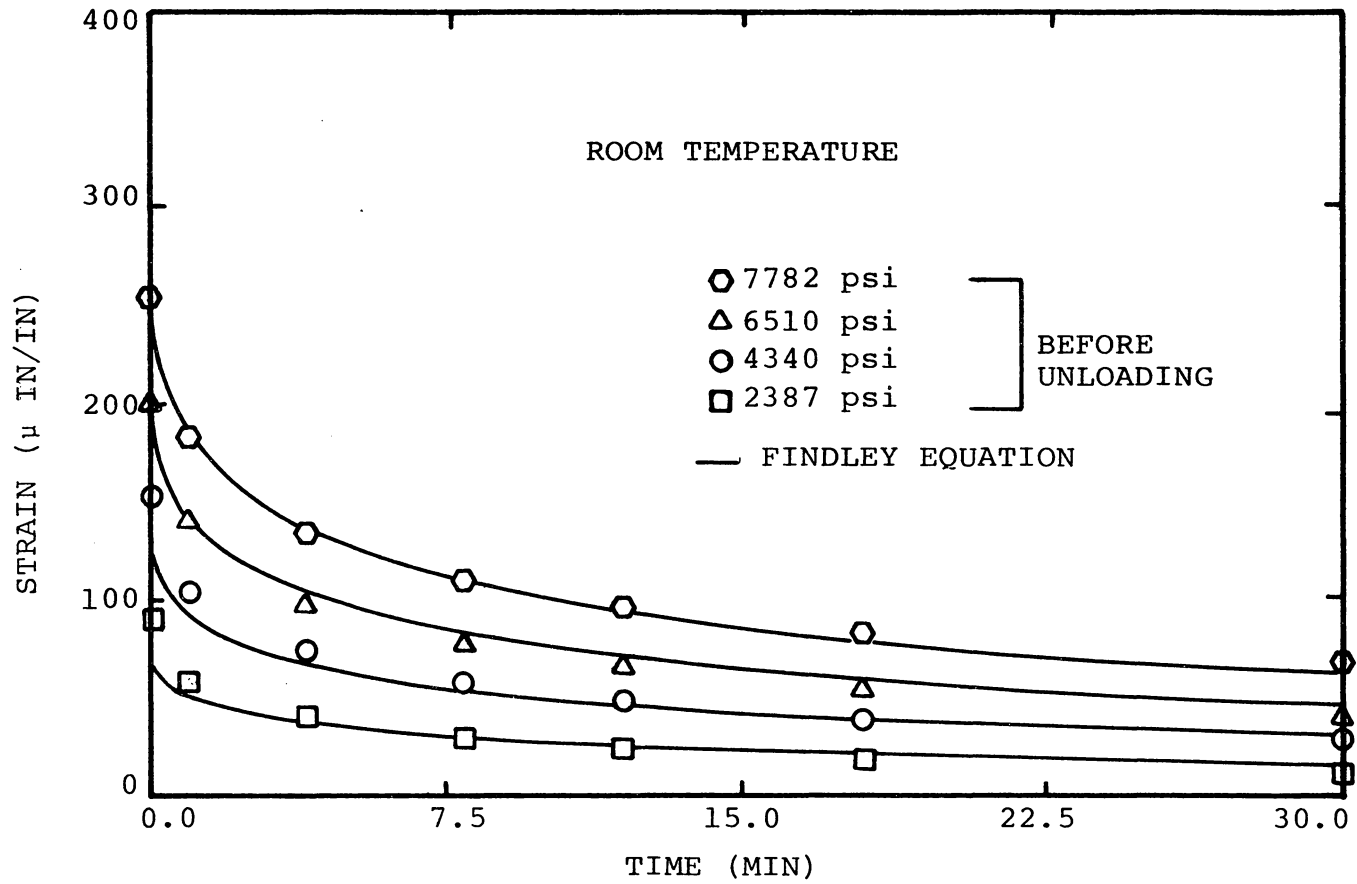


Figure 5.42 Prediction of the recovery response after the short time creep experiments.

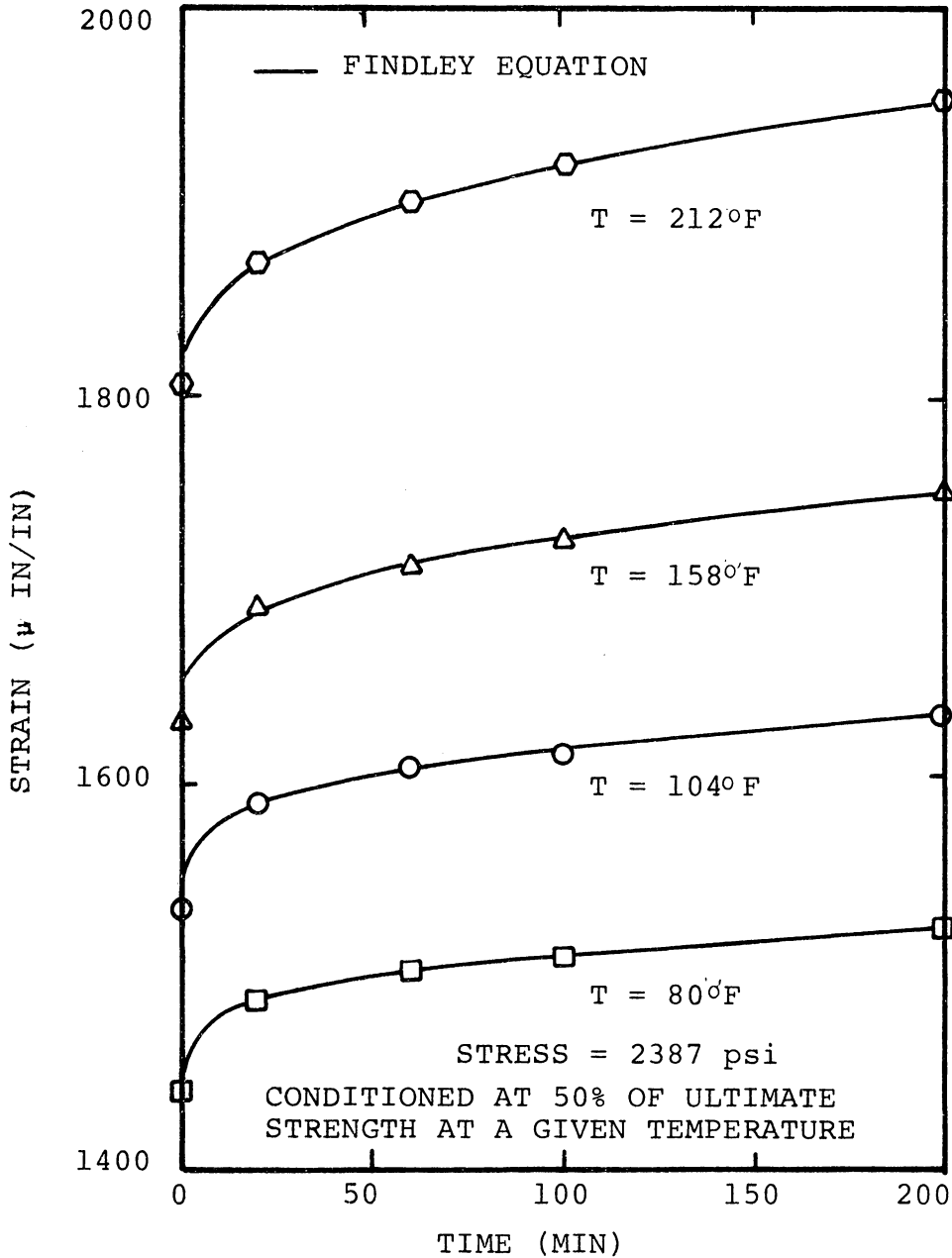


Figure 5.43 Prediction of the short time creep response at elevated temperatures ($\sigma = 2,387$ psi).

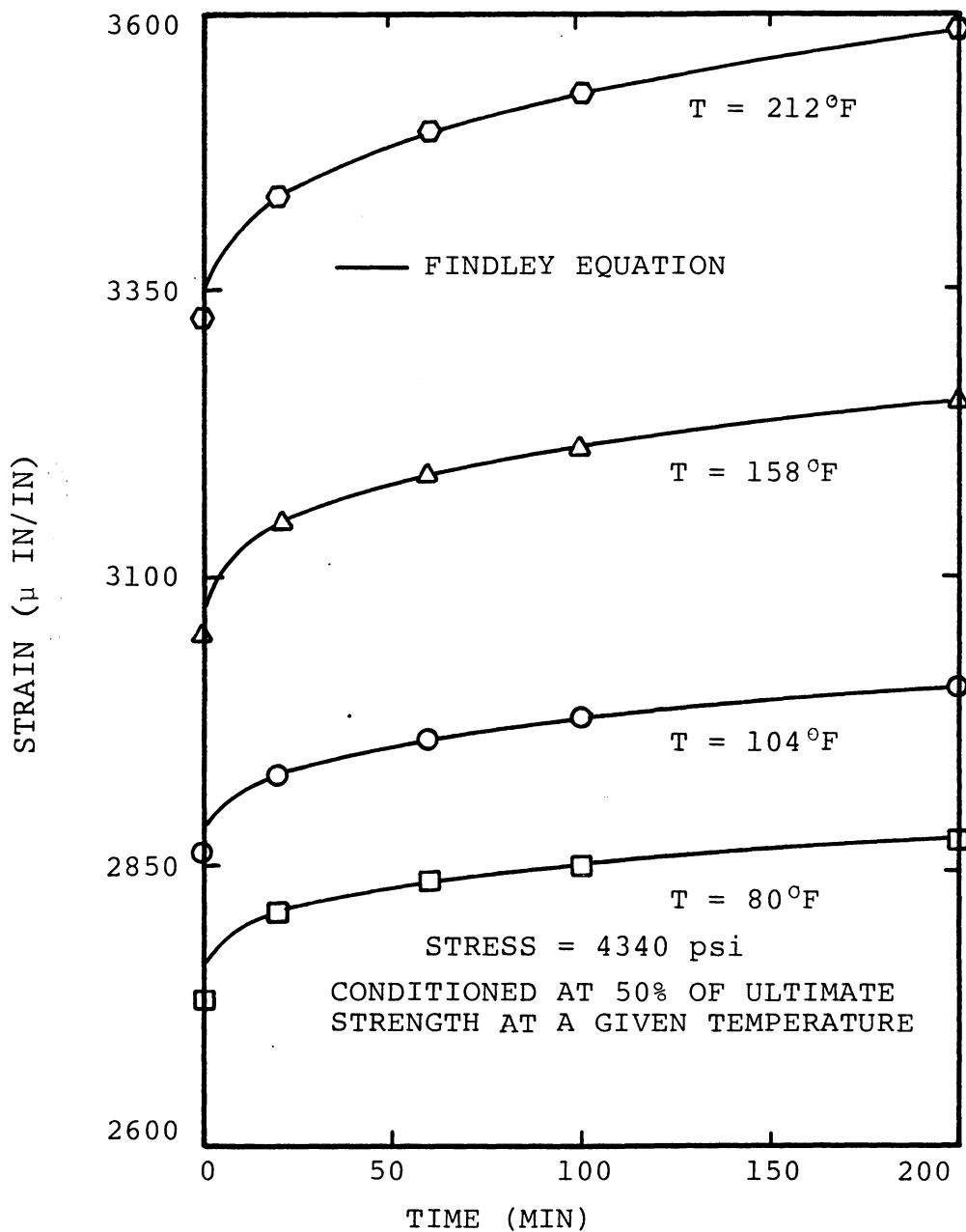


Figure 5.44 Prediction of the short time creep response at elevated temperatures ($\sigma = 4340$ psi).

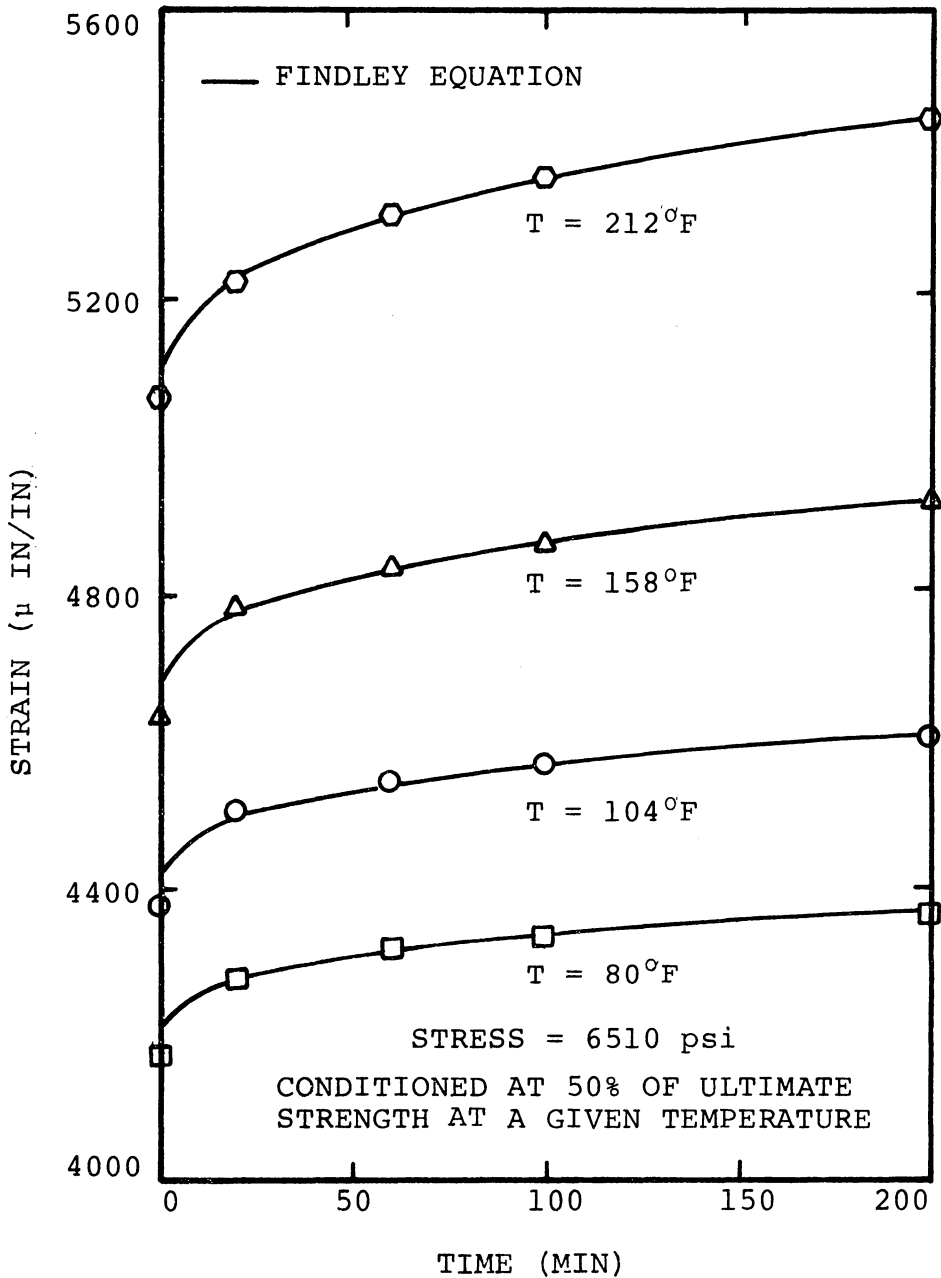


Figure 5.45 Prediction of the short time creep response at elevated temperatures ($\sigma = 6,510$ psi).

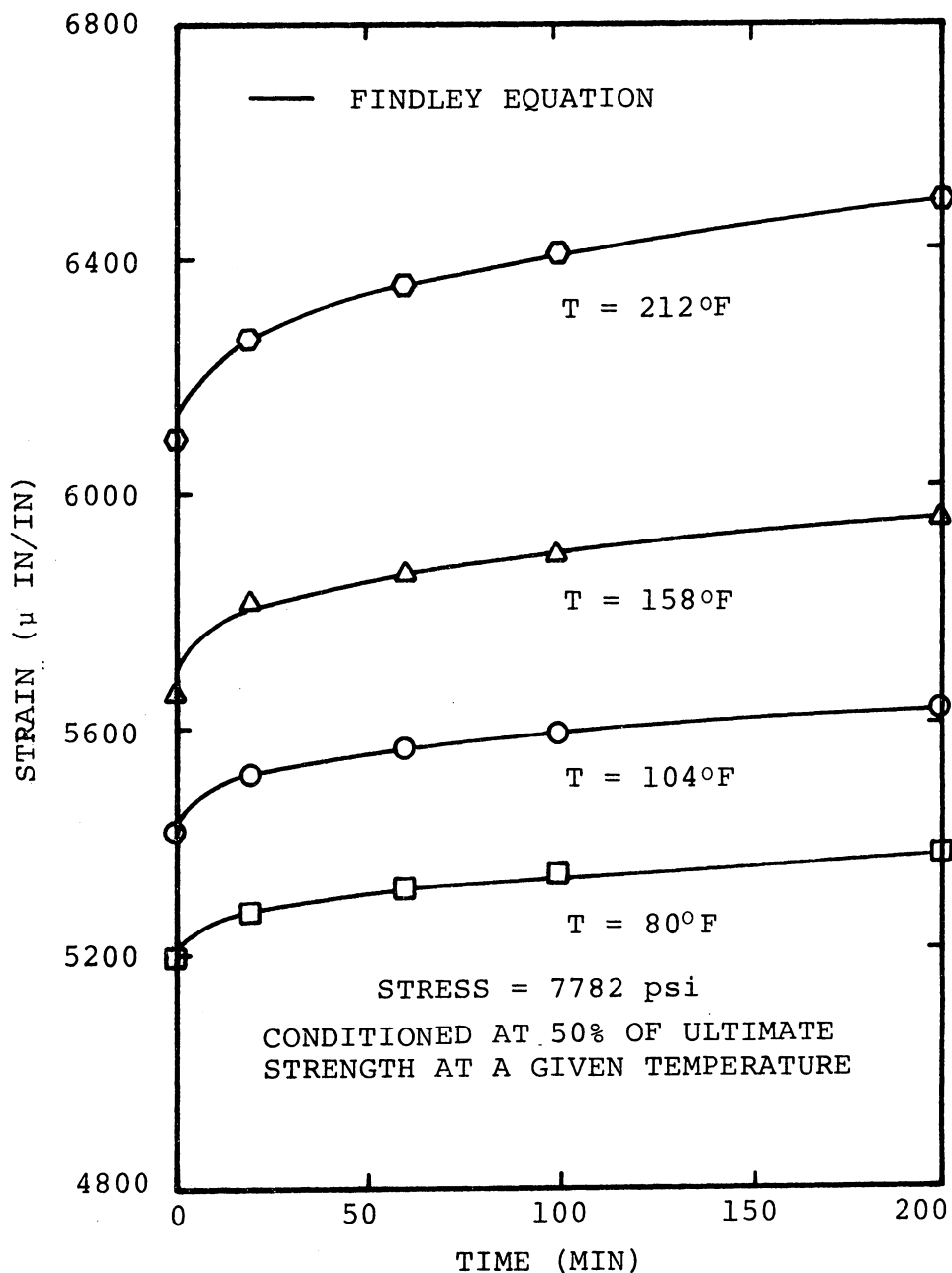


Figure 5.46 Prediction of the short time creep response at elevated temperatures ($\sigma = 7,782$ psi).

Figure 5.35 or Figure 5.36 to 5.38 using either linear interpolation or extrapolation.

Five long time creep tests at elevated temperature were conducted. The duration of tests ranged from 10,000 minutes to 30,000 minutes. Prior to each test, the specimen was conditioned at 50% of ultimate strength at room temperature. Four of these experiments were at 6,510 psi, and the results are shown in Figure 5.47. Excellent agreement was observed between the predictions and the experimental results. Figure 5.48 presents the 30,000 minute creep response at 5,425 psi where the temperature is 185°F. A maximum difference of 50 $\mu\epsilon$ between theory and the experiment was obtained. In all cases the applied stress was less than 50% of the ultimate strength at any test temperature.

Three multiple step loading tests were conducted. Each test was for different time durations and for a different number of step loadings. The first case was a two step loading at room temperature (Figure 5.49). The specimen was loaded at 6,510 psi for an hour, then the stress was increased to 7,782 psi and held constant for another hour. Complete recovery was allowed after the release of the loads. The second case was a three step loading at room temperature (Figure 5.50) where different stress levels were used. The duration of each step was also one hour and complete recovery was obtained after the loadings were released. A

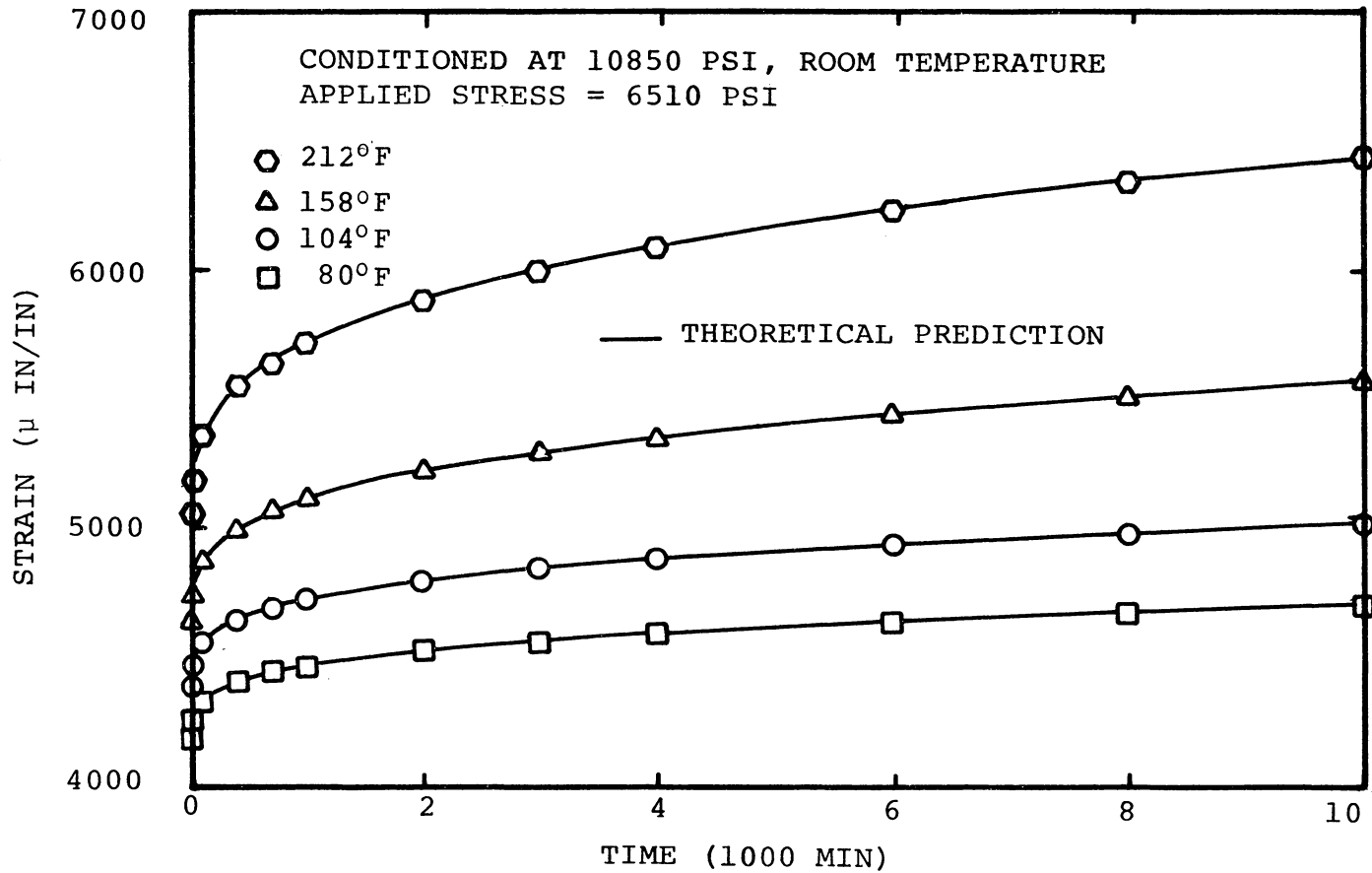


Figure 5.47 Prediction of long time creep response at elevated temperature and at 6,510 psi.

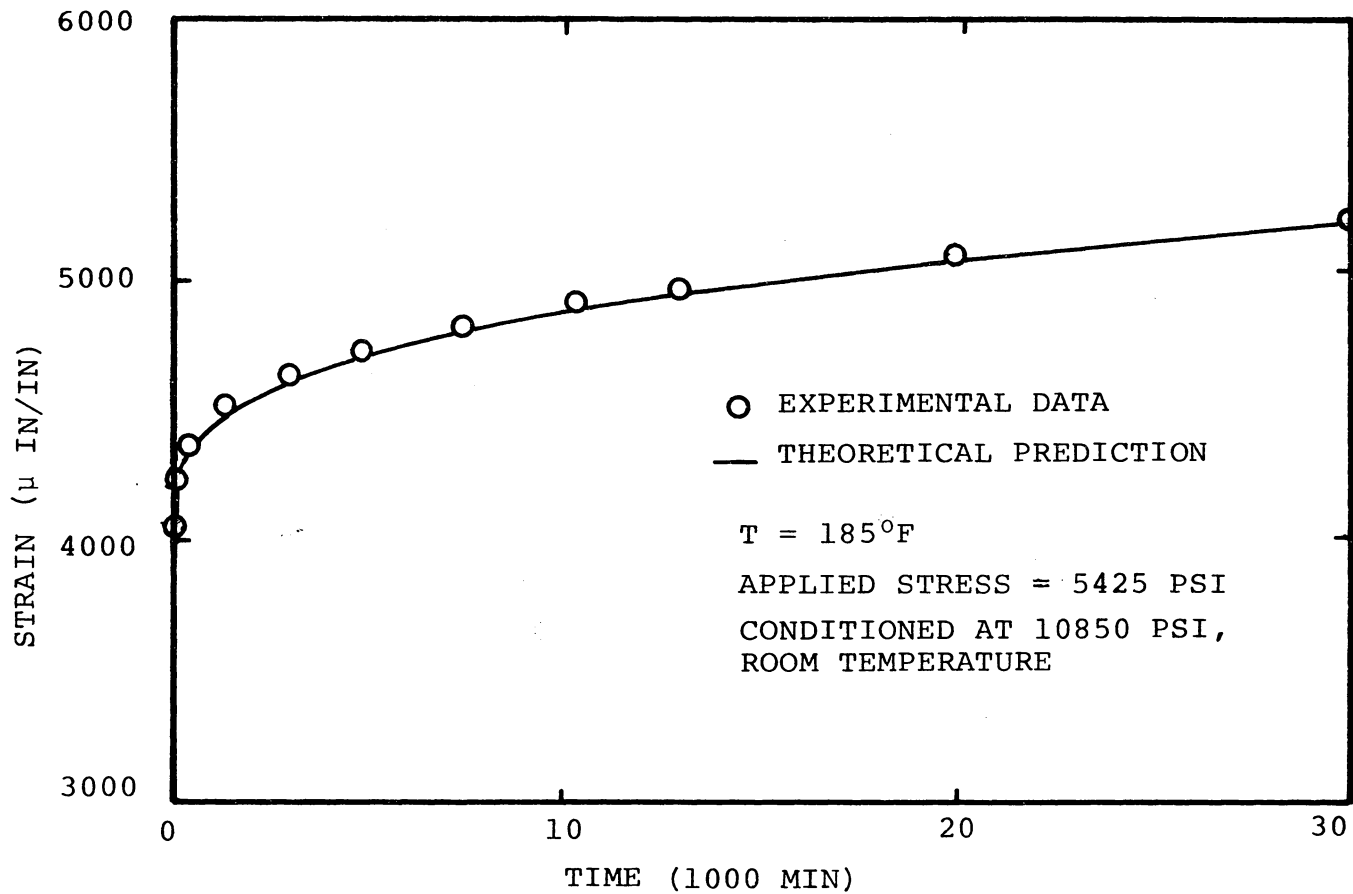


Figure 5.48 Prediction of the long time creep response at 185°F and 5425 psi.

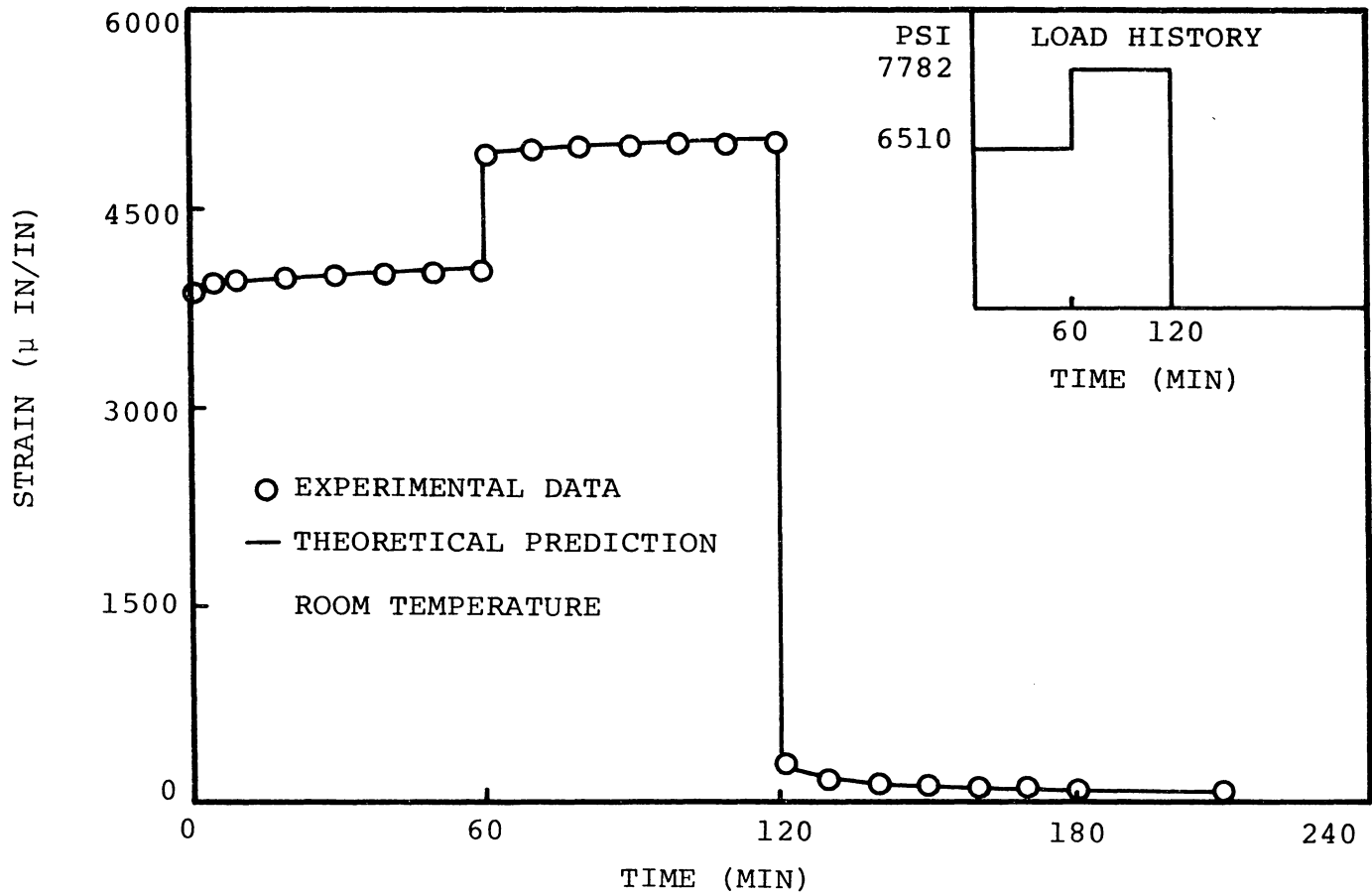


Figure 5.49 Prediction of the creep response at room temperature due to a two step loading.

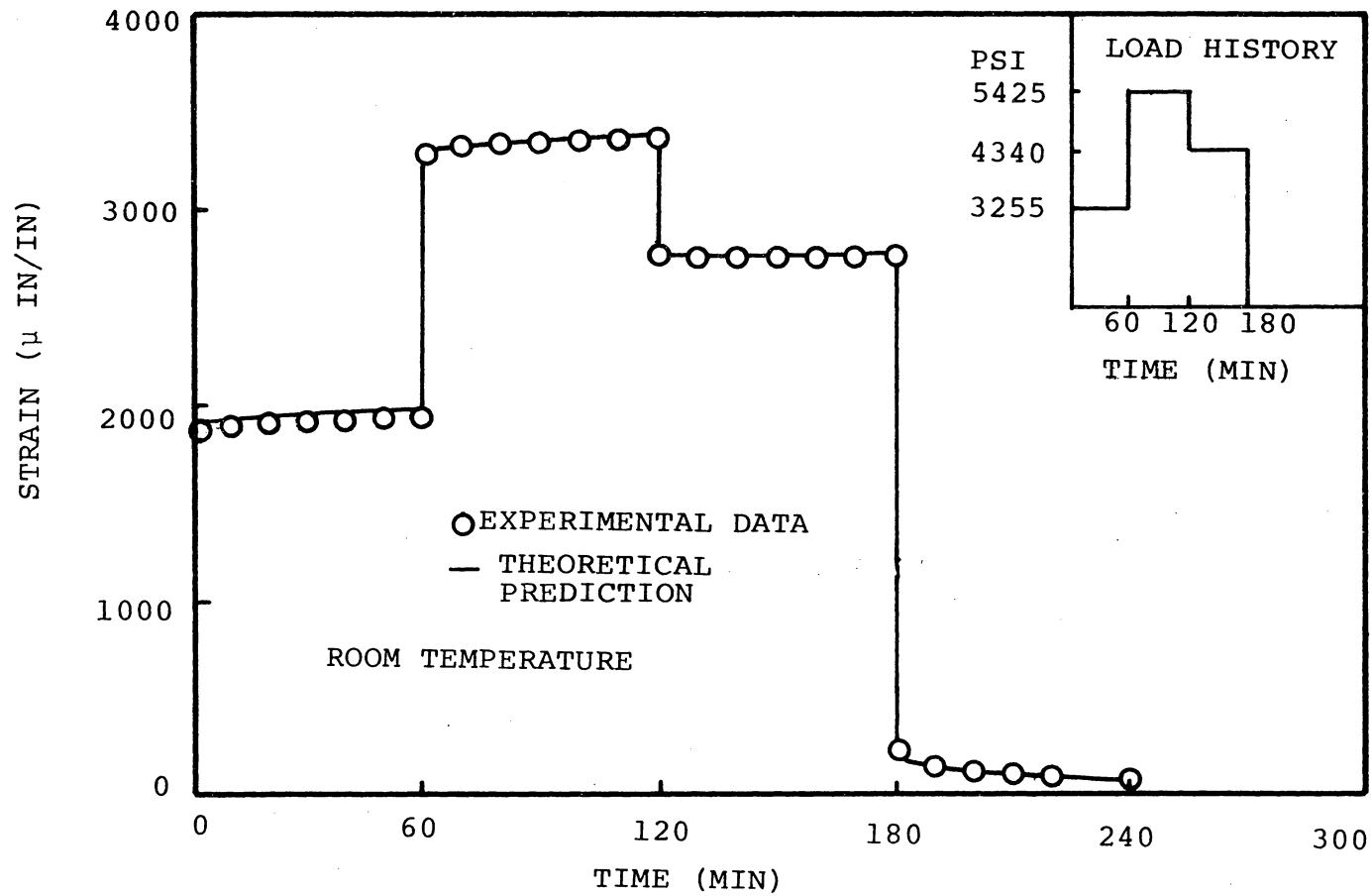


Figure 5.50 Prediction of the creep response at room temperature due to a three step loading.

five step creep loadings (Figure 5.51) was used for the third case where in each step the time interval was different. This test was performed at 131°F and the total duration of the test was over 7,000 minutes. The creep response is shown in Figure 5.52. In the first two cases the specimen was conditioned at 36% of the ultimate strength at room temperature, while in the third case the specimen was conditioned at 50% of the ultimate strength at room temperature.

The predictions of multiple step creep response were based on the modified superposition principle. According to this principle, the creep response due to multiple step loadings can be considered as the summation of the creep response due to each individual load step. Thus, the information required to perform the prediction of multiple step creep are simply the Findley parameters (ϵ_0 , m and n) for each single step creep load contained in the multiple step load. The accuracy of the modified superposition principle has been validated by Findley et al. [68] in their study of nonlinear creep of polyvinyl chloride. In this investigation, the theoretical predictions were aided by a computer program based on the general creep response of multiple step loading (equation (3.12)). In this program only the parameters of each step creep loading and the duration of each load step were needed to perform

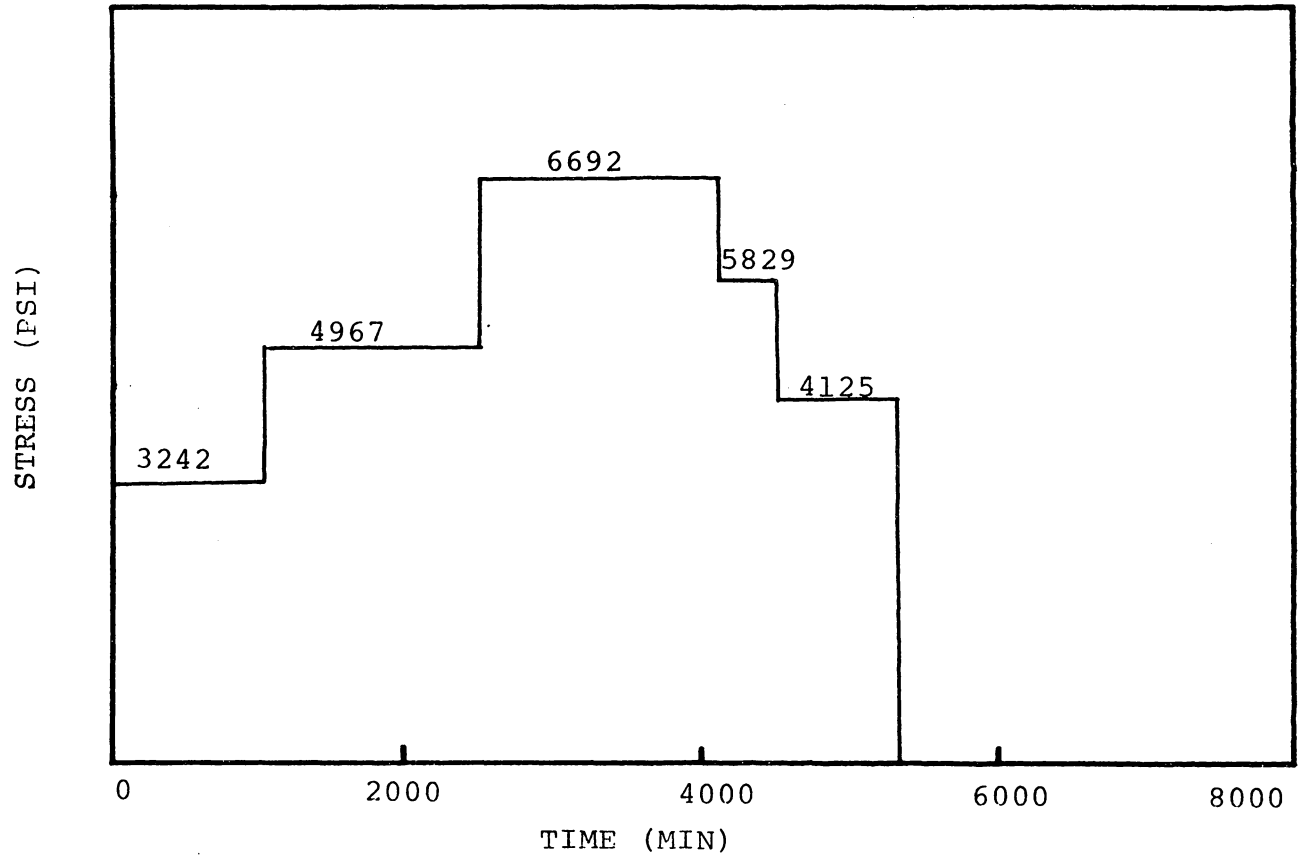


Figure 5.51 Load history for a five step loading.

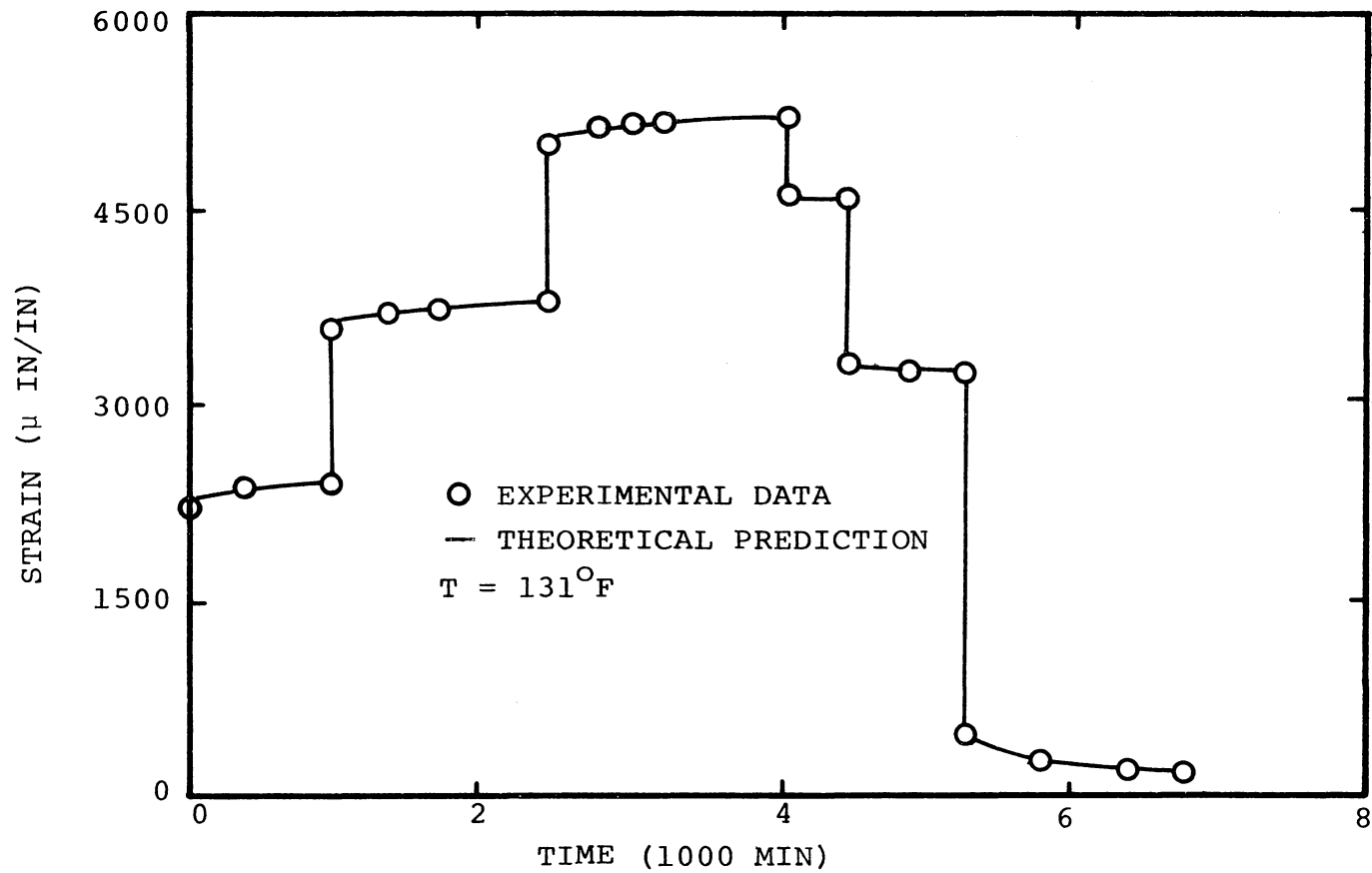


Figure 5.52 Creep response of a five step loading at T = 131°F.

the calculations. As shown in Figures 5.49, 5.50, and 5.52, excellent agreement was achieved between theory and experiment. The maximum error between the theoretical predictions and the experimental results was 3% and occurred at times when the loading had just changed.

In a practical situation, parts made of an SMC-R50 material are put into service in their virgin material state. The creep response of such undamaged specimens is different than those that have been preconditioned. This is perhaps one of the biggest questions about creep characterization using the mechanical conditioning procedure. Thus, comparisons are made between conditioned and unconditioned data [5].

Denton [5] performed creep tests at 73°F and 200°F at various stress levels up to 80% of the static ultimate strength of SMC-R50 at room temperature. Since all of these tests except one were conducted at stress levels beyond the range of creep stress levels used in this study, each parameter (ϵ_0 and m) curve (Figures 5.37 and 5.38) obtained in this study was extrapolated to the highest stress level applied to the virgin specimen. To determine ϵ_0 and m at a desired temperature, a linear interpolation was used. Figures 5.53 to 5.59 present comparisons between the creep response of the virgin specimens and the conditioned specimens. For all of the cases, the creep response of the

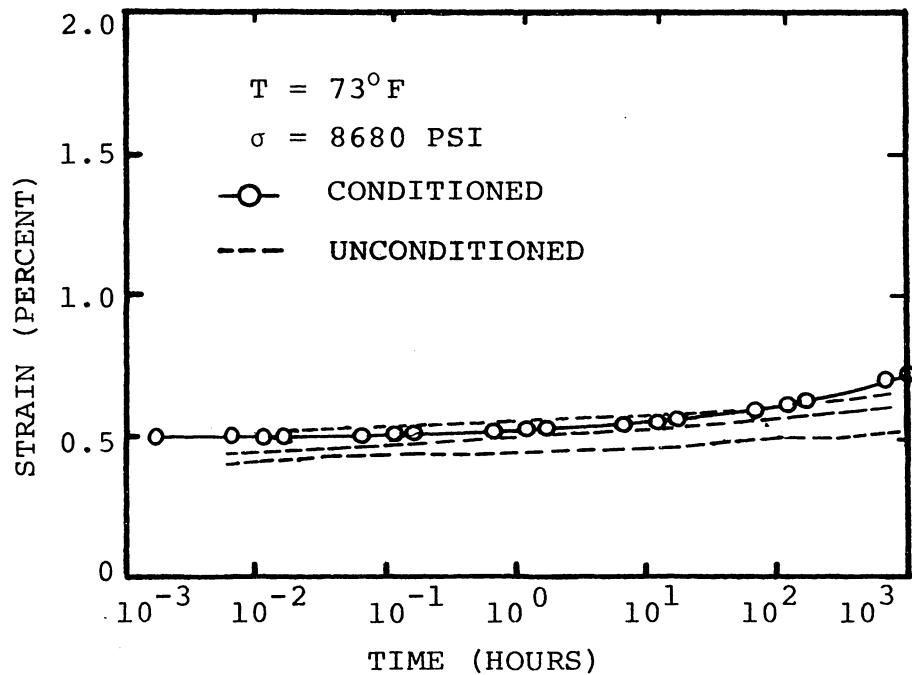


Figure 5.53 Creep response of conditioned and unconditioned specimens at 73°F ($\sigma = 40\%$ of σ_u at 73°F).

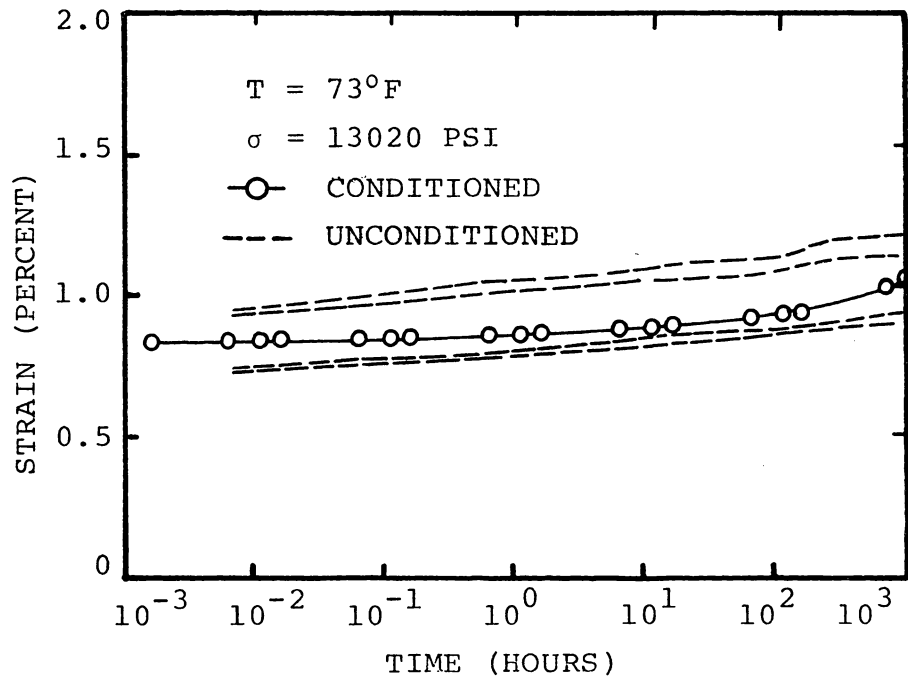


Figure 5.54 Creep response of conditioned and unconditioned specimens at 73°F ($\sigma = 60\%$ of σ_u at 73°F)

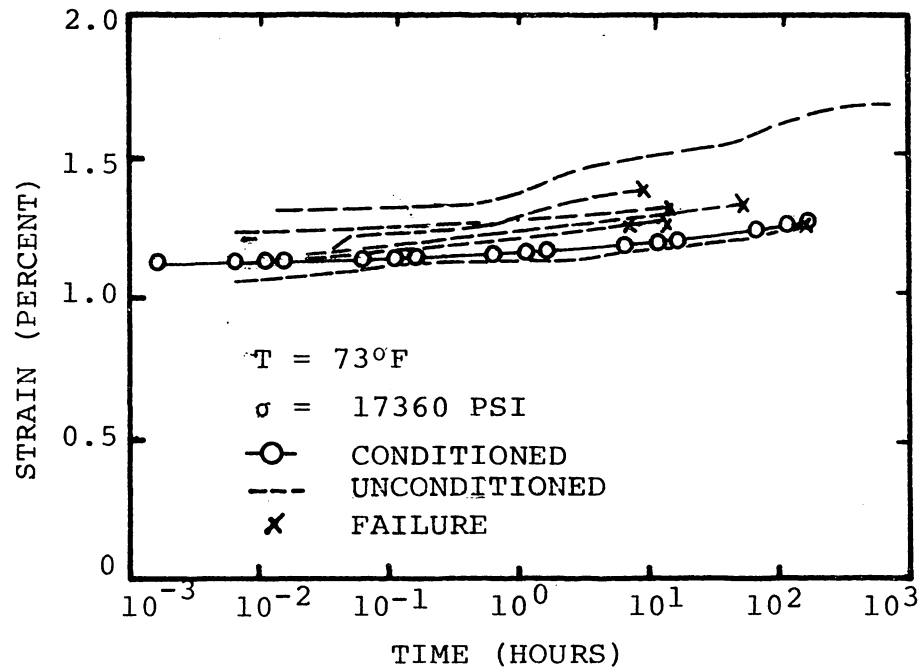


Figure 5.55 Creep response of conditioned and unconditioned specimen at 73°F ($\sigma = 80\%$ of σ_u at 73°F).

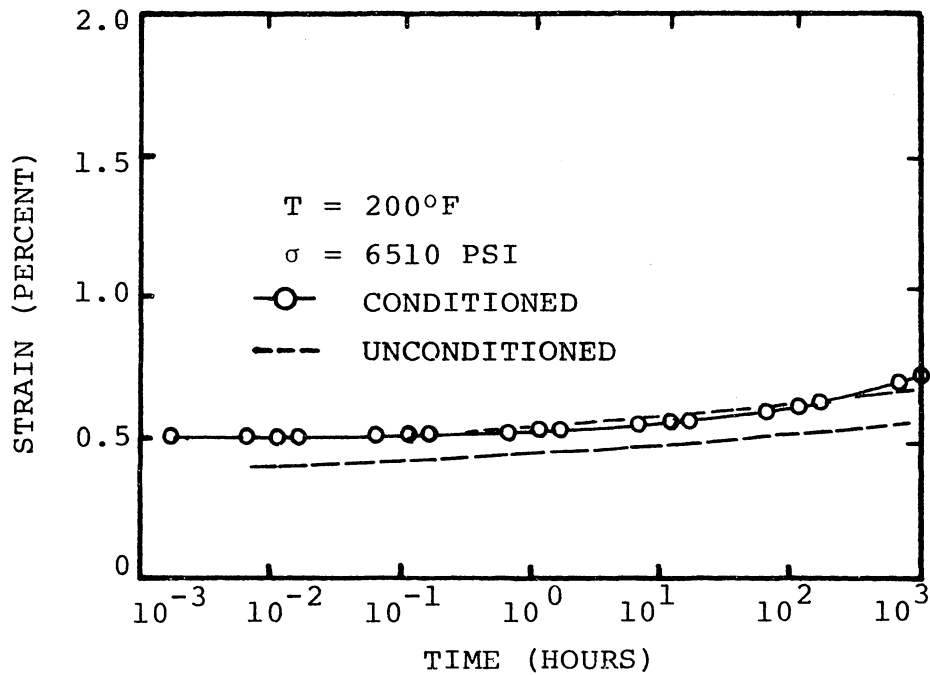


Figure 5.56 Creep response of conditioned and unconditioned specimens at 200°F ($\sigma = 30\%$ of σ_u at 73°F).

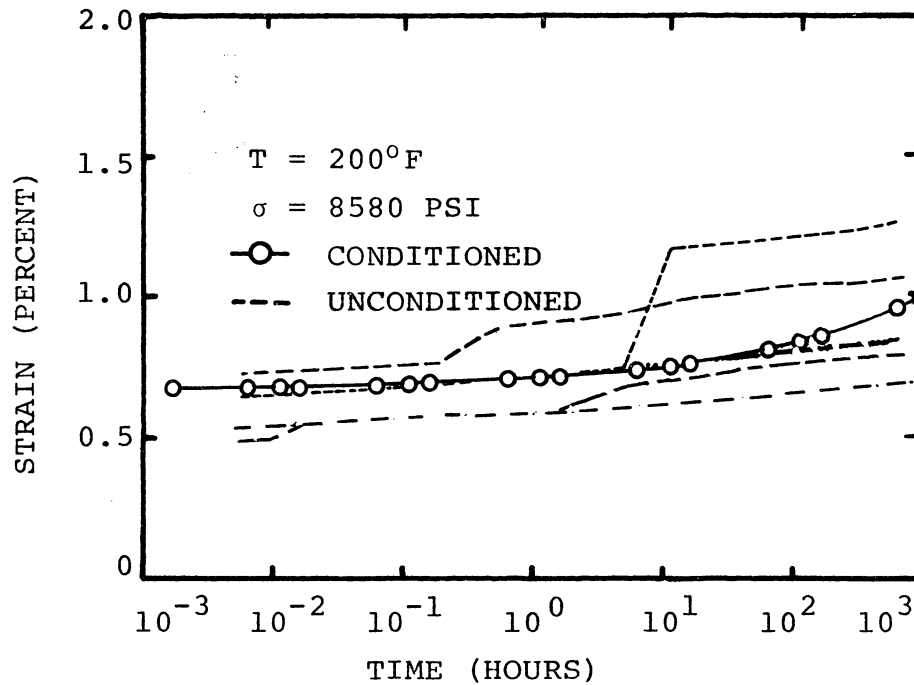


Figure 5.57 Creep response of conditioned and unconditioned specimens at 200°F (σ = 40% of σ_u at 80°).

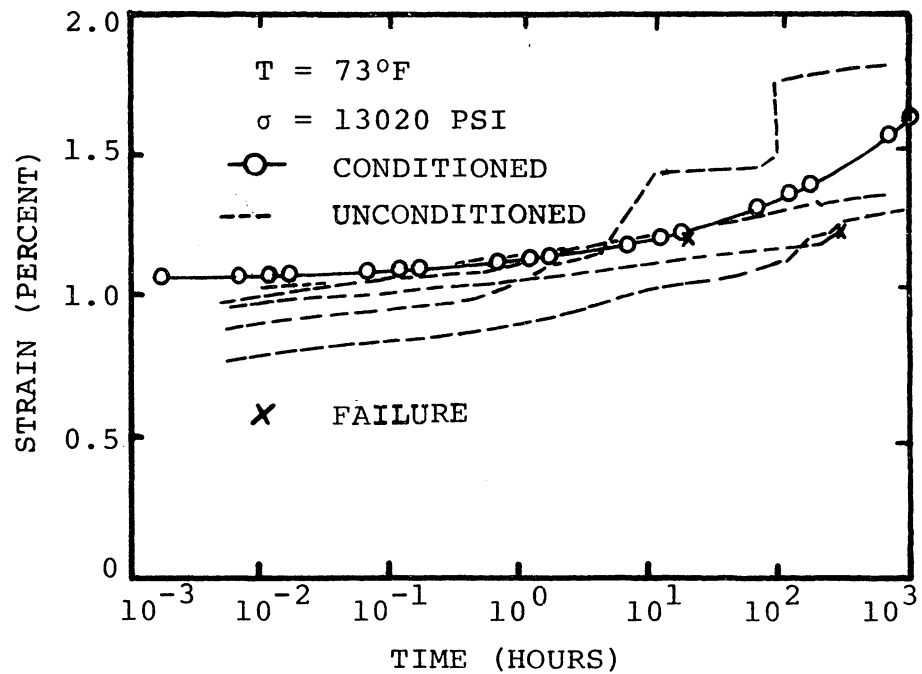


Figure 5.58 Creep response of conditioned and unconditioned specimens at 200°F ($\sigma = 60\%$ of σ_u at 73°F).

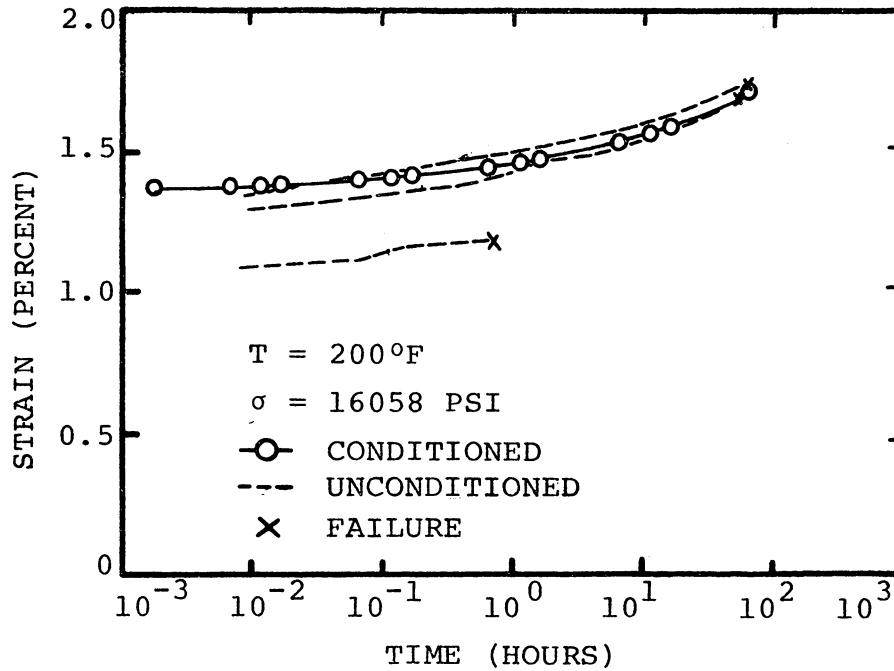


Figure 5.59 Creep response of conditioned and unconditioned specimens at 200°F ($\sigma = 74\%$ of σ_u at 73°F).

conditioned specimens is within the scatter band of that of the virgin specimens under the same test conditions.

5.6 Creep Rupture Results

The time-dependent failure data of SMC-R50 from two sources were used to study the creep rupture phenomenon. These data were obtained by Denton [5] and by Morris [18]. The creep rupture experiments were conducted at five temperature levels, 73°F, 200°F, 293°F, 311°F, and 329°F. For each temperature level, several creep rupture tests were conducted at different stress levels. Two values, the creep stress (i.e. rupture stress) and the failure time, were obtained from each creep rupture test (Table 5.3). Based on these two values, the critical free energy (W_c) to cause failure may be calculated for a given temperature. However, according to equation (3.20), the calculation of the critical energy requires three additional values. These values are initial creep compliance D_0 , transient creep compliance C , and the time exponent n , and are not available in the two references. Thus, to determine the value of critical energy, it is necessary to interpolate and/or extrapolate the experimental results obtained in this study. Each of the four curves of the Findley parameters ϵ_0 and m (as shown in Figures 5.37 and 5.38) were first linearly extended to 17,400 psi, the maximum stress level for the creep rupture data. From the extended curves, four

Table 5.3 List of creep rupture data obtained from Denton [5] and Morris [18], and calculated values of critical free energy

Temperature °F	Stress (ksi)	Failure Time (min)	Critical Free Energy (ksi)	Source
73	17.4	600	0.103	
73	17.4	3180	0.107	
73	17.4	6600	0.109	
200	13.0	18300	0.080	Denton
200	16.1	2940	0.112	
200	16.1	3480	0.113	
293	13.0	450	0.086	
293	13.5	24	0.086	
293	14.0	0.9	0.089	
311	11.7	360	0.074	
311	12.1	90	0.074	Morris
311	12.5	33	0.083	
311	13.0	18	0.078	
329	11.7	42	0.073	
329	12.1	4.2	0.071	
329	12.5	0.7	0.077	

values of a parameter (ϵ_0 or m) were determined for a given stress level and were associated with the four temperature levels used in short time elevated temperature creep experiments. These four values of ϵ_0 or m for a given stress were then fit by a line using the least squares technique and extended to determine the value of ϵ_0 or m at a given temperature level. By the above procedure, the Findley parameters ϵ_0 and m were determined for a given stress and temperature level. The creep compliances D_0 or C were then obtained by dividing ϵ_0 or m by the corresponding stress level. The n -value at a desired temperature was obtained using linear extrapolation.

Based on the analysis described above, the critical free energy (W_c) for each creep rupture data point (as shown in Table 5.3) was calculated using equation (3.20). It was found that for a constant temperature level, the critical free energy was practically independent of stress. It was also found that the critical free energy decreased when the temperature increased (Figure 5.60). The values of critical free energy shown in Figure 5.60 are average values at a given temperature. Based on the values of the critical energy (as shown in Figure 5.60), equation (3.20) was used to obtain the theoretical curves of rupture stress versus log failure time (Figure 5.61). These curves exhibit a linear-like region at short time. The nonlinear

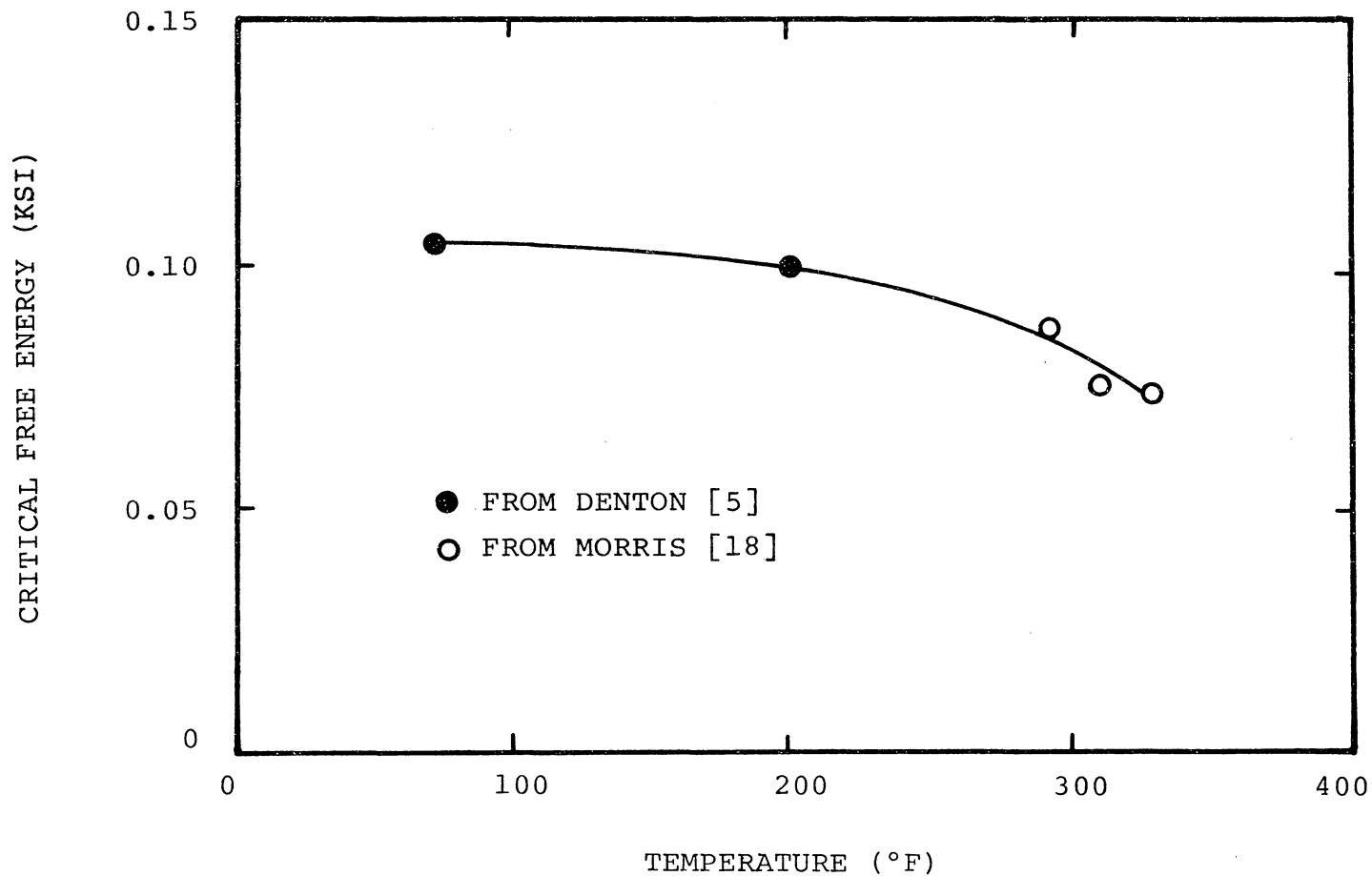


Figure 5.60 The relation between the critical free energy and temperature.

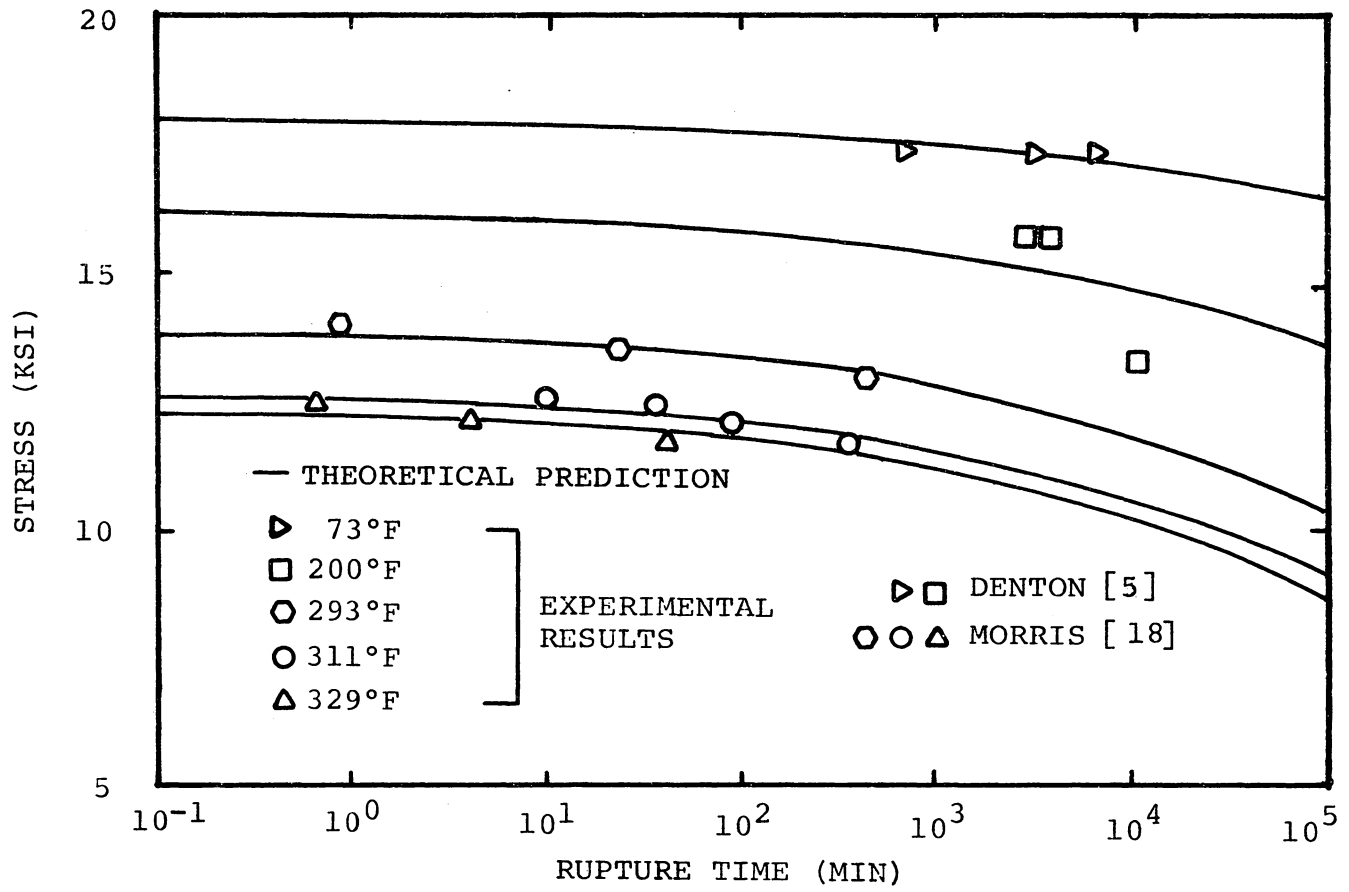


Figure 5.61 Predictions of stress-rupture time using the Reiner-Weisenberg Criterion.

relation between rupture stress and rupture time becomes more significant when the temperature is increased. In Figure 5.61, creep rupture data are also presented. In general, good correlation between the theory and the experimental results was obtained. However, more data is needed at long times to verify this method of predicting creep rupture.

5.7 Summary

The study of the effects of moisture was primarily to determine the extent of environmental conditions where the creep phenomenon would be associated only with applied load and temperature. It was found that the ultimate strength and ultimate strain were essentially constant for specimens stored at room temperature, or for specimens that have been dried and stored at the same conditions. It was assumed that the creep response would likewise be unaffected by the same environmental conditions.

Repeatable creep response could be obtained only after mechanical conditioning. It should be pointed out that the mechanical conditioning procedure introduces damage (micro-cracks) in the specimen. The state of damage is different for the different stress levels used in the mechanical conditioning. Furthermore, the relations between the Findley parameters (ϵ_0 , m , and n) and the applied stress were different for different damage states. Repeatable results

could only be obtained for applied stress levels less than or equal to the stress used in the mechanical conditioning procedure.

The parameters, ϵ_0 , m , and n are functions of the duration of a creep experiment, but approach asymptotic values with time. Accurate prediction of the creep response could be obtained only when the asymptotic values of the parameters were used in the Findley equation. It was also found that the asymptotic values of ϵ_0 and m could be obtained from short-time (200 minutes) creep data if the asymptotic n -value was used to calculate them.

At the same damage level, the asymptotic values of the Findley parameters ϵ_0 and m are hyperbolic sine functions of stress for constant temperature. The n -value increases linearly with temperature, but is independent of stress. It was also found that the Findley equation and the modified superposition principle predicted the creep response due to multiple step loadings.

The critical free energy was found to be a constant for SMC-R50 at a given temperature. It was also found that the critical free energy decreased with an increase in temperature. The time to rupture was predicted using the Reiner-Weissenberg failure criterion. The prediction was fair, however more data at longer times are needed to determine if the failure criterion is accurate.

CHAPTER 6

CONCLUSIONS

The present investigation has centered on two categories; the viscoelastic characterization of SMC-R50 and the usefulness of the Findley equation to predict the creep response of SMC-R50. The material characterization included the study of mechanical conditioning, and the elevated temperature creep response. The theoretical model was used to predict the long-time creep response and the multiple step creep response. Several conclusions have been established in this study:

- (1) The application of mechanical conditioning provides repeatable creep and creep recovery results.
- (2) The Findley parameters ϵ_0 , m , and n are functions of time but approach asymptotic values.
- (3) The Findley equation can be used to describe the creep and creep recovery behavior of SMC-R50.
- (4) The modified superposition principle can be used to predict creep response due to multiple step loadings.
- (5) The critical free energy associated with the creep rupture behavior is independent of stress but is a function of temperature. The stress-rupture time relation can be described by the Reiner-Weissenberg failure criterion.

REFERENCES

1. B. A. Sanders and R. A. Heimbuch, "Engineering Properties of Automotive Fiber Reinforced Plastics," presented at the Society for Experimental Stress Analysis 1977 Fall Meeting, Philadelphia, Pennsylvania, Oct. 11, 1977.
2. D. L. Denton, "Mechanical Properties Characterization of an SMC-R50 Composite," SAE publication, Paper No. 790671, 1979.
3. J. K. Bard and G. G. Warner, "Mold Charge Pattern Versus Isotropy of Chopped Glass/Polyester (SMC) Panels," General Motors Technical Report, MD 76-018, 1976.
4. G. G. Warner, R. J. Reid, and R. A. Heimbuch, "Fatigue Life of E-Glass Polyester Composites," General Motors Technical Report, MD 77-006, 1977.
5. D. L. Denton, "The Mechanical Properties of an SMC-R50 Composite," Composite Technology Update Publication, Owens-Corning Fiberglas Corporation, 1979.
6. R. M. Christensen, "Theory of Viscoelasticity-An Introduction," Academic Press, Inc., New York, 1971.
7. J. D. Ferry, "Viscoelastic Properties of Polymers," John Wiley and Sons, Inc., New York, 1961.
8. H. Leaderman, "Elastic and Creep Properties of Filamentous Materials and Other High Polymers," Textile Foundation, Washington D.C., 1943.
9. W. N. Findley, "Derivation of a Stress-Strain Equation from Creep Data for Plastics," Proc. of first National Congress of Applied Mechanics, 1952, pp. 595-602.
10. W. N. Findley, "Creep Characteristics of Plastics," 1944 Symposium on Plastics, ASTM, 1944, pp. 118-134.
11. W. N. Findley, "Prediction of Stress Relaxation from Creep Tests of Plastics," Proc. of Third National Congress of Applied Mechanics, 1958, pp. 521-526.
12. J. S. Cartner and H. F. Brinson, "The Nonlinear Viscoelastic Behavior of Adhesive and Chopped Fiber Composites," VPI & SU, Blacksburg, VA, VPI-E-78-21, 1978.

13. R. A. Schapery, On the Characterization of Nonlinear Viscoelastic Behavior of Composite Materials," Polymer Engineering and Science, Vol. 9, No. 4, 1969, pp. 295-310.
14. R. A. Schapery, "Viscoelastic Behavior and Analysis of Composite Materials," Mechanics of Composite Materials, edited by G. Sendeckyj, Vol. 2, Academic Press, New York, 1974, pp. 86-168.
15. Y. T. Yeow, "The Time-Temperature Behavior of Graphite Epoxy Laminates," PhD Dissertation, VPI & SU, Blacksburg, VA, 1978.
16. D. A. Dillard and H. F. Brinson, "Nonlinear Viscoelastic Characterization of Graphite/Epoxy Composites," Proc. of the 1982 Joint Conference on Experimental Mechanics, Part 1, Hawaii, 1982, pp. 102-109.
17. H. F. Brinson, D. H. Morris, and Y. T. Yeow, "A New Experimental Method for the Accelerated Characterization of Composite Materials," 6th International Conference for Experimental Stress Analysis, Munich, West Germany, Sept., 1978.
18. D. H. Morris, "A Feasibility Study on the Use of Parameter Methods to Predict Creep-Rupture of Sheet Molding Compound," VPI & SU, Blacksburg, VA, VPI-E-80-7, 1980.
19. D. A. Dillard, "Creep and Creep Rupture of Laminated Graphite/Epoxy Composites," Ph.D Dissertation, VPI & SU, Blacksburg, VA, 1981.
20. W. Flügge, "Viscoelasticity," 2nd Ed., Springer-Verlag, New York, 1975.
21. A. E. Green and R. S. Rivlin, "The Mechanics of Nonlinear Materials with Memory," Archives Rational Mechanics and Analysis, 1(1), 1957, pp. 1-21.
22. Y. T. Yeow, D. H. Morris and H. F. Brinson, "Time Temperature Behavior of a Unidirectional Graphite/Epoxy Composite," Composite Materials: Testing and Design (5th Conference), S. W. Tsai, Ed. ASTM STP 674, 1979, pp. 263-281.
23. D. H. Morris, Y. T. Yeow, and H. F. Brinson, "The Viscoelastic Behavior of the Principal Compliance Matrix of a Uni-directional Graphite/Epoxy Composite," VPI & SU, Blacksburg, VA, VPI-E-79-9, 1979.

24. W. I. Griffith, D. H. Morris, and H. F. Brinson, "The Accelerated Characterization of Viscoelastic Composite Materials," VPI & SU, Blacksburg, VA, VPI-E-80-15, 1980.
25. C. Heil, "The Nonlinear Viscoelastic Response of Resin Matrix Composites," PhD Dissertation, Vrije Universiteit, Brussel, Belgium, 1983.
26. R. A. Schapery, "Further Development of a Thermodynamic Constitutive Theory: Stress Formulation," Purdue University, Report No. 69-2, West Lafayette, IN, 1969.
27. Y. C. Lou and R. A. Schapery, "Viscoelastic Characterization of a Nonlinear Fiber-Reinforced Plastics," Journal of Composite Materials, Vol. 5, 1971, pp. 208-234.
28. R. A. Schapery, S. W. Beckwith and N. Conrad, "Studies on the Viscoelastic Behavior of Fiber-Reinforced Plastics," Texas A&M University, College Station, TX, Report No. MM2702-73-3, 1973.
29. J. C. Halpin, "Characterization of Orthotropic Polymeric Solids," PhD Dissertation, The University of Akron, Akron, OH, 1969.
30. D. F. Sims, "Viscoelastic Creep and Relaxation Behavior of Laminated Composite Plates," PhD Dissertation, Southern Methodist University, Dallas, TX, 1972.
31. D. F. Sims and J. C. Halpin, "Methods for Determining the Elastic and Viscoelastic Response of Composite Materials," Composite Materials: Testing and Design, 3rd Conference, ASTM STP-546, 1974, pp. 46-66.
32. K. L. Jerina, R. A. Schapery, R. W. Tung, and B. A. Sanders, "Viscoelastic Characterization of a Random Fiber Composite Material Employing Micro-Mechanics," Texas A&M University, College Station, TX, Report No. MM3979-80-5, 1980.
33. S. W. Beckwith, "Viscoelastic Characterization of a Nonlinear, Glass/Epoxy Composite Using Micromechanics Theory," Annual Meeting of the JANNAF Structure and Mechanical Behavior Working Group and the Operational Serviceability Working Group, San Francisco, California, February 26, 1975.
34. W. N. Findley and G. Ghosla, "An Equation for Tension Creep of the Three Unfilled Thermoplastics," Journal of Society of Plastic Engineers, Vol. 12, No. 12, 1956, pp. 20-25.

35. W. N. Findley and W. J. Worley, "Short-Time Static Tests and Creep Tests of a Paper Laminated Plastics," Proc. ASTM, Vol. 44, 1944, p. 949.
36. W. N. Findley and J. S. Lai, "Creep and Creep Recovery of 2618 Aluminum Alloy Under Combined Stress with a Representation by a Viscous-Viscoelastic Model," Journal of Applied Mechanics, Vol. 45, 1978, pp. 507-514.
37. U. W. Cho and W. N. Findley, "Creep and Creep Recovery of 304 Stainless Steel under Combined Stress with a Representation by a Viscous-Viscoelastic Model," Journal of Applied Mechanics, Vol. 47, 1980, pp. 755-761.
38. U. W. Cho and W. N. Findley, "Creep and Creep Recovery of 304 Stainless Steel at Low Stresses with Effects of Aging on Creep and Plastic Stains," Journal of Applied Mechanics, Vol. 48, 1981, pp. 785-790.
39. V. B. Gupta and J. Lahiri, "Viscoelastic Behavior of Polypropylene and Glass Reinforced Polypropylene in Creep," Journal of Composite Materials, Vol. 14, 1980, pp. 286-296.
40. W. G. Knauss, "The Mechanics of Polymer Fracture," Applied Mechanics Reviews, Jan. 1973, pp. 1-17.
41. V. R. Regel and V. P. Tamuzh, "Fracture and Fatigue of Polymer and Composites (Survey)," Polymer Mechanics, Vol. 13, No. 3, 1977, pp. 392-408.
42. K. H. Boller, "Tensile Stress Rupture and Creep Characteristics of Two Glass-Fabric Based Plastic Laminates," Forest Products Lab Report, Madison, Wisconsin, 1957.
43. E. M. Wu and D. C. Ruhmann, "Stress Rupture of Glass-Epoxy Composites: Environmental and Stress Effects," ASTM STP 580, 1975.
44. B. D. Coleman, "Statistics and Time Dependence of Mechanical Breakdown in Fibers," Journal of Applied Physics, Vol. 19, 1958, p. 968.

45. C. C. Chiao, "An Accelerated Test for Predicting Lifetime of Organic Fiber Composites," Proceedings of the 3rd Biennial AIME Symposium on Failure Modes in Composites, Las Vegas, Nevada, 1976, pp. 157-169.
46. R. M. Christensen, "Residual-Strength Determination in Polymeric Materials," Lawrence Livermore Laboratory, Livermore, CA, Preprint UCRL-84532, 1980.
47. S. N. Zhurkov, "Kinetic Concept of the Strength of Solids," International Journal of Fracture Mechanics, Vol. 1, 1965, pp. 311-323.
48. R. F. Landel and R. F. Fedors, "Rupture of Amorphous Unfilled Polymers," Fracture Process in Polymeric Solids, edited by R. Rosen, Interscience Publishers, New York, 1964, pp. 361-485.
49. M. J. Crochet, "Symmetric Deformation of Viscoelastic-Plastic Cylinders," Journal of Applied Mechanics, Vol. 33, 1966, pp. 327-334.
50. W. N. Findley and D. B. Peterson, "Prediction of Long-Time Creep with Ten-Year Creep Data on Four Plastic Laminates," Proc. ASTM, Vol. 58, 1958, pp. 841-861.
51. W. N. Findley, H. W. Peithman, and W. J. Worley, "Influence of Temperature on Creep, Stress-Rupture, and Static Properties of Malamine-Resin and Silicone-Resin Glass-Fabric Laminates," National Advisory Committee for Aeronautics, Technical Note 3414, 1955.
52. W. N. Findley, C. H. Adams, and W. J. Worley, "The Effect of Temperature on the Creep of Two Laminated Plastics as Interpreted by the Hyperbolic Sine Law and Activation Energy Theory," Proc. ASTM, Vol. 48, 1948, pp. 1217-1239.
53. A Bertolotti and H. F. Brinson, "A Computer-Based Solution for Evaluating the Parameters in Schapery's Non-Linear Viscoelastic Model," ESM Department, VPI & SU, Blacksburg, VA, Senior Project Report, 1982.
54. W. N. Findley and J. S. Y. Lai, "A Modified Superposition Principle Applied to Creep Of Nonlinear Viscoelastic Material Under Abrupt Changes in State of Combined Stress," Transactions of the Society of Rheology, 11:3, 1967, pp. 361-380.

55. M. Reiner and K. Weissenberg, "A Thermodynamic Theory of the Strength of Materials," Rheology Leaflet, No. 10, 1939, pp. 12-10.
56. O. S. Brüller, "On the Damage Energy of Polymers in Creep," Polymer Engineering and Science, Vol. 18, No. 1, 1978, pp. 42-44.
57. O. S. Brüller, "Energy-Related Failure of Thermoplastics," Polymer Engineering and Science, Vol. 21, No. 3, 1981, pp. 145-150.
58. C. H. Shen and G. S. Springer, "Effects of Moisture and Temperature on the Tensile Strength of Composite Materials," Environmental Effects on Composite Materials, Edited by Springer, Technomic Publishing Company, Inc., Stanford, Conn., 1981.
59. K. B. Kibler, "Time-Dependent Environmental Behavior of Epoxy Matrix Composites," AFML, AFFDL, AFSOR, NASA, NDC and AMMRC, Mechanics of Composites Review, Bergamo Center, Dayton, OH, 1979, pp. 51-61.
60. A. S. D. Wang and P. K. Lin, "Humidity Effects on the Creep Behavior of an Epoxy-Graphite Material," AIAA/SAE 11th Propulsion Conference, Anaheim, CA, AIAA Paper No. 75-1341, 1975.
61. A. C. Loos, G. S. Springer, B. A. Sanders and R. W. Tung, "Moisture Absorption of Polyester-E Glass Composites," Environmental Effects on Composite Materials, Edited by Springer, Technomic Publishing Company, Inc., Stanford, Conn., 1981.
62. A. Hosangadi and T. H. Hahn, "Hygrothermal Degradation of Sheet Molding Compounds," Presented at the Symposium on High Modulus Fiber Composites in Ground Transportation and High Volume Applications, Pittsburgh, PA, Nov. 7, 1983.
63. B. A. Sanders, G. G. Warner, and R. A. Heimbuck, "Mechanical Properties of Three Glass Fiber Reinforced Polyester Materials," General Motors Technical Report, MD76-016, 1976.
64. D. Shirrell, "The Influence of Microstructural Variability Upon the Scatter in Mechanical Properties of R25 Sheet Molding Compounds," Presented at the Symposium on High Modulus Fiber Composites in Ground Transportation and High Volume Applications, Pittsburgh, Nov. 7, 1983.

65. K. L. Reifsnider, E. G. Henneke, II, and W. W. Stinchcomb, "Defect-Property Relationships in Composite Materials," Air Force Materials Laboratory, Wright-Patterson Air Force Base, OH, Report No. AFML-TR-76-81, part IV, 1979.
66. K. L. Reifsnider and J. E. Masters, "Investigation of Characteristic Damage States in Composite Laminates," ASME Publication No. 78-WA/Aero-4, 1978.
67. M. E. Tuttle, "Accelerated Viscoelastic Characterization of T300/5208 Graphite-Epoxy Laminates," PhD Dissertation, VPI & SU, Blacksburg, VA, 1984.
68. K. Onaran and W. N. Findley, "Experimental Determination of Some Kernel Functions in the Multiple Integral Method for Nonlinear Creep of Polyvinyl Chloride," Journal of Applied Mechanics, Vol. 38, 1971, pp. 30-38.

**The vita has been removed from
the scanned document**